

Combinations of single-top-quark production cross-section measurements and $|f_{LV}V_{tb}|$ determinations at $\sqrt{s} = 7$ and 8 TeV with the ATLAS and CMS experiments



The ATLAS and CMS collaborations

E-mail: atlas.publications@cern.ch,
cms-publication-committee-chair@cern.ch

ABSTRACT: This paper presents the combinations of single-top-quark production cross-section measurements by the ATLAS and CMS Collaborations, using data from LHC proton–proton collisions at $\sqrt{s} = 7$ and 8 TeV corresponding to integrated luminosities of 1.17 to 5.1 fb⁻¹ at $\sqrt{s} = 7$ TeV and 12.2 to 20.3 fb⁻¹ at $\sqrt{s} = 8$ TeV. These combinations are performed per centre-of-mass energy and for each production mode: t -channel, tW , and s -channel. The combined t -channel cross-sections are 67.5 ± 5.7 pb and 87.7 ± 5.8 pb at $\sqrt{s} = 7$ and 8 TeV respectively. The combined tW cross-sections are 16.3 ± 4.1 pb and 23.1 ± 3.6 pb at $\sqrt{s} = 7$ and 8 TeV respectively. For the s -channel cross-section, the combination yields 4.9 ± 1.4 pb at $\sqrt{s} = 8$ TeV. The square of the magnitude of the CKM matrix element V_{tb} multiplied by a form factor f_{LV} is determined for each production mode and centre-of-mass energy, using the ratio of the measured cross-section to its theoretical prediction. It is assumed that the top-quark-related CKM matrix elements obey the relation $|V_{td}|, |V_{ts}| \ll |V_{tb}|$. All the $|f_{LV}V_{tb}|^2$ determinations, extracted from individual ratios at $\sqrt{s} = 7$ and 8 TeV, are combined, resulting in $|f_{LV}V_{tb}| = 1.02 \pm 0.04$ (meas.) ± 0.02 (theo.). All combined measurements are consistent with their corresponding Standard Model predictions.

KEYWORDS: Hadron-Hadron scattering (experiments)

ARXIV EPRINT: [1902.07158](https://arxiv.org/abs/1902.07158)

Contents

1	Introduction	1
2	Theoretical cross-section calculations	3
3	Single-top-quark cross-section measurements at $\sqrt{s} = 7$ and 8 TeV	5
4	Combination methodology	6
5	Systematic uncertainties and correlation assumptions	7
5.1	Systematic uncertainties in measured cross-sections	7
5.2	Systematic uncertainties in theoretical cross-section predictions	16
6	Combinations of cross-section measurements	17
6.1	Combinations of t -channel cross-section measurements	17
6.2	Combinations of tW cross-section measurements	18
6.3	Combination of s -channel cross-section measurements	20
6.4	Summary of cross-section combinations	21
7	Combinations of $f_{LV}V_{tb}$ determinations	21
7.1	Results	23
7.2	Stability tests	26
8	Summary	28
A	Systematic uncertainties in cross-section measurements	29
A.1	Systematic uncertainties in t -channel cross-section measurements	29
A.2	Systematic uncertainties in tW cross-section measurements	31
A.3	Systematic uncertainties in s -channel cross-section measurements	34
	The ATLAS collaboration	45
	The CMS collaboration	62

1 Introduction

Measurements of single-top-quark production via the electroweak interaction, a process first observed in proton–antiproton ($p\bar{p}$) collisions at the Tevatron [1, 2], have entered the precision era at the Large Hadron Collider (LHC). It has become possible to measure top-quark properties using single-top-quark events [3]. Single-top-quark production is sensitive to new physics mechanisms [4] that either modify the tWb coupling [5–10] or introduce new

particles and interactions [11–16]. The production rate of single top quarks is proportional to the square of the left-handed coupling at the tWb production vertex, assuming that there are no significant tWd or tWs contributions. In the Standard Model (SM), this coupling is given by the Cabibbo-Kobayashi-Maskawa (CKM) [17, 18] matrix element V_{tb} . Indirect measurements of $|V_{tb}|$, from precision measurements of B -meson decays [19] and from top-quark decays [20–23], rely on the SM assumptions that the CKM matrix is unitary and that there are three quark generations. The most stringent indirect determination comes from a global fit to all available B -physics measurements, resulting in $|V_{tb}| = 0.999105 \pm 0.000032$ [19]. This fit also assumes the absence of any new physics mechanisms that might affect b -quarks. The most precise indirect measurement using top-quark events was performed by the CMS Collaboration in proton–proton (pp) collisions at a centre-of-mass energy of $\sqrt{s} = 7$ TeV, resulting in $|V_{tb}| = 1.007 \pm 0.016$ [23].

A direct estimate of the coupling at the tWb production vertex, $|f_{LV}V_{tb}|$, is obtained from the measured single-top-quark cross-section $\sigma_{\text{meas.}}$ and its corresponding theoretical expectation $\sigma_{\text{theo.}}$,

$$|f_{LV}V_{tb}| = \sqrt{\frac{\sigma_{\text{meas.}}}{\sigma_{\text{theo.}} (V_{tb} = 1)}}. \tag{1.1}$$

The f_{LV} term is a form factor, assumed to be real, that parameterises the possible presence of anomalous left-handed vector couplings [24]. By construction, this form factor is exactly one in the SM, while it can be different from one in models of new physics processes. The direct estimation assumes that $|V_{td}|, |V_{ts}| \ll |V_{tb}|$ [25, 26], and that the tWb interaction involves a left-handed weak coupling, like that in the SM. The $|f_{LV}V_{tb}|$ determination via single-top-quark production is independent of assumptions about the number of quark generations and the unitarity of the CKM matrix [4, 27–29]. Since the indirect determination of $|V_{tb}|$ gives a value close to unity, V_{tb} is considered equal to one in theoretical calculations of the single-top-quark cross-section. The combination of single-top-quark measurements from the Tevatron gives $|f_{LV}V_{tb}| = 1.02^{+0.06}_{-0.05}$ [30].

Single-top-quark production at a hadron collider mostly proceeds, according to the SM prediction, via three modes that can be defined at leading order (LO) in perturbative quantum chromodynamics (QCD): the exchange of a virtual W boson in the t -channel or in the s -channel, and the associated production of a top quark and a W boson (tW). Representative Feynman diagrams for these processes at LO are shown in figure 1.

In pp collisions at the LHC, the process with the largest single-top-quark production cross-section is the t -channel, where a light-flavour quark q from one of the colliding protons interacts with a b -quark by exchanging a space-like virtual W boson, producing a top quark (t -quark) and a recoiling light-flavour quark q' , called the spectator quark. For t -channel production at LO, the b -quark can be considered as directly emitted from the other proton (five-flavour-number scheme or 5FS) or it can come from gluon splitting (four-flavour-number scheme or 4FS) [31]. The kinematic properties of the spectator quark provide distinctive features for this process [32, 33]. The associated production of a W boson and a top quark has the second-largest production cross-section. In a representative process of tW production, a gluon interacts with an initial b -quark by exchanging a virtual b -quark,

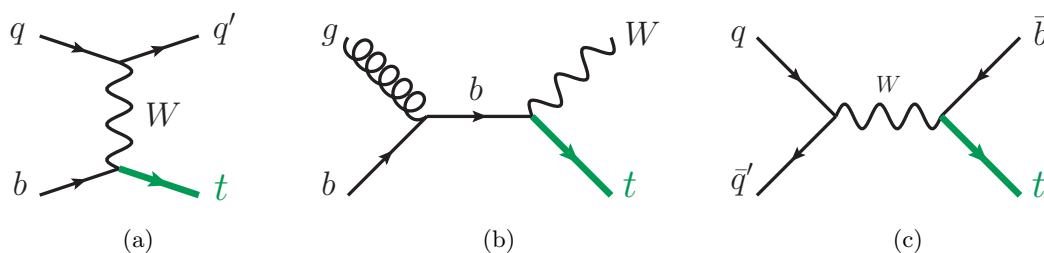


Figure 1. Representative Feynman diagrams at LO in QCD and in the five-flavour-number scheme for single-top-quark production in (a) the t -channel, (b) tW production, and (c) the s -channel.

producing a t -quark and a W boson. The measurement of this process suffers from a large background from top-quark pair ($t\bar{t}$) production [34, 35]. The s -channel cross-section is the smallest at the LHC. In this process, a quark–antiquark pair annihilates to produce a time-like virtual W boson, which decays to a t -quark and a \bar{b} -quark. This process was observed in $p\bar{p}$ collisions at the Tevatron [36] and evidence of it was reported by the ATLAS Collaboration in pp collisions at $\sqrt{s} = 8$ TeV [37].

In this paper, the t -channel, tW , and s -channel single-top-quark cross-section measurements by the ATLAS and CMS experiments are combined for each production mode, separately at pp centre-of-mass energies of 7 and 8 TeV. A combined determination of $|f_{LV}V_{tb}|$ is also presented, using as inputs the values of $|f_{LV}V_{tb}|^2$ calculated from the measured and predicted single-top-quark cross-sections in the three production modes at $\sqrt{s} = 7$ and 8 TeV. Using the same approach, results are also shown for $|f_{LV}V_{tb}|$ combinations for each production mode.

The theoretical cross-section calculations are described in section 2. Section 3 presents the cross-section measurements. The combination methodology is briefly described in section 4. Section 5 is devoted to a discussion of systematic uncertainties in the cross-section measurements as well as theoretical calculations, where the latter affect the $|f_{LV}V_{tb}|$ extraction in particular. The assumptions made about the correlation of uncertainties between the two experiments, as well as between theoretical calculations, are also discussed. Section 6 presents the combination of cross-sections for each production mode at the same centre-of-mass energy. In section 7, determinations of $|f_{LV}V_{tb}|$ are performed using all single-top-quark cross-section measurements together or by production mode. Stability tests are also shown and discussed. In section 8, the results are summarised.

2 Theoretical cross-section calculations

The theoretical predictions for the single-top-quark production cross-sections are calculated at next-to-leading order (NLO) in the strong coupling constant α_s , at NLO with next-to-next-to-leading-logarithm (NNLL) resummation (named NLO+NNLL), and at next-to-next-to-leading order (NNLO). The difference between 4FS and 5FS is small [38, 39], and the calculations use the 5FS. The NLO prediction is used in the V_{tb} combination for the t -channel and s -channel, while the NLO+NNLL prediction is used for tW , as explained

below. The NLO prediction is calculated with HATHOR (v2.1) [40, 41]. Uncertainties comprise the scale uncertainty, the α_s uncertainty, and the parton distribution function (PDF) uncertainty. The scale uncertainty is evaluated by varying the renormalisation and factorisation scales up and down together by a factor of two. The combination of the PDF+ α_s uncertainty is calculated according to the PDF4LHC prescription [42] from the envelope of the uncertainties at 68% confidence level (CL) in the MSTW2008 NLO, CT10 NLO [43], and NNPDF2.3 [44] PDF sets.

The NLO+NNLL predictions [45] are available for all single-top-quark production modes [46–48]. Uncertainties in these calculations are estimated by varying the renormalisation and factorisation scales between $m_t/2$ and $2m_t$, where m_t is the top-quark mass, and from the 90% CL uncertainties in the MSTW2008 NNLO [49, 50] PDF set. The evaluation of the PDF uncertainties is provided by the author of refs. [46–48] and is not fully compatible with the PDF4LHC prescription. The t -channel cross-sections at $\sqrt{s} = 7$ and 8 TeV are also computed at NNLO in α_s [51], with the renormalisation and factorisation scales set to m_t . This results in cross-sections which are about 0.3% and 0.6% lower than the NLO values at $\sqrt{s} = 7$ and 8 TeV respectively. However, only a limited number of scale variations are evaluated [51].

A summary of all the available theoretical cross-section predictions for t -channel, tW , and s -channel production, $\sigma_{\text{theo.}}^{t\text{-chan.}}$, $\sigma_{\text{theo.}}^{tW}$, and $\sigma_{\text{theo.}}^{s\text{-chan.}}$ respectively, with their uncertainties is shown in table 1.

In this paper, NLO predictions serve as the reference for the t - and s -channel processes, following the prescriptions presented above, because higher-order calculations and their uncertainties are not fully computed and available for the parameter values of choice. The advantage of the NLO cross-section calculations is that the configurable parameters in HATHOR can be set according to those used to generate the ATLAS and CMS simulation samples. The t - and s -channel processes do not interfere at NLO [52]. For these two processes, the entire phase space is included in the integration in order to obtain the total cross-section. The tW cross-section prediction, $\sigma_{\text{theo.}}^{tW}$, is available at NLO [41] and NLO+NNLL [47, 53]. The tW process at NLO interferes with the $t\bar{t}$ process at LO with the subsequent decay $\bar{t} \rightarrow W\bar{b}$. In the NLO prediction for tW production provided in ref. [41], a kinematic cut-off is imposed on the transverse momentum (p_T) of the outgoing b -quark, suppressing the contribution from $t\bar{t}$ production. Since the treatment of this interference in HATHOR is still being developed [54, 55], the NLO+NNLL calculation is used as reference for tW production. For the reference cross-section predictions, uncertainties corresponding to the dependence on m_t and on the LHC beam energy, E_{beam} , are evaluated. The m_t dependence is estimated by varying its central value of 172.5 GeV (the value used in the simulation samples used to measure the single-top-quark cross-sections) by ± 1 GeV, using the functional form proposed in ref. [56]. The theoretical calculations are performed at a given centre-of-mass energy while the energy of the LHC beam is measured with an uncertainty. The single-top-quark cross-sections are assumed to depend on E_{beam} according to the model given in ref. [57], with a relative uncertainty $\delta E_{\text{beam}}/E_{\text{beam}}$ of 0.1% [58]. The theoretical cross-sections that are used as reference are marked with a \dagger in table 1.

\sqrt{s}	Process	Accuracy	$\sigma_{\text{theo.}}$ [pb]
7 TeV	t -channel	NLO [†]	$63.9_{-1.3}^{+1.9}$ (scale) ± 2.2 (PDF+ α_s) ± 0.7 (m_t) ± 0.1 (E_{beam})
		NLO+NNLL	$64.6_{-1.7}^{+2.6}$ (scale+PDF+ α_s)
		NNLO	$63.7_{-0.3}^{+0.5}$ (scale)
	tW	NLO	$13.2_{-0.6}^{+0.5}$ (scale) ± 1.3 (PDF+ α_s)
		NLO+NNLL [†]	15.74 ± 0.40 (scale) $_{-1.14}^{+1.10}$ (PDF+ α_s) ± 0.28 (m_t) ± 0.04 (E_{beam})
	s -channel	NLO [†]	$4.29_{-0.10}^{+0.12}$ (scale) ± 0.14 (PDF+ α_s) ± 0.10 (m_t) ± 0.01 (E_{beam})
NLO+NNLL		$4.63_{-0.18}^{+0.20}$ (scale+PDF+ α_s)	
8 TeV	t -channel	NLO [†]	$84.7_{-1.7}^{+2.6}$ (scale) ± 2.8 (PDF+ α_s) ± 0.8 (m_t) ± 0.2 (E_{beam})
		NLO+NNLL	$87.8_{-1.9}^{+3.4}$ (scale+PDF+ α_s)
		NNLO	$84.2_{-0.2}^{+0.3}$ (scale)
	tW	NLO	$18.77_{-0.82}^{+0.77}$ (scale) ± 1.70 (PDF+ α_s)
		NLO+NNLL [†]	22.37 ± 0.60 (scale) ± 1.40 (PDF+ α_s) ± 0.38 (m_t) ± 0.06 (E_{beam})
	s -channel	NLO [†]	$5.24_{-0.12}^{+0.15}$ (scale) ± 0.16 (PDF+ α_s) ± 0.12 (m_t) ± 0.01 (E_{beam})
NLO+NNLL		5.61 ± 0.22 (scale+PDF+ α_s)	

Table 1. Predicted cross-sections for single-top-quark production at $\sqrt{s} = 7$ and 8 TeV at the LHC. Uncertainties include scale and PDF+ α_s variations, except for the NNLO predictions, which only contain the scale variation. The PDF+ α_s uncertainties are evaluated according to the PDF4LHC prescription only for the NLO predictions. The uncertainties associated with the top-quark mass m_t and beam energy E_{beam} are also given for the NLO predictions for the t - and s -channels, and for the NLO+NNLL prediction for tW production. The value of m_t is set to 172.5 GeV in all predictions. The cross-sections marked with [†] are those used in the $|f_{\text{LV}}V_{tb}|$ combination.

3 Single-top-quark cross-section measurements at $\sqrt{s} = 7$ and 8 TeV

The t -channel single-top-quark production cross-sections, $\sigma_{t\text{-chan.}}$, were measured by the ATLAS and CMS Collaborations at $\sqrt{s} = 7$ TeV [59, 60] and 8 TeV [32, 33]. Evidence of tW production was reported at $\sqrt{s} = 7$ TeV by ATLAS [61] and CMS [62], while at $\sqrt{s} = 8$ TeV its cross-section, σ_{tW} , was measured by both experiments [34, 35]. Evidence of s -channel production was reported by ATLAS, with a measured cross-section, $\sigma_{s\text{-chan.}}$, at $\sqrt{s} = 8$ TeV [37], whereas CMS set upper limits on the s -channel production cross-section at $\sqrt{s} = 7$ and 8 TeV. The observed (expected) significance of the CMS measurement at $\sqrt{s} = 8$ TeV is 2.3 (0.8) standard deviations [63].

The ATLAS and CMS analyses use similar approaches to measure the single-top-quark production cross-sections. Both experiments select events containing at least one prompt isolated lepton (electron or muon) and at least one high- p_T jet. The analyses use various multivariate analysis (MVA) techniques, such as boosted decision trees [64–66], neural networks [67], or the matrix element method (MEM) [68, 69], to separate the signal from background. To measure the cross-section, analyses perform a binned maximum-likelihood fit to data using the distribution of the corresponding MVA discriminator. Exceptions are the ATLAS s -channel and CMS t -channel measurements at $\sqrt{s} = 8$ TeV. In the ATLAS s -channel analysis, the fit is performed simultaneously to the MEM discriminant

		ATLAS		CMS	
\sqrt{s}	Process	σ [pb]	Lumi. [fb^{-1}]	σ [pb]	Lumi. [fb^{-1}]
7 TeV	t -channel	68 ± 8	4.59	67.2 ± 6.1	1.17–1.56
	tW	16.8 ± 5.7	2.05	16^{+5}_{-4}	4.9
	s -channel	—	—	7.1 ± 8.1	5.1
8 TeV	t -channel	$89.6^{+7.1}_{-6.3}$	20.2	83.6 ± 7.8	19.7
	tW	$23.0^{+3.6}_{-3.9}$	20.3	23.4 ± 5.4	12.2
	s -channel	$4.8^{+1.8}_{-1.5}$	20.3	13.4 ± 7.3	19.7

Table 2. Summary of the single-top-quark cross-section measurements published by the ATLAS and CMS Collaborations at $\sqrt{s} = 7$ and 8 TeV. Total uncertainties are shown. Small differences between the integrated luminosity values in different analyses within the same experiment and centre-of-mass energy are due to different luminosity calibrations at the time of publication.

in the signal region and the lepton-charge distribution in the W +jets control region. The CMS t -channel measurement at $\sqrt{s} = 8$ TeV is based on a simultaneous fit to the absolute pseudorapidity (η) distributions of the recoiling light-flavour jet in events with negative and with positive lepton charge. The analyses measuring different single-top-quark production modes within the same experiment and at the same centre-of-mass energy have disjoint signal regions. Both experiments simulate the single-top-quark processes using the NLO POWHEG-BOX generator [70–74] for the matrix-element (ME) calculations. ATLAS also uses the POWHEG-BOX generator to simulate top-quark-pair background events, while CMS uses the LO MADGRAPH generator [75]. The PYTHIA [76] event generator is used for modelling the parton shower (PS), hadronisation and the underlying event in both the single-top-quark and $t\bar{t}$ processes. The cross-sections are measured assuming a value of 172.5 GeV for m_t for all top-quark processes and all centre-of-mass energies. A summary of the uncertainties in each measurement is shown in table 2, with details given in appendix A.

4 Combination methodology

The ATLAS and CMS single-top-quark production cross-section measurements shown in table 2 are combined, and the combined $|f_{LV}V_{tb}|$ value determined, using the best linear unbiased estimator (BLUE) method [77–79]. The BLUE method is applied iteratively in order to reduce a possible bias arising from the dependence of systematic uncertainties on the central value of the cross-section [80]. Convergence is reached when the central value changes by less than 0.01% compared with the previous iteration. In each iteration, the BLUE method minimises the global χ^2 by adjusting the weight for each input measurement [79]. The global χ^2 is calculated taking correlations into account. The sum of weights is required to be equal to one. Negative weights are allowed; these indicate strong correlations [81]. The number of degrees of freedom is $n - 1$, where n is number of measurements in the combination. The χ^2 and n are then used to calculate a corresponding probability [79].

The systematic uncertainties are scaled with the cross-section in each iteration, i.e. they are treated as relative uncertainties. The data and simulation statistical uncertainties are not scaled [80]. The systematic uncertainties in the s -channel cross-section combination are also not scaled because the s -channel measurements have large backgrounds.

Following the same strategy as in the input measurements by the ATLAS and CMS Collaborations, the combined cross-sections are reported at $m_t = 172.5$ GeV, not including the uncertainty associated with the m_t variation. The shift in the combined cross-section due to a variation of ± 1 GeV in the top-quark mass is given where this information is available. For the determination of the combined $|f_{LV}V_{tb}|$ value, the uncertainty in the measured cross-sections due to a variation of ± 1 GeV in the mass is considered. Uncertainties in the measurements are symmetrised, before combination, by averaging the magnitude of the downward and upward variations. More details are given in sections 5 and 6.

5 Systematic uncertainties and correlation assumptions

In order to combine single-top-quark cross-section measurements and $|f_{LV}V_{tb}|$ values, the sources of uncertainty are grouped into categories. While the categorisation and evaluation of uncertainties varies somewhat between experiments and between measurements, each individual measurement considers a complete set of uncertainties. Assumptions are made about correlations between similar sources of uncertainty in different measurements, as explained in section 5.1. Uncertainties associated with theoretical predictions are taken into account in the $|f_{LV}V_{tb}|$ combination. The correlations between similar uncertainties in different theoretical predictions are discussed in section 5.2.

5.1 Systematic uncertainties in measured cross-sections

Systematic uncertainties in the ATLAS t -channel measurements at $\sqrt{s} = 7$ and 8 TeV are evaluated using pseudoexperiments, except the background normalisation uncertainties, which are constrained in the fit to data. In the ATLAS tW measurements at $\sqrt{s} = 7$ and 8 TeV and the s -channel measurement at $\sqrt{s} = 8$ TeV, systematic uncertainties are included as nuisance parameters in profile-likelihood fits. Systematic uncertainties in the CMS t -channel and tW measurements at $\sqrt{s} = 7$ and 8 TeV are included as nuisance parameters in fits to data, except the theory modelling uncertainties in signal and backgrounds, described below, which are evaluated using pseudoexperiments. All systematic uncertainties in the CMS s -channel measurements at $\sqrt{s} = 7$ and 8 TeV are obtained through pseudoexperiments, except the background normalisation uncertainties, which are constrained in the fit to data. In the analyses where systematic uncertainties are included as nuisance parameters, the total uncertainty presented in table 2 is evaluated by varying all the nuisance parameters in the fit simultaneously. To extract the impact of each source of this type of uncertainty, these analyses use approximate procedures which neglect the correlations between sources of uncertainty introduced by the fits. Throughout this paper, individual uncertainties are taken as reported by the input analyses, regardless of the method used to determine them. The total uncertainties are evaluated as the sum in quadrature of individual contributions.

Although the sources of systematic uncertainty and the procedures used to estimate their impact on the measured cross-section are partially different in the individual analyses, it is still possible to identify contributions that describe similar physical effects. These contributions are listed below; they are grouped together, and only the resulting categories are used in the combination. Categories are treated as uncorrelated among each other. For each source of uncertainty, correlations between different measurements are assumed to be positive, unless explicitly mentioned otherwise. The stability of the cross-section and $|f_{LV}V_{tb}|$ combinations is studied by varying the correlation assumptions for the dominant uncertainties, as discussed in section 7.2.

The uncertainties in each category are listed below, with the correlation assumptions across experiments given in parentheses. These correlations correspond to those used in the cross-section combinations. They are also valid for the combination of the $|f_{LV}V_{tb}|$ extractions, unless explicitly mentioned otherwise. The symbol “—” means that the uncertainty is either considered only in the ATLAS or the CMS measurement, or is not considered at all. A summary of uncertainties in the cross-section measurements together with the corresponding correlation assumptions between experiments is provided in appendix A.

Data statistical (Correlation 0): this statistical uncertainty arises from the limited size of the data sample. It is uncorrelated between ATLAS and CMS, between production modes, and between centre-of-mass energies.

Simulation statistical (Correlation 0 and — for CMS tW at $\sqrt{s} = 7$ TeV and s -channel at $\sqrt{s} = 8$ TeV): this statistical uncertainty comes from the limited size of simulated event samples. It is uncorrelated between ATLAS and CMS, between production modes, and between centre-of-mass energies. For the CMS tW analysis at $\sqrt{s} = 7$ TeV and s -channel analysis at $\sqrt{s} = 8$ TeV, this uncertainty is evaluated as part of the total statistical uncertainty, which is also considered uncorrelated, as discussed above. More details are given in appendices A.2 and A.3.

Integrated luminosity (Correlation 0.3): this uncertainty originates from the systematic uncertainty in the integrated luminosity, as determined by the individual experiments using the methods described in refs. [82–85]. It affects the determination of both the signal and background yields. The integrated-luminosity uncertainty has a component that is correlated between ATLAS and CMS, arising from imperfect knowledge of the beam currents during van der Meer scans in the LHC accelerator [86], and an uncorrelated component from the long-term luminosity monitoring that is experiment-specific. At $\sqrt{s} = 7$ TeV, these components are 0.5% and 1.7% respectively for ATLAS and 0.5% and 2.1% respectively for CMS. At $\sqrt{s} = 8$ TeV, they are 0.6% and 1.8% respectively for ATLAS and 0.7% and 2.5% respectively for CMS. At both centre-of-mass energies, the correlation coefficient between the integrated-luminosity uncertainty in ATLAS and CMS at the same centre-of-mass energy is $\rho = 0.3$. Within the same experiment, the integrated-luminosity uncertainty is assumed to be correlated between production modes and uncorrelated between centre-of-mass energies. In section 7.2, it is shown that the combined $|f_{LV}V_{tb}|^2$ result does not depend significantly on the correlation assumptions.

Theory modelling: this category contains the uncertainties in the modelling of the simulated single-top-quark processes, as well as smaller contributions from the modelling of the $t\bar{t}$ and W +jets background processes. Both signal and background modelling are included because the uncertainties in all top-quark processes are closely related. These include initial- and final-state radiation (ISR/FSR), renormalisation and factorisation scales, NLO matching method, PS and hadronisation modelling, and PDF uncertainties. For the tW process, the uncertainty due to the treatment of interference between tW and $t\bar{t}$ final states is also included, as discussed below. These modelling uncertainties in signal and background processes are summed in quadrature in each input measurement.

- *Scales and radiation modelling* (Correlation 1)

The renormalisation and factorisation scales and ISR/FSR uncertainties account for missing higher-order corrections in the perturbative expansion and the amount of initial- and final-state radiation in simulated signal and background processes. In the ATLAS measurements of all three production modes, these uncertainties are estimated using dedicated single-top-quark and $t\bar{t}$ simulated event samples, by consistently varying the renormalisation and factorisation scales and the amount of ISR/FSR in accordance with a measurement of additional jet activity in $t\bar{t}$ events at $\sqrt{s} = 7$ TeV [87, 88]. In the ATLAS t -channel measurements, they are also estimated in W +jets simulated event samples, by varying the scale and matching parameters in the ALPGEN LO multileg generator [89] at $\sqrt{s} = 7$ TeV and by varying the parameters controlling the scale in the SHERPA LO multileg generator [90] at $\sqrt{s} = 8$ TeV. In the CMS measurements, these uncertainties are estimated by varying the renormalisation and factorisation scales, and ISR/FSR, consistently in the simulated event samples. In the CMS t -channel measurement at $\sqrt{s} = 8$ TeV, this uncertainty applies only to the signal modelling since the modelling of the dominant $t\bar{t}$ and W +jets background processes is obtained from data. However, for the t -channel analysis at $\sqrt{s} = 7$ TeV, the scales are varied in the simulated signal, $t\bar{t}$, W +jets and other single-top-quark processes. The same approach is followed in the CMS s -channel measurements at both centre-of-mass energies. The tW cross-section measurements of CMS account for this uncertainty only in the tW signal and $t\bar{t}$ background, given the negligible contributions from the W +jets and other single-top-quark processes in the dilepton final state.

Although the methods are apparently different, they mostly address the same uncertainty, hence this uncertainty is considered correlated between ATLAS and CMS. It is also considered correlated between production modes and centre-of-mass energies. The combined $|f_{LV}V_{tb}|$ result does not depend significantly on this correlation assumption, as discussed in section 7.2.

- *NLO matching* (Correlation 1 for t -channel and — for tW and s -channel)

The ATLAS measurements include an uncertainty to account for different NLO matching methods implemented in different NLO event generators. This is evaluated in single-top-quark and $t\bar{t}$ simulations by comparing the POWHEG-BOX,

MC@NLO [91, 92], and MADGRAPH5_aMC@NLO [93] event generators, all interfaced to HERWIG [94] (with JIMMY [95] for the underlying-event modelling). In the CMS t -channel measurement at $\sqrt{s} = 7$ TeV, the NLO matching uncertainty is evaluated by comparing POWHEG-BOX with CompHEP [96, 97]. In the CMS t -channel analysis at $\sqrt{s} = 8$ TeV, this uncertainty accounts for different NLO matching methods in the t -channel signal event generator, as well as for differences between event generation in the 4FS and 5FS, by comparing POWHEG-BOX with MADGRAPH. The NLO matching uncertainty is considered correlated between ATLAS and CMS, between production modes, and between centre-of-mass energies. In the CMS tW and s -channel analyses at $\sqrt{s} = 7$ and 8 TeV, this uncertainty is not considered, since the modelling uncertainties in the scheme to remove overlap with $t\bar{t}$ are dominant in the tW analysis and the renormalisation/factorisation scale is dominant in the s -channel analysis. The results of the stability test for this uncertainty are shown in section 7.2.

- *Parton shower and hadronisation* (Correlation 1)

In both experiments, the difference between the PYTHIA and HERWIG showering programs is considered in the jet energy scale (JES) [98–101] and b -tagging calibration [102–106]. The ATLAS analyses additionally include an uncertainty in the PS and hadronisation modelling in simulated single-top-quark and $t\bar{t}$ events, evaluated by comparing the POWHEG-BOX event generator interfaced to PYTHIA or to HERWIG. The CMS analyses additionally include an uncertainty in the $t\bar{t}$ and W +jets backgrounds estimated with the MADGRAPH event generator interfaced to PYTHIA. It is evaluated in simulated event samples where the value of the ME/PS matching threshold in the MLM method [107] is doubled or halved from its initial value. The CMS t -channel measurement at $\sqrt{s} = 8$ TeV does not consider this uncertainty in the $t\bar{t}$ and W +jets backgrounds since the distribution and normalisation of the $t\bar{t}$ and W +jets processes are derived mostly from data. In the CMS tW analyses at $\sqrt{s} = 7$ and 8 TeV, the contributions of the W +jets and other single-top-quark processes in the dilepton final state are negligible.

This uncertainty is considered correlated between ATLAS and CMS, between different production modes, and between different centre-of-mass energies. The combined $|f_{LV}V_{tb}|$ result does not depend significantly on this correlation assumption, as shown in section 7.2.

- *Parton distribution functions* (Correlation 1)

The PDF uncertainty is evaluated following the PDF4LHC procedures [42, 108, 109] and is considered correlated between ATLAS and CMS, between different production modes, and between different centre-of-mass energies.

- *tW and $t\bar{t}$ interference* (Correlation 1 for tW and — for t - and s -channels)

The tW process interferes with $t\bar{t}$ production at NLO [110–112]. In both ATLAS and CMS, two simulation approaches are compared: diagram removal (DR) [110] and diagram subtraction (DS) [27, 110]. In the DR approach, all NLO diagrams that overlap

with the doubly resonant $t\bar{t}$ contributions are removed from the calculation of the tW amplitude. This approach accounts for the interference term, but it is not gauge invariant (though the effect is numerically negligible) [110]. In the DS approach, a subtraction term is built into the amplitude to cancel out the $t\bar{t}$ component close to the top-quark resonance while respecting gauge invariance.

The DR approach is the default, and the comparison with the DS approach is used to assess this systematic uncertainty. For the tW analyses, this uncertainty is considered correlated between the two experiments and between different centre-of-mass energies.

- *Modelling of the top-quark p_T spectrum* (Correlation —)

In the CMS tW and s -channel analyses at $\sqrt{s} = 8$ TeV, the simulated $t\bar{t}$ events are reweighted to correct the p_T spectrum of the generated top quarks, which was found to be significantly harder than the spectrum observed in data in differential cross-section measurements [113, 114]. To estimate the uncertainty related to this mismodelling, the tW measurement is repeated without the reweighting, and the change relative to the default result is taken as the uncertainty. In the CMS s -channel analysis, the measurement is repeated with the effect of the weights removed and doubled. The resulting variation in the cross-section is symmetrised. This uncertainty is not considered in the CMS t -channel measurement at $\sqrt{s} = 8$ TeV where the modelling of the $t\bar{t}$ background is extracted from data. In the ATLAS measurements, modelling uncertainties in the top-quark p_T spectrum in $t\bar{t}$ events [115] are covered by the PS and hadronisation uncertainty and they are found to be small in comparison with other systematic uncertainties. This uncertainty is considered correlated between the CMS tW and s -channel analyses at $\sqrt{s} = 8$ TeV.

- *Dependence on the top-quark mass* (Correlation 1)

The measured single-top-quark cross-sections shown in table 2 assume a nominal m_t value of 172.5 GeV. The dependence of the measured cross-section on m_t is estimated for the ATLAS t -channel measurements at $\sqrt{s} = 7$ and 8 TeV and for the ATLAS tW measurement at $\sqrt{s} = 8$ TeV. It is determined using dedicated simulations of single-top-quark and $t\bar{t}$ samples with different m_t values. The cross-section measurements assuming the different m_t values are interpolated using a first- or a second-order polynomial, for which the constant term is given by the central value of $m_t = 172.5$ GeV. The CMS measurements at $\sqrt{s} = 8$ TeV provide information for a variation of ± 2 GeV in the top-quark mass, which is scaled to a ± 1 GeV shift assuming a linear dependence. For the CMS t -channel and tW measurements at $\sqrt{s} = 8$ TeV, the changes in cross-sections are symmetrised and reported as uncertainties. In the CMS s -channel analysis, the change in the cross-section is determined for the up and down variation of m_t . No estimates are available for the CMS t -channel analysis at $\sqrt{s} = 7$ TeV, the ATLAS and CMS tW analyses at $\sqrt{s} = 7$ TeV or the ATLAS s -channel analysis at $\sqrt{s} = 8$ TeV. The top-quark-mass uncertainty is small

for each measurement, thus the impact of not evaluating it for these measurements is negligible.

In this paper, a symmetrised uncertainty in the measured cross-section due to a variation of ± 1 GeV in the top-quark mass is considered. When the full cross-section dependence on the top-quark mass is available for a given production mode at a given centre-of-mass energy, the sign of the dependence of the uncertainty per unit of mass is taken into account in the correlations. In the case of the CMS t -channel and tW measurements at $\sqrt{s} = 8$ TeV, where the sign of the dependence is not available, it is assumed that the sign is the same as for the ATLAS measurement, since the phase space and background composition are comparable between CMS and ATLAS. Given that the uncertainty in the measured cross-section is considered for the same m_t variation and considering the sign of the dependence when available, this uncertainty is considered correlated between ATLAS and CMS and between different centre-of-mass energies and uncorrelated between the t -channel and tW production modes.

Background normalisation (Correlation 0): three background uncertainties are considered: in top-quark background ($t\bar{t}$ and other single-top-quark processes), in other background determined from simulation (W/Z +jets, diboson, and other smaller background channels), and in background estimated from data (multijet background from misidentified and non-prompt leptons). The exceptions are the t -channel measurements at $\sqrt{s} = 7$ TeV, where the background from simulation includes top-quark background, as shown in tables 9–13 in appendix A. The normalisation of the main background processes is determined from data, either by inclusion of normalisation uncertainties as nuisance parameters in the fit used to extract the signal, or through dedicated techniques based on data. In the t -channel and s -channel measurements, the uncertainties in the theoretical cross-section predictions for the top-quark, W/Z +jets, and diboson processes are included. In the tW measurements, the uncertainties in the theoretical cross-section predictions for the top-quark and diboson processes are taken into account. In the ATLAS measurements of the t -channel process at $\sqrt{s} = 7$ and 8 TeV, the uncertainty in the multijet background is estimated by comparing background estimates made using different techniques based on simulation and data samples. In the ATLAS tW analyses at $\sqrt{s} = 7$ and 8 TeV, the normalisation uncertainty in the background from misidentified and non-prompt leptons is obtained from variations in the data-based estimate. In the ATLAS s -channel analysis, the uncertainty assigned to the normalisation of the multijet background is based on control samples. For all CMS measurements, background normalisations are constrained in the fits to data. In the CMS measurements of the t -channel and s -channel processes, the uncertainties in the multijet background are assessed by comparing the results of alternative background estimation methods based on data. Hence, the associated uncertainties are considered uncorrelated between ATLAS and CMS, between different production modes, and between different centre-of-mass energies.

Jets: in the analyses, the uncertainties related to the reconstruction and energy calibration of jets are propagated through variations in the modelling of the detector response.

These uncertainties, classified in categories as JES, jet identification (JetID), and jet energy resolution (JER), are discussed below.

- *Jet energy scale* (Correlation 0 and — for JES flavour)

The JES is derived using information from data and simulation. Its uncertainty increases with increasing $|\eta|$ and decreases with increasing p_T of the reconstructed jet.

For all of the ATLAS measurements, except the tW measurement at $\sqrt{s} = 7$ TeV, the JES uncertainty is split into components originating from the jet calibration procedure; most of them are derived from in situ techniques based on data [98, 99]. These components are categorised as modelling, detector, calibration method, and statistical components, which are grouped into the “JES common” uncertainty, as well as a flavour-dependence component (“JES flavour”), which accounts for the flavour composition of the jets and the calorimeter response to jets of different flavours. The modelling of additional pp collisions in each bunch-crossing (pile-up) is considered separately, as discussed below. The η -dependent component is dominant for the t -channel production mode. Thus, the JES common uncertainty is considered uncorrelated between the t -channel and the other single-top-quark production modes. For the tW analysis at $\sqrt{s} = 8$ TeV, the modelling component, which is constrained in the fit to data, is dominant. The uncertainty in the flavour composition of the jets is dominant for the s -channel.

For the CMS measurements, sources contributing to the JES uncertainty are combined together into the “JES common” uncertainty, and the effect is propagated to the cross-section measurements through η - and p_T -dependent JES uncertainties [100, 101]. The jet energy corrections and their corresponding uncertainties are extracted from data. The JES uncertainty is estimated from its effect on the normalisation and shape of the discriminant in each analysis. The JES uncertainty is considered uncorrelated between the t -channel and the other single-top-quark production modes because it is dominated by the forward jet in the t -channel.

The correlation between the JES common uncertainty (or the JES uncertainty for the tW measurement at $\sqrt{s} = 7$ TeV) in ATLAS and the JES uncertainty in CMS follows the prescription in refs. [116, 117], with the slight differences for the t -channel described above. The JES common (or JES) uncertainty is considered uncorrelated between ATLAS and CMS, between centre-of-mass energies, and between production modes. Within the ATLAS experiment, the JES common uncertainty is considered correlated between tW and s -channel and uncorrelated between t -channel and the other production modes. For the ATLAS t -channel analyses, a correlation of 0.75 is assumed between $\sqrt{s} = 7$ and 8 TeV, since these analyses are mainly affected by the same uncertainty components. This correlation value is estimated by comparing variations of the JES uncertainty components in these two measurements.

In all CMS measurements and in the ATLAS tW measurement at $\sqrt{s} = 7$ TeV, the JES uncertainty is not split and therefore the JES flavour uncertainty is included in the overall JES uncertainty. For the ATLAS measurements where this component

is available, the JES flavour uncertainty is considered correlated between different production modes and uncorrelated between centre-of-mass energies.

The JES uncertainty is one of the dominant contributions in most of the single-top-quark measurements. To ensure the robustness of the results against the correlation assumptions for this large uncertainty, the combination is performed with alternative correlation values, as discussed in section 7.2.

- *Jet identification* (Correlation —)

In the ATLAS measurements, the JetID uncertainty includes the jet and vertex reconstruction efficiency uncertainties. In the CMS measurements, this uncertainty is included in the JES uncertainty. For ATLAS, it is considered correlated between the different production modes at the same centre-of-mass energy and uncorrelated for the other cases.

- *Jet energy resolution* (Correlation 0)

The uncertainty in the JER, which is not split into components, is extracted from data. Generally, the JER uncertainty is propagated via a nuisance parameter in the signal extraction fit, except for the ATLAS t -channel measurements at $\sqrt{s} = 7$ and 8 TeV, and the CMS s -channel measurement, where this uncertainty is determined using pseudoexperiments. The JER uncertainty is considered uncorrelated between ATLAS and CMS, and between centre-of-mass energies. It is considered correlated between different production modes.

Detector modelling: this category includes the uncertainty in the modelling of leptons, magnitude of the missing transverse momentum (E_T^{miss}), and identification of jets from b -quarks (b -tagging).

- *Lepton modelling* (Correlation 0)

The lepton modelling uncertainty includes components associated with the lepton energy scale and resolution, reconstruction and trigger efficiencies. This uncertainty is considered uncorrelated between ATLAS [118–121] and CMS [122] and between different centre-of-mass energies, since it is determined from data. It is considered correlated between different production modes.

- *Hadronic part of the high-level trigger* (Correlation —)

In the CMS t -channel cross-section measurement at $\sqrt{s} = 7$ TeV, the high-level trigger (HLT) criteria for the electron channel are based on the presence of an electron together with a b -tagged jet. In this analysis, the uncertainty in the modelling of the hadronic part of the HLT requirement is determined from data. This uncertainty is only evaluated in this one measurement.

- E_T^{miss} modelling (Correlation 0)

The ATLAS measurements include separate components for the uncertainties in the energy scale and resolution of the E_T^{miss} [123]. The CMS measurements account for a

combined E_T^{miss} scale and resolution uncertainty [100, 124], arising from the jet-energy uncertainties. Additionally, CMS accounts for an uncertainty in E_T^{miss} arising from energy deposits in the detector that are not included in the reconstruction of leptons, photons, and jets. The E_T^{miss} uncertainty is considered uncorrelated between ATLAS and CMS, and between different centre-of-mass energies. It is considered correlated between production modes, except for the ATLAS and CMS tW analyses at $\sqrt{s} = 8$ TeV, where it is considered uncorrelated with the other production modes because the E_T^{miss} uncertainty is constrained in the fit to data. In the ATLAS tW analysis at $\sqrt{s} = 7$ TeV, this uncertainty is included in the pile-up modelling uncertainty.

- *b-tagging* (Correlation 0)

In the ATLAS analyses, b -tagging modelling uncertainties are split into components associated with b -quark, c -quark, and light-flavour quark and gluon jets [102–104]. They are evaluated by varying the p_T -dependence (η -dependence in the case of light-flavour jets) of the flavour-dependent scale factors applied to each jet in simulation within a range that reflects the systematic uncertainty in the measured tagging efficiency and misidentification rates. This uncertainty is not considered in the ATLAS tW analysis at $\sqrt{s} = 7$ TeV because no b -tagging criterion is applied in the event selection. In the CMS measurements, the uncertainties in b -tagging efficiency and misidentification rates of jets initiated by light-flavour quarks and gluons are derived from data, using control samples [105, 106]. The CMS uncertainties are propagated to the cross-section measurements using pseudoexperiments. Exceptions are the t -channel measurement at $\sqrt{s} = 7$ TeV and the tW measurement at $\sqrt{s} = 8$ TeV, where these uncertainties are constrained in the fit to data.

The two collaborations split up the different sources of systematic uncertainties related to b -tagging in a different way. However, the different sources are combined by adding their contributions in quadrature to obtain a single b -tagging uncertainty per analysis. This means that the b -tagging uncertainty also contains the uncertainties associated with the misidentification rates of jets initiated by charm quarks, light-flavour quarks and gluons. The resulting uncertainty is considered uncorrelated between ATLAS and CMS, and between different centre-of-mass energies. It is considered correlated between different production modes.

- *Pile-up modelling* (Correlation 0)

In both ATLAS and CMS, simulated events are reweighted to match the distribution of the average number of interactions per bunch-crossing in data. The corresponding uncertainty is obtained from in situ techniques based on data and simulated event samples. In the ATLAS analyses at $\sqrt{s} = 7$ TeV, the uncertainty due to pile-up is derived from the impact of the reweighting on E_T^{miss} . In the ATLAS analyses at $\sqrt{s} = 8$ TeV, this uncertainty is evaluated as a component of the JES, separated into four terms (number of primary vertices, average number of collisions per bunch-crossing, average pile-up energy density in the calorimeter, and p_T dependence) since the pile-up calibration (assuming average conditions during 8 TeV data-taking) is

applied to both data and simulation before selecting and calibrating the jets [117]. In CMS, the reweighting uses a model with a free parameter that can be interpreted as an effective cross-section for inelastic pp interactions. This uncertainty is obtained from a fit to the number of additional primary vertices in simulation. In the CMS analyses, this uncertainty is introduced as a nuisance parameter in the fit. The only exception is the s -channel measurement, where the pile-up uncertainty is estimated from pseudoexperiments. In all cases, the effects of pile-up on the jet energy and the isolation of leptons are taken into account in the jet and lepton uncertainties respectively. The pile-up uncertainty is considered uncorrelated between ATLAS and CMS and between different centre-of-mass energies. It is considered correlated between different production modes [116, 117].

5.2 Systematic uncertainties in theoretical cross-section predictions

The systematic uncertainties in the combined $|f_{LV}V_{tb}|$ value are evaluated from uncertainties in the individual cross-section measurements $\sigma_{\text{meas.}}$ and the theoretical predictions $\sigma_{\text{theo.}}$. The uncertainties associated with $\sigma_{\text{theo.}}$ are discussed in section 2; they are summarised in table 1. The correlation assumptions for the systematic uncertainties related to the theoretical cross-section are explained below. In section 7.2, the stability of the $|f_{LV}V_{tb}|$ combination against variations in the correlations is examined. For clarity, the correlations are given in parentheses next to the systematic-uncertainty name. These correlations are used in the combination of the $|f_{LV}V_{tb}|$ extractions.

PDF+ α_s (Correlation 1 for centre-of-mass energies and 0.5 for production modes): the PDF uncertainty is considered correlated between centre-of-mass energies and 50% correlated between production modes, since different production modes have one initial-state particle in common (a quark or a gluon), but not both.

Renormalisation and factorisation scales (Correlation 1 for t -channel and s -channel and 0 for tW): the renormalisation and factorisation scale uncertainties in $\sigma_{\text{theo.}}$ are considered correlated between production modes and centre-of-mass energies, except between the tW production mode and the other production modes, where they are considered uncorrelated because the tW prediction is computed at a different order in perturbation theory.

Top-quark mass (Correlation 1): the uncertainty due to m_t is evaluated by varying m_t from its central value of 172.5 GeV by ± 1 GeV and evaluating the corresponding change in cross-section using the parameterisation given in ref. [56], as discussed in section 2. This uncertainty is considered correlated between centre-of-mass energies and production modes.

E_{beam} (Correlation 1): the uncertainty in the cross-section due to the uncertainty in E_{beam} is estimated by computing the cross-section variation corresponding to a ± 1 standard deviation shift in the beam-energy uncertainty. It is considered correlated between centre-of-mass energies and production modes.

6 Combinations of cross-section measurements

The cross-section measurements described in section 3 are combined at each centre-of-mass energy for each production mode. Systematic uncertainties are categorised and correlation assumptions are employed according to section 5. The combinations are performed using the iterative BLUE method, as described in section 4.

As discussed in section 4, the uncertainty in the measured cross-section associated with the m_t variation is not considered in the combination of cross-sections. However, the shift in the combined cross-section resulting from a variation of ± 1 GeV in the top-quark mass is provided where this information is available. This is calculated by repeating the combination with the up-shifted and down-shifted input cross-sections. In measurements where only the magnitude of the shift is available for one experiment, the sign of the shift is assumed to be the same for both experiments, as discussed in section 5.1. If the uncertainty associated with the m_t variation is not available for one or both of the input measurements, then no shift in the combined cross-section is given.

Additional information about the uncertainties considered in the combination of cross-section measurements is provided in appendix A.

6.1 Combinations of t -channel cross-section measurements

The combination of the ATLAS and CMS t -channel cross-section measurements at $\sqrt{s} = 7$ TeV [59, 60] results, after one iteration, in

$$\sigma_{t\text{-chan.}} = 67.5 \pm 2.4 \text{ (stat.)} \pm 5.0 \text{ (syst.)} \pm 1.1 \text{ (lumi.) pb} = 67.5 \pm 5.7 \text{ pb.}$$

The relative uncertainty is 8.4%, which improves on the uncertainty of 9.1% in the most precise individual measurement from CMS [60]. The χ^2 for the combination is 0.01, corresponding to a probability of 93%. The CMS weight in the combination is 0.58, while the ATLAS weight is 0.42. The overall correlation between the two measurements is 20%. The contribution from each uncertainty category to the total uncertainty in the combined t -channel cross-section measurement at $\sqrt{s} = 7$ TeV is shown in table 3(a).

The combination of the ATLAS and CMS t -channel cross-section measurements at $\sqrt{s} = 8$ TeV [32, 33] results, after two iterations, in a cross-section of

$$\sigma_{t\text{-chan.}} = 87.7 \pm 1.1 \text{ (stat.)} \pm 5.5 \text{ (syst.)} \pm 1.5 \text{ (lumi.) pb} = 87.7 \pm 5.8 \text{ pb.}$$

The relative uncertainty is 6.7%, which improves on the uncertainty of 7.5% in the most precise individual measurement from ATLAS [32]. The χ^2 for the combination is 0.59, corresponding to a probability of 44%. This probability is lower than the probability of the combination at $\sqrt{s} = 7$ TeV because of the differences between the ATLAS and CMS measured cross-sections and their small uncertainties. The ATLAS weight in the combination is 0.68, while the CMS weight is 0.32. The overall correlation between the two measurements is 42%. This is larger than the correlation between the measurements at $\sqrt{s} = 7$ TeV because the statistical and detector uncertainties are lower, thus increasing the importance of the theory modelling uncertainty (which is correlated between the two

(a)			(b)		
$\sigma_{t\text{-chan.}}, \sqrt{s} = 7 \text{ TeV}$			$\sigma_{t\text{-chan.}}, \sqrt{s} = 8 \text{ TeV}$		
Combined cross-section	67.5 pb		Combined cross-section	87.7 pb	
Uncertainty category	Uncertainty		Uncertainty category	Uncertainty	
	[%]	[pb]		[%]	[pb]
Data statistical	3.5	2.4	Data statistical	1.3	1.1
Simulation statistical	1.4	0.9	Simulation statistical	0.6	0.5
Integrated luminosity	1.7	1.1	Integrated luminosity	1.7	1.5
Theory modelling	5.1	3.5	Theory modelling	5.3	4.7
Background normalisation	1.9	1.3	Background normalisation	1.2	1.1
Jets	3.4	2.3	Jets	2.6	2.3
Detector modelling	3.4	2.3	Detector modelling	1.8	1.6
Total syst. unc. (excl. lumi.)	7.5	5.0	Total syst. unc. (excl. lumi.)	6.3	5.5
Total syst. unc. (incl. lumi.)	7.6	5.2	Total syst. unc. (incl. lumi.)	6.5	5.7
Total uncertainty	8.4	5.7	Total uncertainty	6.7	5.8

Table 3. Contribution from each uncertainty category to the combined t -channel cross-section ($\sigma_{t\text{-chan.}}$) uncertainty at (a) $\sqrt{s} = 7 \text{ TeV}$ and (b) $\sqrt{s} = 8 \text{ TeV}$. The total uncertainty is computed by adding in quadrature all the individual systematic uncertainties (including the uncertainty in the integrated luminosity) and the statistical uncertainty in data. Correlations of systematic uncertainties between experiments are presented in appendix A.1.

experiments), as shown in appendix A.1. The contribution from each uncertainty category to the total uncertainty in the combined t -channel cross-section measurement at $\sqrt{s} = 8 \text{ TeV}$ is shown in table 3(b).

At both centre-of-mass energies, the uncertainties from theory modelling are found to be dominant. Details of the central values, the impact of individual sources of uncertainties, and their correlations between experiments at $\sqrt{s} = 7$ and 8 TeV can be found in appendix A.1.

The shift in the combined cross-section at $\sqrt{s} = 8 \text{ TeV}$ from a variation of $\pm 1 \text{ GeV}$ in the top-quark mass is $\mp 0.8 \text{ pb}$, which is similar to the shifts in the input measurements for the same m_t variation. The shift in the combined cross-section at $\sqrt{s} = 7 \text{ TeV}$ is not evaluated since no estimate is available for the CMS input measurement at $\sqrt{s} = 7 \text{ TeV}$.

6.2 Combinations of tW cross-section measurements

The combination of the ATLAS and CMS tW cross-section measurements at $\sqrt{s} = 7 \text{ TeV}$ [61, 62] yields, after two iterations, a cross-section of

$$\sigma_{tW} = 16.3 \pm 2.3 \text{ (stat.)} \pm 3.3 \text{ (syst.)} \pm 0.7 \text{ (lumi.) pb} = 16.3 \pm 4.1 \text{ pb.}$$

The relative uncertainty is 25%, which improves on the uncertainty of 28% in the most precise individual measurement from CMS [62]. The χ^2 for the combination is 0.01, corresponding to a probability of 91%. The CMS weight in the combination is 0.59, while the

(a)			(b)		
$\sigma_{tW}, \sqrt{s} = 7 \text{ TeV}$			$\sigma_{tW}, \sqrt{s} = 8 \text{ TeV}$		
Combined cross-section	16.3 pb		Combined cross-section	23.1 pb	
Uncertainty category	Uncertainty		Uncertainty category	Uncertainty	
	[%]	[pb]		[%]	[pb]
Data statistical	14.0	2.3	Data statistical	4.7	1.1
Simulation statistical	0.8	0.1	Simulation statistical	0.8	0.2
Integrated luminosity	4.4	0.7	Integrated luminosity	3.6	0.8
Theory modelling	13.9	2.3	Theory modelling	11.8	2.7
Background normalisation	6.0	1.0	Background normalisation	2.2	0.5
Jets	11.5	1.9	Jets	6.2	1.4
Detector modelling	6.2	1.0	Detector modelling	4.9	1.1
Total syst. unc. (excl. lumi.)	20.0	3.3	Total syst. unc. (excl. lumi.)	14.4	3.3
Total syst. unc. (incl. lumi.)	20.5	3.3	Total syst. unc. (incl. lumi.)	14.8	3.4
Total uncertainty	24.8	4.1	Total uncertainty	15.6	3.6

Table 4. Contribution from each uncertainty category to the combined tW cross-section (σ_{tW}) uncertainty at (a) $\sqrt{s} = 7 \text{ TeV}$ and (b) $\sqrt{s} = 8 \text{ TeV}$. The total uncertainty is computed by adding in quadrature all the individual systematic uncertainties (including the uncertainty in the integrated luminosity) and the statistical uncertainty in data. Correlations of systematic uncertainties between experiments are presented in appendix A.2.

ATLAS weight is 0.41. The overall correlation between the two measurements is 17%. The contribution from each uncertainty category to the total uncertainty in the combined tW cross-section measurement at $\sqrt{s} = 7 \text{ TeV}$ is shown in table 4(a).

The combination of the ATLAS and CMS tW cross-section measurements at $\sqrt{s} = 8 \text{ TeV}$ [34, 35] results, after two iterations, in

$$\sigma_{tW} = 23.1 \pm 1.1 \text{ (stat.)} \pm 3.3 \text{ (syst.)} \pm 0.8 \text{ (lumi.) pb} = 23.1 \pm 3.6 \text{ pb.}$$

The relative uncertainty is 15.6%, which improves on the uncertainty of 16.5% in the most precise individual measurement from ATLAS [34]. The χ^2 for the combination is 0.01, corresponding to a probability of 94%. The ATLAS weight in the combination is 0.70, while the CMS weight is 0.30. The overall correlation between the two measurements is 40%. Similar to the t -channel, this is larger than the correlation between the measurements at $\sqrt{s} = 7 \text{ TeV}$ due to the increased importance of the theory modelling uncertainties. The contribution from each uncertainty category to the total uncertainty in the combined tW cross-section measurement at $\sqrt{s} = 8 \text{ TeV}$ is shown in table 4(b).

At both centre-of-mass energies, the uncertainties in the theory modelling are found to be dominant. The jet uncertainties are also important. Details of the central values, the impact of individual sources of uncertainties, and their correlations between experiments at $\sqrt{s} = 7$ and 8 TeV are presented in appendix A.2.

$\sigma_{s\text{-chan.}}, \sqrt{s} = 8 \text{ TeV}$		
Combined cross-section	4.9 pb	
Uncertainty category	Uncertainty	
	[%]	[pb]
Data statistical	16	0.8
Simulation statistical	12	0.6
Integrated luminosity	5	0.2
Theory modelling	14	0.7
Background normalisation	8	0.4
Jets	13	0.6
Detector modelling	8	0.4
Total syst. unc. (excl. lumi.)	25	1.2
Total syst. unc. (incl. lumi.)	25	1.2
Total uncertainty	30	1.4

Table 5. Contribution from each uncertainty category to the combined s -channel cross-section ($\sigma_{s\text{-chan.}}$) uncertainty at $\sqrt{s} = 8 \text{ TeV}$. The total uncertainty is computed by adding in quadrature all the individual systematic uncertainties (including the uncertainty in the integrated luminosity) and the statistical uncertainty in data. Correlations of systematic uncertainties between experiments are presented in appendix A.3.

The shift in the combined cross-section at $\sqrt{s} = 8 \text{ TeV}$ from a variation of $\pm 1 \text{ GeV}$ in the top-quark mass is $\pm 1.1 \text{ pb}$, which is similar in magnitude to that in the input measurements for the same m_t variation. The shift in the combined cross-section at $\sqrt{s} = 7 \text{ TeV}$ is not evaluated since no estimates are available for the input measurements at $\sqrt{s} = 7 \text{ TeV}$.

6.3 Combination of s -channel cross-section measurements

The ATLAS and CMS s -channel cross-section measurements suffer from large backgrounds, and the cross-section measurements have large uncertainties. Since the systematic uncertainties mainly affect the background prediction, they are not scaled in the iterative BLUE procedure. Only the luminosity uncertainty is scaled with the central value. The combination of the ATLAS and CMS s -channel cross-section measurements at $\sqrt{s} = 8 \text{ TeV}$ [37, 63] results, after two iterations, in a cross-section of

$$\sigma_{s\text{-chan.}} = 4.9 \pm 0.8 \text{ (stat.)} \pm 1.2 \text{ (syst.)} \pm 0.2 \text{ (lumi.) pb} = 4.9 \pm 1.4 \text{ pb.}$$

The relative uncertainty is 30%, very similar to the most precise individual measurement from ATLAS [37]. The χ^2 for the combination is 1.45, corresponding to a probability of 23%. The ATLAS weight in the combination is 0.99, while the CMS weight is 0.01. The overall correlation between the two measurements is 15%. The contribution from each uncertainty category to the total uncertainty in the combined s -channel cross-section measurement at $\sqrt{s} = 8 \text{ TeV}$ is shown in table 5.

Since the ATLAS measurement has a large weight in the combination, the importance of each uncertainty in the combination is similar to that in the ATLAS measurement, as presented in appendix A.3.

The shift in the combined cross-section at $\sqrt{s} = 8$ TeV from a variation in the top-quark mass is not evaluated since no estimate is available for the ATLAS input measurement.

6.4 Summary of cross-section combinations

A summary of the cross-sections measured by ATLAS and CMS and their combinations in all single-top-quark production modes at each centre-of-mass energy is shown in figure 2. The measurements are compared with the theoretical predictions shown in table 1: NNLO for t -channel only, NLO and NLO+NNLL for all three production modes. For the NLO calculation, the renormalisation- and factorisation-scale uncertainties and the sum in quadrature of the contributions from scale, PDF, and α_s are shown separately. Only the scale uncertainty is shown for the NNLO calculation. For the NLO+NNLL calculation, the sum in quadrature of the contributions from scale, PDF, and α_s is shown. All measurements are in good agreement with their corresponding theoretical predictions within their total uncertainties.

The stability of the combinations of the cross-section measurements to variations in the correlation assumptions, discussed in section 5, is checked for the theory modelling, JES, the most important contributions to the theoretical cross-section predictions (i.e. PDF+ α_s and scale) and the integrated luminosity. The results of these tests show that their impacts on the cross-section combinations are very small, similar to the stability tests for the combination of the $|f_{LV}V_{tb}|$ values discussed in section 7.2.

7 Combinations of $|f_{LV}V_{tb}|$ determinations

The measured cross-section for a given single-top-quark production mode, $\sigma_{\text{meas.}}$, has a linear dependence on $|f_{LV}V_{tb}|^2$ as defined in eq. (1.1). Thus, a value of $|f_{LV}V_{tb}|^2$ is extracted from each cross-section measurement and the corresponding theoretical prediction (presented in sections 3 and 2 respectively). These values are then combined per channel, and in an overall $|f_{LV}V_{tb}|^2$ combination. In the overall combination, the value from the CMS measurement of $\sigma_{s\text{-chan.}}$ is excluded. The reason for excluding the CMS s -channel analysis from the overall $|f_{LV}V_{tb}|^2$ combination is that, at the same centre-of-mass energy, the CMS t -channel determination has strong correlations with the s -channel determination, which contains relatively large uncertainties. The strong correlation between these two measurements makes the combined $|f_{LV}V_{tb}|^2$ value strongly dependent on the correlation assumptions for the dominant uncertainties. This results in a large variation of the combined $|f_{LV}V_{tb}|^2$ value for different correlation assumptions.

All uncertainties in $\sigma_{\text{meas.}}$ and $\sigma_{\text{theo.}}$ are propagated to the $|f_{LV}V_{tb}|^2$ values, taking into account the correlations described in section 5. The combined value of $|f_{LV}V_{tb}|^2$ is evaluated using the reference theoretical cross-section central values marked with a † in table 1, where it can also be seen that the E_{beam} uncertainty is negligible compared to other uncertainties. For the most precise measurements (i.e. for $\sigma_{t\text{-chan.}}$ cross-section

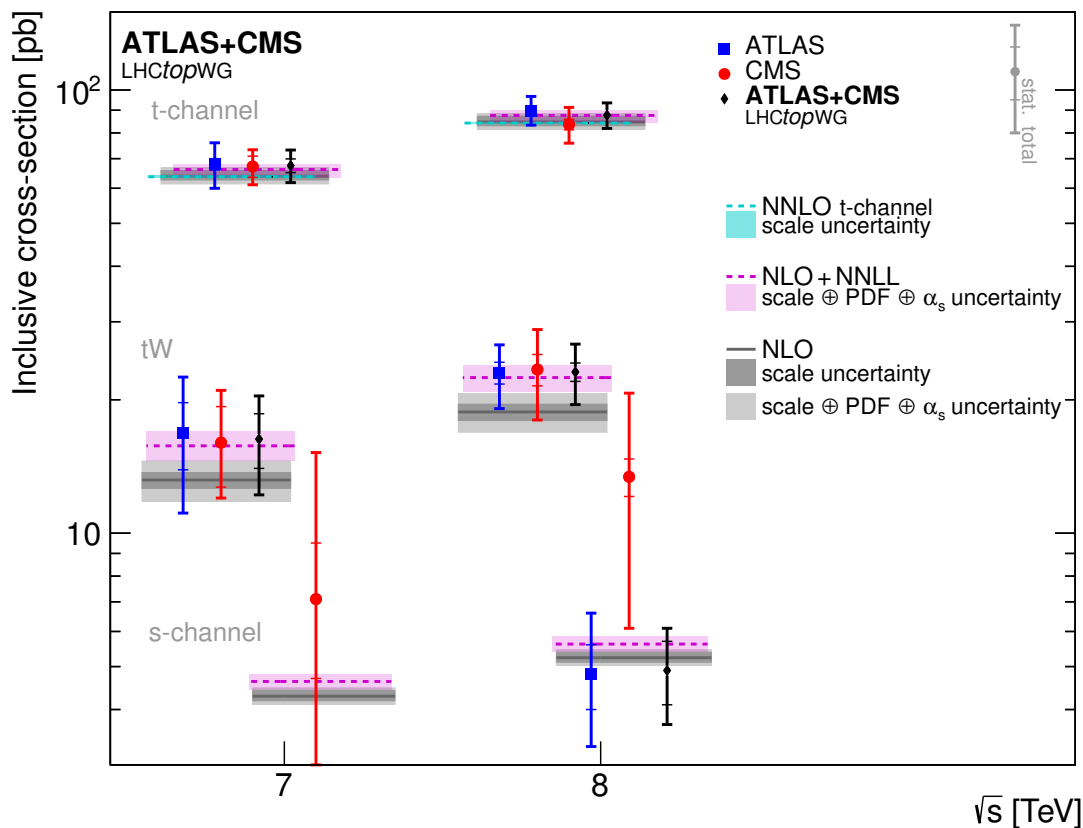


Figure 2. Single-top-quark cross-section measurements performed by ATLAS and CMS, together with the combined results shown in sections 6.1–6.3. These measurements are compared with the theoretical predictions at NLO and NLO+NNLL for all three production modes and the prediction at NNLO for t -channel only. The corresponding theoretical uncertainties are also presented. The scale uncertainty for the NNLO prediction is small and is presented as a narrow band under the dashed line.

measurements at $\sqrt{s} = 8$ TeV), which have a large expected impact on the combination, the other theoretical calculations from table 1 are used as cross-checks.

Table 6 contains a summary of the individual $|f_{LV}V_{tb}|^2$ determinations that are the inputs to the overall $|f_{LV}V_{tb}|^2$ combination, together with their experimental and theoretical uncertainties using the reference theoretical cross-sections and uncertainties. For the same processes and at the same centre-of-mass energies, there are some important differences between uncertainty categories. In analyses based on t -channel events at $\sqrt{s} = 7$ TeV, the data statistical uncertainty is larger in CMS than in ATLAS because the two experiments use data samples of different size. Differences in the category of jet uncertainties are due to the evaluation of the JES uncertainty in ATLAS using pseudoexperiments, while this uncertainty is introduced as a nuisance parameter in the fit in CMS. At $\sqrt{s} = 8$ TeV, the difference between ATLAS and CMS in the background-normalisation category is due to the different techniques used to estimate each background uncertainty. Additional details are discussed in appendix A.1. In the CMS tW analysis at $\sqrt{s} = 7$ TeV, the uncertainty

associated with the size of the simulated samples is evaluated as part of the total statistical uncertainty. The large difference in the pile-up uncertainty between ATLAS and CMS is due to the different methods used to assess this uncertainty, as discussed in section 5.1. At $\sqrt{s} = 8$ TeV, the sizes of the data and simulated samples used in the CMS tW analysis are smaller than in the ATLAS analysis, resulting in larger data and simulation statistical uncertainties. The large difference between the two experiments in the category of jet uncertainties arises because the JES uncertainty in ATLAS is evaluated in different categories mostly using pseudoexperiments, while in CMS the JES uncertainty is introduced as a nuisance parameter in the fit. Further details are discussed in appendix A.2. In the CMS s -channel analysis, the uncertainty associated with the size of the simulated samples is evaluated as part of the total statistical uncertainty. More details are discussed in appendix A.3.

7.1 Results

The combination of $|f_{LV}V_{tb}|^2$ is performed using the inputs from all three single-top-quark production modes. Using the same method, the combination of $|f_{LV}V_{tb}|^2$ is also performed separately for each production mode for comparison.

Combining the $|f_{LV}V_{tb}|^2$ values extracted from the t -channel and tW cross-section measurements at $\sqrt{s} = 7$ and 8 TeV from ATLAS and CMS, as well as the ATLAS s -channel measurement at $\sqrt{s} = 8$ TeV, results in

$$|f_{LV}V_{tb}|^2 = 1.05 \pm 0.02 \text{ (stat.)} \pm 0.06 \text{ (syst.)} \pm 0.01 \text{ (lumi.)} \pm 0.04 \text{ (theo.)} = 1.05 \pm 0.08,$$

with a relative uncertainty of 7.4%. The contribution from each experimental uncertainty category to the total uncertainty in the combined $|f_{LV}V_{tb}|^2$ value is shown in table 7. The theory modelling uncertainties in signal and background processes, discussed in section 5.1, dominate the experimental uncertainty and the total uncertainty. The theoretical cross-section uncertainty is the second-largest contribution to the total uncertainty in the combined $|f_{LV}V_{tb}|^2$ value. Changes in the combined $|f_{LV}V_{tb}|^2$ value from using alternative NNLO and NLO+NNLL theoretical predictions for the t -channel are less than 1%.

Figure 3 illustrates the correlations between the input measurements in the combination. The correlations are all below 0.6. The largest correlations are generally between the measurements in the same experiment at the same centre-of-mass energy, and for those that have large contributions from the same theory modelling components, such as the ATLAS s -channel measurement, which has a correlation of over 0.5 with each of the tW measurements.

The BLUE weights for each of the contributing measurements are shown in table 8. The t -channel measurements at $\sqrt{s} = 8$ TeV have the largest weight in the combination, followed by the t -channel measurements at $\sqrt{s} = 7$ TeV. The tW measurements have smaller cross-section uncertainties than the s -channel measurements, but, in addition to the correlation between tW and s -channel measurements, the tW measurements are also more correlated with the t -channel measurements in each experiment. The negative weights indicate the presence of large correlations between the corresponding measurement and some of the other measurements [81].

	<i>t</i> -channel ATLAS 8 TeV	<i>t</i> -channel CMS 8 TeV	<i>t</i> -channel ATLAS 7 TeV	<i>t</i> -channel CMS 7 TeV	<i>tW</i> ATLAS 8 TeV	<i>tW</i> CMS 8 TeV	<i>tW</i> ATLAS 7 TeV	<i>tW</i> CMS 7 TeV	<i>s</i> -channel ATLAS 8 TeV
$ f_{LV}V_{tb} ^2$	1.06	0.99	1.06	1.05	1.03	1.05	1.07	1.02	0.92
Uncertainties:									
Data statistical	0.01	0.03	0.03	0.06	0.06	0.09	0.18	0.21	0.15
Simulation statistical	0.01	0.01	0.02	0.02	0.01	0.03	0.02	–	0.11
Integrated luminosity	0.02	0.03	0.02	0.02	0.05	0.03	0.07	0.04	0.05
Theory modelling									
ISR/FSR, ren./fact. scale	0.04	0.02	0.03	0.04	0.09	0.13	0.05	0.03	0.06
NLO match., generator	0.03	0.05	0.02	0.04	0.03	–	0.11	–	0.10
Parton shower	0.02	–	–	0.01	0.02	0.15	0.16	0.10	0.02
PDF	0.01	0.02	0.03	0.01	0.01	0.02	0.02	0.02	0.03
DS/DR scheme	–	–	–	–	0.04	0.02	–	0.06	–
Top-quark p_T rew.	–	–	–	–	–	<0.01	–	–	–
Background normalisation									
Top-quark bkg.	<0.01	0.02	0.02	0.01	0.02	0.02	0.06	0.06	0.05
Other bkg. from sim.	0.01	<0.01	<0.01	0.03	0.02	0.03	0.09	0.04	0.05
Bkg. from data	<0.01	0.02	0.01	0.01	<0.01	–	0.02	–	0.01
Jets									
JES common	0.03	0.04	0.08	0.01	0.05	0.04	0.17	0.15	0.05
JES flavour	<0.01	–	0.02	–	0.02	–	–	–	0.01
JetID	<0.01	–	0.01	–	<0.01	–	0.05	–	0.01
JER	<0.01	0.01	0.02	<0.01	0.07	0.01	0.02	0.04	0.11
Detector modelling									
Leptons	0.02	0.01	0.03	0.04	0.03	0.02	0.07	0.05	0.02
HLT (had. part)	–	–	–	0.02	–	–	–	–	–
E_T^{miss} scale	<0.01	<0.01	0.03	<0.01	0.06	<0.01	–	0.03	0.01
E_T^{miss} res.	<0.01	–	–	–	<0.01	–	–	–	0.01
<i>b</i> -tagging	0.01	0.02	0.04	0.02	0.01	0.01	–	0.02	0.07
Pile-up	<0.01	0.01	<0.01	0.01	0.03	<0.01	0.11	0.01	0.01
Top-quark mass	0.01	<0.01	0.01	–	0.05	0.05	–	–	–
Theoretical cross-section									
PDF+ α_s	0.03	0.03	0.04	0.04	0.06	0.07	0.08	0.07	0.03
Ren./fact. scale	0.03	0.03	0.03	0.03	0.03	0.03	0.03	0.03	0.02
Top-quark mass	0.01	0.01	0.01	0.01	0.02	0.02	0.02	0.02	0.02
E_{beam}	<0.01	<0.01	<0.01	<0.01	<0.01	<0.01	<0.01	<0.01	<0.01
Total systematic uncertainty	0.09	0.09	0.13	0.10	0.18	0.23	0.34	0.24	0.24
Total uncertainty	0.09	0.10	0.13	0.12	0.19	0.24	0.38	0.32	0.28

Table 6. Results of the ATLAS and CMS individual $|f_{LV}V_{tb}|^2$ determinations that are the inputs to the overall $|f_{LV}V_{tb}|^2$ combination together with their experimental uncertainties. The values of $|f_{LV}V_{tb}|^2$ may slightly differ from those published for the different analyses since in this paper the theoretical cross-sections used are those marked with † in table 1. Experimental uncertainties contributing less than 1% are denoted by <0.01. Entries with – mean that this uncertainty was not evaluated for this analysis. Descriptions of the background categories and of the correlations of systematic uncertainties between experiments are presented in appendix A.

Combined $f_{LV}V_{tb} ^2$	1.05	
Uncertainty category	Uncertainty	
	[%]	$\Delta f_{LV}V_{tb} ^2$
Data statistical	1.8	0.02
Simulation statistical	0.9	0.01
Integrated luminosity	1.3	0.01
Theory modelling	4.5	0.05
Background normalisation	1.3	0.01
Jets	2.6	0.03
Detector modelling	1.6	0.02
Top-quark mass	0.7	0.01
Theoretical cross-section	4.3	0.04
Total syst. unc. (excl. lumi.)	7.1	0.07
Total syst. unc. (incl. lumi.)	7.2	0.08
Total uncertainty	7.4	0.08

Table 7. Contributions from each experimental and theoretical uncertainty category to the overall $|f_{LV}V_{tb}|^2$ combination. The total uncertainty is computed by adding in quadrature all of the individual systematic uncertainties (including the integrated luminosity and theoretical cross-section) and the statistical uncertainty in data.

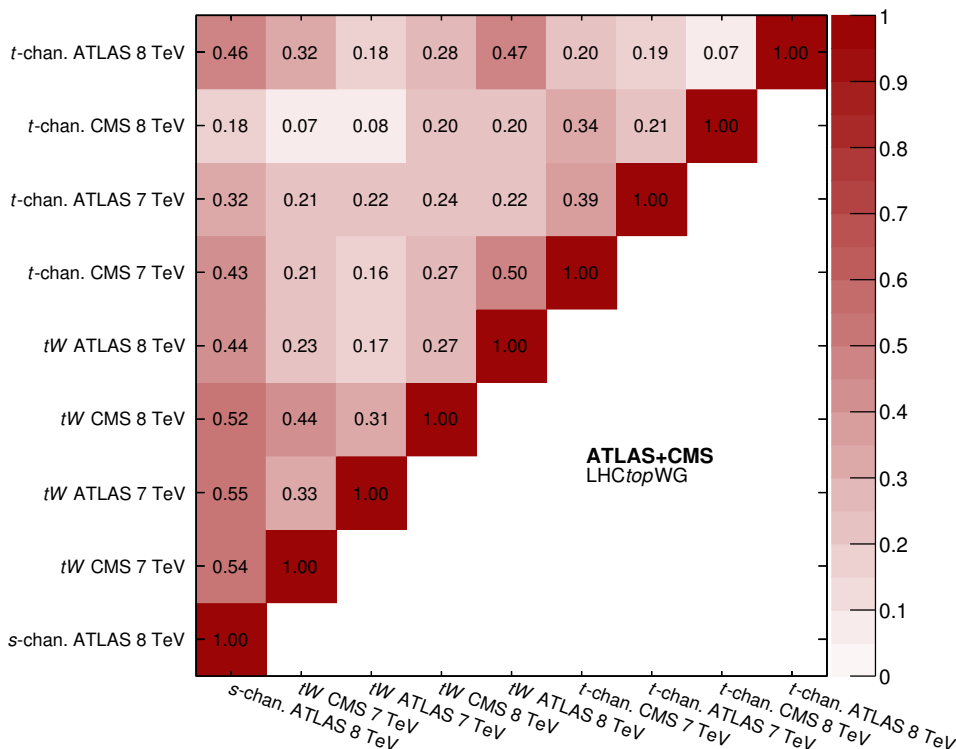


Figure 3. Correlation matrix of the overall $|f_{LV}V_{tb}|^2$ combination. Each bin corresponds to a measurement in a given production mode, experiment, and at a given centre-of-mass energy.

Process	\sqrt{s}	Experiment	BLUE weight
t -channel	8 TeV	ATLAS	0.56
		CMS	0.27
	7 TeV	ATLAS	0.07
		CMS	0.15
tW	8 TeV	ATLAS	0.05
		CMS	-0.04
	7 TeV	ATLAS	-0.02
		CMS	0.02
s -channel	8 TeV	ATLAS	-0.07

Table 8. BLUE weights for the overall $|f_{LV}V_{tb}|^2$ combination.

The combined $|f_{LV}V_{tb}|$ value from the cross-section measurements at $\sqrt{s} = 7$ and 8 TeV, including uncertainties in σ_{theo} for each production mode, is

$$\begin{aligned}
 |f_{LV}V_{tb}| &= 1.02 \pm 0.01 \text{ (stat.)} \pm 0.03 \text{ (syst.)} \pm 0.01 \text{ (lumi.)} \pm 0.02 \text{ (theo.)} \\
 &= 1.02 \pm 0.04 \text{ (meas.)} \pm 0.02 \text{ (theo.)} = 1.02 \pm 0.04,
 \end{aligned}$$

with a relative uncertainty of 3.7%, which improves on the precision of 4.7% of the most precise individual $|f_{LV}V_{tb}|$ extraction, which comes from the ATLAS t -channel analysis at $\sqrt{s} = 8$ TeV [32]. This is a 30% improvement over the Tevatron combination [30].

The $|f_{LV}V_{tb}|$ values are also combined for each production mode, combining across experiments and centre-of-mass energies. For the s -channel, the ATLAS and CMS measurements at $\sqrt{s} = 8$ TeV are combined. The results are

$$\begin{aligned}
 t\text{-channel} : |f_{LV}V_{tb}| &= 1.02 \pm 0.01 \text{ (stat.)} \pm 0.03 \text{ (syst.)} \pm 0.01 \text{ (lumi.)} \pm 0.02 \text{ (theo.)} \\
 &= 1.02 \pm 0.04 \text{ (meas.)} \pm 0.02 \text{ (theo.)} = 1.02 \pm 0.04, \\
 tW : |f_{LV}V_{tb}| &= 1.02 \pm 0.03 \text{ (stat.)} \pm 0.07 \text{ (syst.)} \pm 0.02 \text{ (lumi.)} \pm 0.04 \text{ (theo.)} \\
 &= 1.02 \pm 0.09 \text{ (meas.)} \pm 0.04 \text{ (theo.)} = 1.02 \pm 0.09, \\
 s\text{-channel} : |f_{LV}V_{tb}| &= 0.97 \pm 0.08 \text{ (stat.)} \pm 0.12 \text{ (syst.)} \pm 0.02 \text{ (lumi.)} \pm 0.02 \text{ (theo.)} \\
 &= 0.97 \pm 0.15 \text{ (meas.)} \pm 0.02 \text{ (theo.)} = 0.97 \pm 0.15.
 \end{aligned}$$

The relative uncertainties are 3.9%, 8.4% and 15.0% respectively. In all cases, these results are more precise than the best individual determinations of $|f_{LV}V_{tb}|$, which have uncertainties of 4.7%, 9.9% and 20.8% for the t -channel [32], tW [34] and s -channel [37] analyses respectively.

Figure 4 shows a summary of the $|f_{LV}V_{tb}|$ combinations. The combination is dominated by the t -channel analyses.

7.2 Stability tests

The stability of the combination of the $|f_{LV}V_{tb}|^2$ values to variations in the correlation assumptions, discussed in section 5, is checked for the dominant uncertainty contributions.

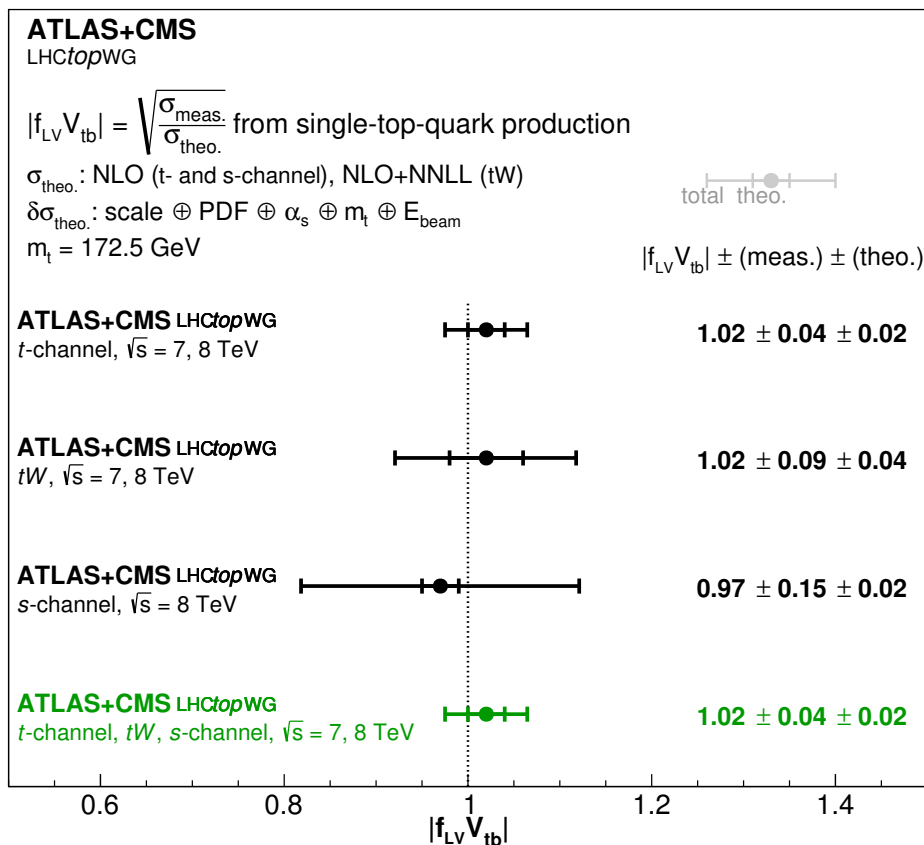


Figure 4. The combined $|f_{LV}V_{tb}|$ value extracted from the t -channel and tW cross-section measurements at $\sqrt{s} = 7$ and 8 TeV from ATLAS and CMS, as well as the ATLAS s -channel measurement at $\sqrt{s} = 8$ TeV, is shown together with the combined $|f_{LV}V_{tb}|$ values for each production mode. The theoretical predictions for t -channel and s -channel production are computed at NLO accuracy, while the theoretical predictions for tW are calculated at NLO+NNLL accuracy. The $\sigma_{\text{theo.}}$ uncertainties used to compute $|f_{LV}V_{tb}|$ include scale, PDF+ α_s , m_t , and E_{beam} variations.

The correlation values are varied for the theory modelling, JES, and the most important contributions to the theoretical cross-section predictions (i.e. PDF+ α_s and scale). Because of the scheme that is used for the correlations, stability tests are also performed for the uncertainties associated with the integrated luminosity. Figure 5 summarises the results of these stability tests, where the correlations between ATLAS and CMS (and also between centre-of-mass energies for the integrated luminosity) are varied.

The uncertainties in the theory modelling category (i.e. scales and radiation modelling, NLO matching, and PS and hadronisation) are varied from their default value of fully correlated to half correlated and to the more extreme tests of uncorrelated and half anti-correlated. The JES category is varied from its default value of uncorrelated to half correlated and half anti-correlated and the more extreme variation of fully correlated. The theoretical cross-section uncertainties, PDF+ α_s and scale, are varied from their default values of fully correlated to half correlated, uncorrelated and half anti-correlated. For the integrated luminosity, the correlation between ATLAS and CMS is varied from its default

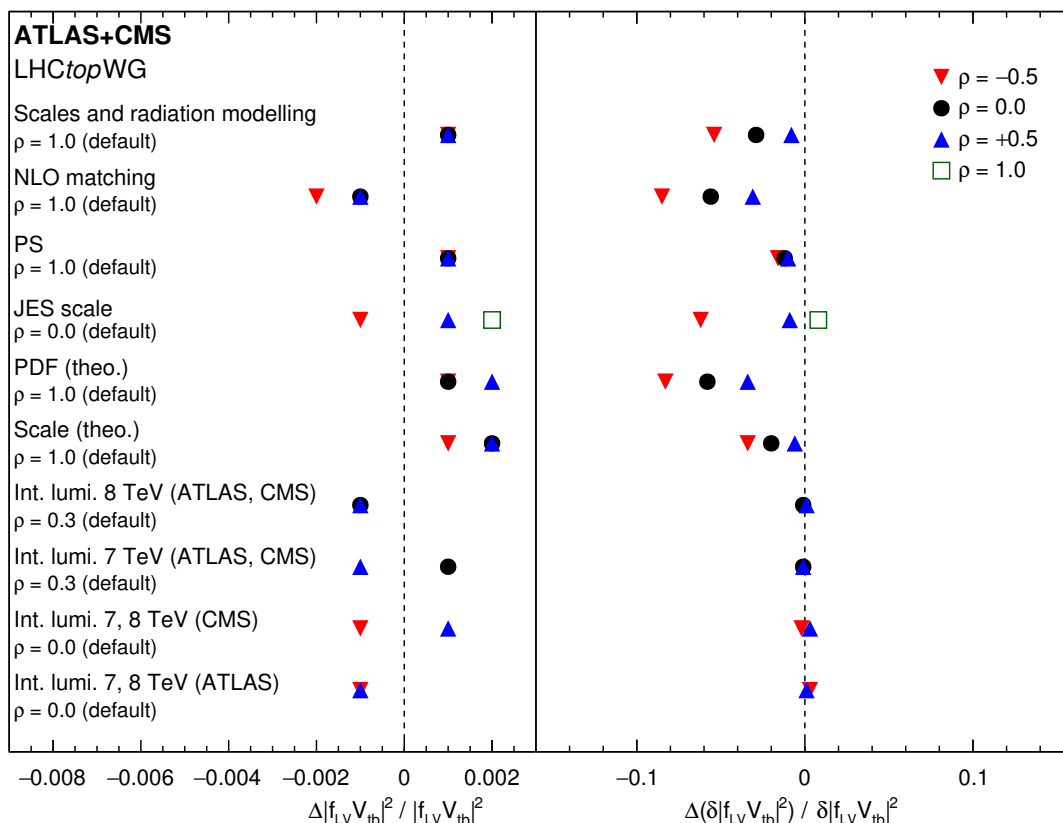


Figure 5. Results of the stability tests performed by varying of the correlation assumptions in different uncertainty categories: theory modelling (scales and radiation modelling, NLO matching, and PS and hadronisation), JES, dominant theoretical cross-section predictions (i.e. PDF+ α_s and scale) and integrated luminosity. Two or three variations are considered depending on the uncertainty category. The corresponding relative shifts (with shift = varied – nominal) in the central value, $\Delta|f_{LV}V_{tb}|^2/|f_{LV}V_{tb}|^2$, and in its uncertainty, $\Delta(\delta|f_{LV}V_{tb}|^2)/(\delta|f_{LV}V_{tb}|^2)$, are shown.

value of 30% correlated to half correlated and uncorrelated. The correlation between different centre-of-mass energies for each experiment is varied from the default of uncorrelated to half and fully correlated. The correlation of the theoretical scale uncertainty between different processes is also tested. For all variations, the relative changes in the central value of the combined $|f_{LV}V_{tb}|$ are significantly smaller ($<0.5\%$) than the relative total uncertainty of 3.7%. Additionally, the relative changes in the total uncertainty are below 0.004, i.e., less than 10% of the total uncertainty of 0.04. These tests show that the result of the combination is robust and does not critically depend on any of the correlation assumptions. The cross-section combinations similarly do not depend significantly on any of the correlation assumptions.

8 Summary

The combinations of single-top-quark production cross-section measurements in the t -channel, tW , and s -channel production modes are presented, using data from LHC pp

collisions collected by the ATLAS and CMS Collaborations. The combinations for each production mode are performed at $\sqrt{s} = 7$ and 8 TeV, using data corresponding to integrated luminosities of 1.17 to 5.1 fb $^{-1}$ at $\sqrt{s} = 7$ TeV, and of 12.2 to 20.3 fb $^{-1}$ at $\sqrt{s} = 8$ TeV. The combined t -channel cross-sections are found to be 67.5 ± 5.7 pb and 87.7 ± 5.8 pb at $\sqrt{s} = 7$ and 8 TeV respectively. The values of the combined tW cross-sections at $\sqrt{s} = 7$ and 8 TeV are 16.3 ± 4.1 pb and 23.1 ± 3.6 pb respectively. For the s -channel cross-section, the combination yields 4.9 ± 1.4 pb at $\sqrt{s} = 8$ TeV. The square of the magnitude of the CKM matrix element V_{tb} multiplied by a form factor accounting for possible contributions from physics beyond the SM, f_{LV} , is determined from each production mode at each centre-of-mass energy, using the ratio of the measured cross-section to its theoretical prediction, and assuming that the top-quark-related CKM matrix elements obey the relation $|V_{td}|, |V_{ts}| \ll |V_{tb}|$. The values of $|f_{LV}V_{tb}|^2$ extracted from individual ratios at $\sqrt{s} = 7$ and 8 TeV yield a combined value of $|f_{LV}V_{tb}| = 1.02 \pm 0.04$ (meas.) ± 0.02 (theo.). All combined measurements are consistent with their corresponding SM predictions.

A Systematic uncertainties in cross-section measurements

The single-top-quark cross-sections measured by the ATLAS and CMS Collaborations at $\sqrt{s} = 7$ and 8 TeV, as well as the uncertainties and their correlations between experiments, are summarised in tables 9–13 for the t -channel, tW , and s -channel production modes. Similar to the approach that is followed in combinations using the BLUE method, the total uncertainty in these tables is evaluated as the sum in quadrature of the individual uncertainties. To obtain the impact of each source of uncertainty, the input analyses use either pseudoexperiments or approximate procedures which neglect the correlations between sources of uncertainty introduced by the fit to data. In the latter case, this may lead to small changes in the total uncertainty compared with the input measurements presented in table 2. The likelihood fit includes all nuisance parameters at the same time to evaluate the total uncertainty. The method used by each input analysis to evaluate the individual uncertainties is described below.

A.1 Systematic uncertainties in t -channel cross-section measurements

The t -channel cross-sections measured by the ATLAS and CMS Collaborations at $\sqrt{s} = 7$ TeV [59, 60] and $\sqrt{s} = 8$ TeV [32, 33], as well as the uncertainties and their correlations between experiments, are shown in tables 9 and 10 respectively. The total uncertainty given for each measurement is the sum in quadrature of the individual uncertainties. This is slightly different from the total uncertainty shown in table 2 for the CMS measurements at $\sqrt{s} = 7$ and 8 TeV since the total uncertainty is evaluated, through the fit, by varying all nuisance parameters at the same time.

In table 9, the CMS result at $\sqrt{s} = 7$ TeV has a larger data statistical uncertainty than the ATLAS result because the two experiments use data samples of different size (see table 2). In the background-normalisation category, the “Bkg. from MC” uncertainty refers to the tW , s -channel, $t\bar{t}$, W/Z +jets, and diboson backgrounds. In the ATLAS measurement, the normalisation uncertainty in the multijet background is estimated by comparing

	ATLAS ($\sigma_{t\text{-chan.}}, \sqrt{s} = 7\text{TeV}$)		CMS ($\sigma_{t\text{-chan.}}, \sqrt{s} = 7\text{TeV}$)		
Cross-section	68.0 pb		67.2 pb		
Uncertainty category	Uncertainty		Uncertainty		ρ
Data statistical		2.7%		5.8%	0.0
Simulation statistical		1.9%		1.9%	0.0
Integrated luminosity		1.8%		2.2%	0.3
Theory modelling	Ren./fact. scales, ISR/FSR	2.6%	Ren./fact. scales	3.5%	1.0
	NLO match., PS ($t\bar{t}$, t -chan.)	2.2%	Sig. modelling (NLO method)	4.3%	1.0
			Parton shower	0.8%	1.0
	PDF	3.2%	PDF	1.4%	1.0
Category subtotal		4.7%		5.8%	0.85
Background norm.	Bkg. from MC: norm.	1.6%	Bkg. from MC: norm.	2.7%	0.0
	Bkg. from MC/data: multijet norm.	1.4%	Bkg. from data: multijet norm.	1.3%	0.0
Category subtotal		2.1%		3.0%	0.0
Jets	JES common	7.6%	JES	0.9%	0.0
	JES flavour	1.8%			0.0
	JetID	1.1%			0.0
	JER	1.9%	JER	0.3%	0.0
Category subtotal		8.1%		0.9%	0.0
Detector modelling	Lepton modelling	2.8%	Lepton modelling	3.5%	0.0
			HLT (had. part)	1.5%	0.0
	E_T^{miss} modelling	2.6%	E_T^{miss} modelling	0.1%	0.0
	b -tagging	3.9%	b -tagging	2.2%	0.0
	Pile-up	0.2%	Pile-up	0.6%	0.0
Category subtotal		5.5%		4.4%	0.0
Total uncertainty		11.7%		10.2%	0.20

Table 9. Measured cross-sections, uncertainty components, their magnitudes (relative to the individual measurements) and the correlation (ρ) between the ATLAS and CMS $\sigma_{t\text{-chan.}}$ measurements at $\sqrt{s} = 7$ TeV. Uncertainties in the same row can be compared between experiments, as detailed in the text. The naming conventions follow those of the corresponding experiments.

background estimates made using different techniques based on data and simulation samples, while in the CMS measurement, it is estimated from the difference between alternative methods based on data. There is also a large difference between the two experiments in the jets category. As discussed in section 5.1, the uncertainty in each JES component in the ATLAS measurement is evaluated using pseudoexperiments. The CMS measurement is a BLUE combination of three different measurements, two of which introduce JES components as a nuisance parameter in the fit. Since these fits use additional control regions, the impact of the JES is reduced. In addition, the JES uncertainty in the analyses at $\sqrt{s} = 7$ TeV is smaller for CMS [100] than for ATLAS [99].

In the analyses at $\sqrt{s} = 8$ TeV, summarised in table 10, the difference between ATLAS and CMS in the background normalisation category is due to the different techniques used to estimate each background uncertainty. The “Other bkg. from MC” uncertainty includes the contributions from the tW , s -channel, $t\bar{t}$, W/Z +jets, and diboson backgrounds in the ATLAS analysis, and the tW , s -channel, Z +jets, and diboson backgrounds in the CMS analysis. In the ATLAS measurement, the normalisation uncertainties associated with the

	ATLAS ($\sigma_{t\text{-chan.}}, \sqrt{s} = 8 \text{ TeV}$)		CMS ($\sigma_{t\text{-chan.}}, \sqrt{s} = 8 \text{ TeV}$)		
Cross-section	89.6 pb		83.6 pb		
Uncertainty category	Uncertainty		Uncertainty		ρ
Data statistical		1.4%		2.7%	0.0
Simulation statistical		0.8%		0.7%	0.0
Integrated luminosity		1.9%		2.6%	0.3
Theory modelling	Ren./fact. scales	3.6%	Ren./fact. scales	1.9%	1.0
	NLO match.	3.3%	NLO match., 4FS vs 5FS	4.9%	1.0
	Parton shower	2.1%			1.0
	PDF	1.3%	PDF	1.9%	1.0
Category subtotal	5.5%		5.6%		0.84
Background norm.	$t\bar{t}$, tW and s -chan. norm.	0.1%	$t\bar{t}$ and W +jets norm.	2.2%	0.0
	Other bkg. from MC: norm.	0.9%	Other bkg. from MC: norm.	0.3%	0.0
	Bkg. from MC/data: multijet norm.	0.3%	Bkg. from data: multijet norm.	2.3%	0.0
Category subtotal	1.0%		3.2%		0.0
Jets	JES common	3.2%	JES	4.2%	0.0
	JES flavour	0.2%			0.0
	JetID	0.1%			0.0
	JER	0.4%	JER	0.7%	0.0
Category subtotal	3.2%		4.3%		0.0
Detector modelling	Lepton modelling	1.9%	Lepton modelling	0.6%	0.0
	E_T^{miss} scale	0.4%	E_T^{miss} modelling	0.3%	0.0
	E_T^{miss} resolution	0.2%			0.0
	b -tagging	1.1%	b -tagging	2.5%	0.0
	Pile-up	0.3%	Pile-up	0.7%	0.0
Category subtotal	2.3%		2.7%		0.0
Total uncertainty	7.3%		9.0%		0.42

Table 10. Measured cross-sections, uncertainty components, their magnitudes (relative to the individual measurements) and the correlation (ρ) between the ATLAS and CMS $\sigma_{t\text{-chan.}}$ measurements at $\sqrt{s} = 8 \text{ TeV}$. Uncertainties in the same row can be compared between experiments, as detailed in the text. The naming conventions follow those of the corresponding experiments.

top-quark, W/Z +jets, diboson, and multijet backgrounds are estimated using pseudoexperiments. Variations in the theoretical cross-section predictions for these processes are also considered, except for the multijet background, where the results obtained from data and simulation samples analysed with various techniques are compared. In the CMS measurement, the uncertainty in the multijet background is estimated from the difference between alternative methods based on data. The normalisations of the $t\bar{t}$ and W +jets backgrounds are included as nuisance parameters in the fit, while the shapes of their distributions are adjusted by corrections based on data in control regions.

A.2 Systematic uncertainties in tW cross-section measurements

The tW cross-sections measured by the ATLAS and CMS Collaborations at $\sqrt{s} = 7 \text{ TeV}$ [61, 62] and $\sqrt{s} = 8 \text{ TeV}$ [34, 35], as well as the uncertainties and their correlations between experiments, are shown in tables 11 and 12 respectively.

In table 11, the CMS measurement at $\sqrt{s} = 7 \text{ TeV}$ takes into account the uncertainty associated with the size of the simulated event samples using the Barlow-Beeston

	ATLAS (σ_{tW} , $\sqrt{s} = 7\text{TeV}$)		CMS (σ_{tW} , $\sqrt{s} = 7\text{TeV}$)		
Cross-section	16.8 pb		16.0 pb		
Uncertainty category	Uncertainty		Uncertainty		ρ
Data statistical		17.0%		20.8%	0.0
Simulation statistical		2.0%		0.0%	0.0
Integrated luminosity		7.0%		4.3%	0.3
Theory modelling	ISR/FSR, scales	5.0%	ISR/FSR, scales	2.8%	1.0
	$tW/t\bar{t}$ NLO match.	10.0%			1.0
	$tW/t\bar{t}$ PS	15.0%	tW ME/PS match. thr.	10.1%	1.0
	PDF	2.0%	PDF	2.1%	1.0
			DR/DS scheme	5.9%	1.0
Category subtotal	18.8%		12.2%		0.74
Background norm.	$t\bar{t}$ norm.	6.0%	$t\bar{t}$ norm.	6.0%	0.0
	Z +jets, diboson norm.	8.0%	Z/γ^* +jets norm.	4.2%	0.0
	Bkg. from data: fake lept. norm.	2.0%			0.0
Category subtotal	10.2%		7.3%		0.0
Jets	JES	16.0%	JES	15.1%	0.0
	JetID	5.0%			0.0
	JER	2.0%	JER	3.6%	0.0
Category subtotal	16.9%		15.6%		0.0
Detector modelling	Lepton modelling	7.0%	Lepton modelling	5.2%	0.0
			E_T^{miss} modelling	2.5%	0.0
			b -tagging	1.9%	0.0
	Pile-up	10.0%	Pile-up	1.5%	0.0
Category subtotal	12.2%		6.2%		0.0
Total uncertainty	35.1%		30.6%		0.17

Table 11. Measured cross-sections, uncertainty components, their magnitudes (relative to the individual measurements) and the correlation (ρ) between the ATLAS and CMS σ_{tW} measurements at $\sqrt{s} = 7\text{ TeV}$. Uncertainties in the same row can be compared between experiments, as detailed in the text. The naming conventions follow those of the corresponding experiments.

method [125]. This contribution is included as part of the total statistical uncertainty. This uncertainty is therefore considered to be zero for the CMS measurement to avoid double-counting. Since the statistical uncertainties in the data and simulation are uncorrelated between the two experiments, this choice has almost no effect on the combination. In the ATLAS analysis, the normalisation uncertainty in the misidentified lepton (fake lept.) background is conservatively taken to be 100%, based on comparisons in data. The E_T^{miss} uncertainties are included in the pile-up modelling uncertainty. The b -tagging uncertainty is not considered because no b -tagging criterion is required in the event selection. The large difference in the pile-up uncertainty between ATLAS and CMS arises from different methods employed by the experiments to assess this uncertainty, as discussed in section 5.1.

In table 12, the tW measurement by CMS at $\sqrt{s} = 8\text{ TeV}$ is based on the first half of the $\sqrt{s} = 8\text{ TeV}$ data sample. This leads to a larger data statistical uncertainty for CMS than for ATLAS. For the same reason, the sizes of the simulated event samples are smaller, resulting in a larger simulation statistical uncertainty in the CMS result. In the ATLAS measurement, the normalisation uncertainty in the multijet background is estimated by comparing estimates made using different techniques on data and simulation

	ATLAS (σ_{tW} , $\sqrt{s} = 8$ TeV)		CMS (σ_{tW} , $\sqrt{s} = 8$ TeV)		
Cross-section	23.0 pb		23.4 pb		
Uncertainty category	Uncertainty		Uncertainty		ρ
Data statistical		5.8%		8.1%	0.0
Simulation statistical		0.5%		2.4%	0.0
Integrated luminosity		4.6%		3.0%	0.3
Theory modelling	ISR/FSR	8.8%	Ren./fact. scales	12.4%	1.0
	NLO match.	2.5%			1.0
	Parton shower	1.7%	Parton shower	14.1%	1.0
	PDF	0.6%	PDF	1.7%	1.0
	$tW/t\bar{t}$ overlap	3.5%	tW DR/DS scheme	2.1%	1.0
			Top-quark p_T reweight.	0.4%	0.0
Category subtotal	10.0%		19.0%		0.75
Background norm.	$t\bar{t}$ norm.	1.9%	$t\bar{t}$ norm.	1.7%	0.0
	Z +jets, diboson norm.	2.0%	Z +jets norm.	2.6%	0.0
	Bkg. from data: fake lept. norm.	0.3%			0.0
Category subtotal	2.8%		3.1%		0.0
Jets	JES common	5.3%	JES	3.8%	0.0
	JES flavour	1.9%			0.0
	JetID	0.2%			0.0
	JER	6.5%	JER	0.9%	0.0
Category subtotal	8.6%		3.9%		0.0
Detector modelling	Lepton modelling	3.0%	Lepton modelling	1.8%	0.0
	E_T^{miss} scale	5.5%	E_T^{miss} modelling	0.4%	0.0
	E_T^{miss} resolution	0.2%			0.0
	b -tagging	1.0%	b -tagging	0.9%	0.0
	Pile-up	2.7%	Pile-up	0.4%	0.0
Category subtotal	6.9%		2.0%		0.0
Total uncertainty	16.8%		21.7%		0.40

Table 12. Measured cross-sections, uncertainty components, their magnitudes (relative to the individual measurements) and the correlation (ρ) between the ATLAS and CMS σ_{tW} measurements at $\sqrt{s} = 8$ TeV. Uncertainties in the same row can be compared between experiments, as detailed in the text. The naming conventions follow those of the corresponding experiments.

samples, while in the CMS measurement, the uncertainty contribution of the multijet background is estimated from the difference between alternative methods based on data. In the ATLAS analysis, the misidentified lepton and non-prompt (fake lept.) background has a normalisation uncertainty of 60%, based on comparisons in data, to account for possible mismodelling of the jet multiplicity and jet acceptance. There is a large difference between the two experiments in the jets category. As discussed in section 5.1, the JES uncertainty in the ATLAS measurement is evaluated in different categories. The detector modelling component of the JES common uncertainty is constrained in the fit to data. In the CMS measurement, different components of the JES uncertainty are grouped together, and the group is introduced as a nuisance parameter in the fit. The E_T^{miss} modelling uncertainty is smaller for the CMS measurement due to the use of low- p_T jets, which allows this uncertainty to be constrained in the fit to data, as discussed in section 5.1.

	ATLAS ($\sigma_{s\text{-chan.}}, \sqrt{s} = 8 \text{ TeV}$)		CMS ($\sigma_{s\text{-chan.}}, \sqrt{s} = 8 \text{ TeV}$)		
Cross-section	4.8 pb		13.4 pb		
Uncertainty category	Uncertainty		Uncertainty		ρ
Data statistical		16.0%		10.0%	0.0
Simulation statistical		12.0%		0.0%	0.0
Integrated luminosity		5.0%		4.0%	0.3
Theory modelling	Ren./fact. scales	7.0%	Ren./fact. scales	30.0%	1.0
	$t\bar{t}$, t -chan. generator	11.0%			1.0
	Parton shower	2.0%	Parton shower	7.0%	1.0
	PDF	3.0%	PDF	7.0%	1.0
			Top-quark p_T reweight.	6.0%	0.0
Category subtotal	13.5%		32.2%		0.56
Background norm.	t -chan., $t\bar{t}$ norm.	5.0%	t -chan., $t\bar{t}$ norm.	12.0%	0.0
	W/Z +jets, diboson norm.	6.0%	W/Z +jets, diboson norm.	12.0%	0.0
	Bkg. from data: multijet norm.	1.0%	Bkg. from data: multijet norm.	2.0%	0.0
Category subtotal	7.9%		17.1%		0.0
Jets	JES common	5.0%	JES	32.5%	0.0
	JES flavour	1.0%			0.0
	JetID	1.0%			0.0
	JER	12.0%	JER	10.2%	0.0
Category subtotal	13.1%		34.1%		0.0
Detector modelling	Lepton modelling	2.4%	Lepton modelling	1.0%	0.0
	E_T^{miss} scale	1.0%	E_T^{miss} modelling	6.0%	0.0
	E_T^{miss} res	1.0%			0.0
	b -tagging	8.0%	b -tagging	14.0%	0.0
	Pile-up	1.0%	Pile-up	9.0%	0.0
Category subtotal	8.5%		17.7%		0.0
Total uncertainty	30.2%		54.0%		0.15

Table 13. Measured cross-sections, uncertainty components, their magnitudes (relative to the individual measurements) and the correlation (ρ) between the ATLAS and CMS $\sigma_{s\text{-chan.}}$ measurements at $\sqrt{s} = 8 \text{ TeV}$. Uncertainties in the same row can be compared between experiments, as detailed in the text. The naming conventions follow those of the corresponding experiments.

A.3 Systematic uncertainties in s -channel cross-section measurements

The s -channel cross-sections measured by the ATLAS and CMS Collaborations at $\sqrt{s} = 8 \text{ TeV}$ [37, 63], as well as the uncertainties and their correlations between experiments, are shown in table 13.

The CMS measurement takes into account the uncertainty associated with the size of the simulated event samples using the Barlow-Beeston method [125]. The contribution is included in the total statistical uncertainty. This uncertainty is therefore considered to be zero for the CMS measurement to avoid double-counting. Since the statistical uncertainties in the data and simulation are uncorrelated between the two experiments, this choice has almost no effect on the combination. The result from ATLAS has smaller uncertainties. This is attributed to the use of the latest simulation samples with tuned parameters [126] as well as the use of the matrix element method in the ATLAS analysis. In addition, all systematic uncertainties are profiled in the ATLAS analysis, while in the CMS analysis, major

uncertainties, including those from jets and in the theory modelling category, are excluded from the fit and evaluated using pseudoexperiments. The total uncertainties in table 13 are slightly different from the uncertainties shown in table 2 because here the uncertainties are summed in quadrature, while in the input analyses the impacts of at least some of the uncertainties are included in the fits to data. In particular, the difference between the relative total uncertainty shown in table 2 for the ATLAS measurement, i.e. 34.4%, and the relative total uncertainty shown in table 13 is due to the usage of an approximate procedure to compute the individual uncertainty contributions. Possible correlation terms between the systematic uncertainties introduced by the fit are not included here.

Acknowledgments

We thank CERN for the very successful operation of the LHC, as well as the support staff from our institutions without whom ATLAS and CMS could not be operated efficiently. We acknowledge the support of ANPCyT, Argentina; YerPhI, Armenia; ARC, Australia; BMFWF and FWF, Austria; ANAS, Azerbaijan; SSTC, Belarus; CNPq and FAPESP, Brazil; NSERC, NRC and CFI, Canada; CERN; CONICYT, Chile; CAS, MOST and NSFC, China; COLCIENCIAS, Colombia; MSMT CR, MPO CR and VSC CR, Czech Republic; D NRF and DNSRC, Denmark; IN2P3-CNRS, CEA-DRF/IRFU, France; SRNSFG, Georgia; BMBF, HGF, and MPG, Germany; GSRT, Greece; RGC, Hong Kong SAR, China; ISF and Benozziyo Center, Israel; INFN, Italy; MEXT and JSPS, Japan; CNRST, Morocco; NWO, Netherlands; RCN, Norway; MNiSW and NCN, Poland; FCT, Portugal; MNE/IFA, Romania; MES of Russia and NRC KI, Russian Federation; JINR; MESTD, Serbia; MSSR, Slovakia; ARRS and MIZŠ, Slovenia; DST/NRF, South Africa; MINECO, Spain; SRC and Wallenberg Foundation, Sweden; SERI, SNSF and Cantons of Bern and Geneva, Switzerland; MOST, Taiwan; TAEK, Turkey; STFC, United Kingdom; DOE and NSF, United States of America. In addition, individual groups and members have received support from BCKDF, CANARIE, CRC and Compute Canada, Canada; COST, ERC, ERDF, Horizon 2020, and Marie Skłodowska-Curie Actions, European Union; Investissements d’Avenir Labex and IDEX, ANR, France; DFG and AvH Foundation, Germany; Herakleitos, Thales and Aristeia programmes co-financed by EU-ESF and the Greek NSRF, Greece; BSF-NSF and GIF, Israel; CERCA Programme Generalitat de Catalunya, Spain; The Royal Society and Leverhulme Trust, United Kingdom. We acknowledge the enduring support for the construction and operation of the LHC and the CMS detector provided by the following funding agencies: BMBWF and FWF (Austria); FNRS and FWO (Belgium); CNPq, CAPES, FAPERJ, FAPERGS, and FAPESP (Brazil); MES (Bulgaria); CERN; CAS, MoST, and NSFC (China); COLCIENCIAS (Colombia); MSES and CSF (Croatia); RPF (Cyprus); SENESCYT (Ecuador); MoER, ERC IUT, and ERDF (Estonia); Academy of Finland, MEC, and HIP (Finland); CEA and CNRS/IN2P3 (France); BMBF, DFG, and HGF (Germany); GSRT (Greece); NKFI (Hungary); DAE and DST (India); IPM (Iran); SFI (Ireland); INFN (Italy); MSIP and NRF (Republic of Korea); MES (Latvia); LAS (Lithuania); MOE and UM (Malaysia); BUAP, CINVESTAV, CONACYT, LNS, SEP, and UASLP-FAI (Mexico); MOS (Montenegro); MBIE (New Zealand); PAEC (Pakistan);

MSHE and NSC (Poland); FCT (Portugal); JINR (Dubna); MON, RosAtom, RAS, RFBR, and NRC KI (Russia); MESTD (Serbia); SEIDI, CPAN, PCTI, and FEDER (Spain); MOSTR (Sri Lanka); Swiss Funding Agencies (Switzerland); MST (Taipei); ThEPCenter, IPST, STAR, and NSTDA (Thailand); TUBITAK and TAEK (Turkey); NASU and SFFR (Ukraine); STFC (United Kingdom); DOE and NSF (U.S.A.).

Individuals have received support from the Marie-Curie programme and the European Research Council and Horizon 2020 Grant, contract No. 675440 (European Union); the Leventis Foundation; the A.P. Sloan Foundation; the Alexander von Humboldt Foundation; the Belgian Federal Science Policy Office; the Fonds pour la Formation à la Recherche dans l’Industrie et dans l’Agriculture (FRIA-Belgium); the Agentschap voor Innovatie door Wetenschap en Technologie (IWT-Belgium); the F.R.S.-FNRS and FWO (Belgium) under the “Excellence of Science — EOS” — be.h project n. 30820817; the Beijing Municipal Science & Technology Commission, No. Z181100004218003; the Ministry of Education, Youth and Sports (MEYS) of the Czech Republic; the Lendület (“Momentum”) Programme and the János Bolyai Research Scholarship of the Hungarian Academy of Sciences, the New National Excellence Program ÚNKP, the NKFIA research grants 123842, 123959, 124845, 124850, and 125105 (Hungary); the Council of Science and Industrial Research, India; the HOMING PLUS programme of the Foundation for Polish Science, cofinanced from European Union, Regional Development Fund, the Mobility Plus programme of the Ministry of Science and Higher Education, the National Science Center (Poland), contracts Harmonia 2014/14/M/ST2/00428, Opus 2014/13/B/ST2/02543, 2014/15/B/ST2/03998, and 2015/19/B/ST2/02861, Sonata-bis 2012/07/E/ST2/01406; the National Priorities Research Program by Qatar National Research Fund; the Programa Estatal de Fomento de la Investigación Científica y Técnica de Excelencia María de Maeztu, grant MDM-2015-0509 and the Programa Severo Ochoa del Principado de Asturias; the Thalís and Aristeia programmes cofinanced by EU-ESF and the Greek NSRF; the Rachadapisek Sompot Fund for Postdoctoral Fellowship, Chulalongkorn University and the Chulalongkorn Academic into Its 2nd Century Project Advancement Project (Thailand); the Welch Foundation, contract C-1845; and the Weston Havens Foundation (U.S.A.).

In addition, we gratefully acknowledge the computing centres and personnel of the Worldwide LHC Computing Grid for delivering so effectively the computing infrastructure essential to our analyses. In particular, the support from CERN, the ATLAS Tier-1 facilities at TRIUMF (Canada), NDGF (Denmark, Norway, Sweden), CC-IN2P3 (France), KIT/GridKA (Germany), INFN-CNAF (Italy), NL-T1 (Netherlands), PIC (Spain), ASGC (Taiwan), RAL (U.K.) and BNL (U.S.A.), the Tier-2 facilities worldwide and large non-WLCG resource providers is acknowledged gratefully. Major contributors of ATLAS computing resources are listed in ref. [127].

Open Access. This article is distributed under the terms of the Creative Commons Attribution License ([CC-BY 4.0](https://creativecommons.org/licenses/by/4.0/)), which permits any use, distribution and reproduction in any medium, provided the original author(s) and source are credited.

References

- [1] CDF collaboration, *First observation of electroweak single top quark production*, *Phys. Rev. Lett.* **103** (2009) 092002 [[arXiv:0903.0885](#)] [[INSPIRE](#)].
- [2] D0 collaboration, *Observation of single top quark production*, *Phys. Rev. Lett.* **103** (2009) 092001 [[arXiv:0903.0850](#)] [[INSPIRE](#)].
- [3] A. Giammanco and R. Schwienhorst, *Single top-quark production at the Tevatron and the LHC*, *Rev. Mod. Phys.* **90** (2018) 035001 [[arXiv:1710.10699](#)] [[INSPIRE](#)].
- [4] T.M.P. Tait and C.P. Yuan, *Single top quark production as a window to physics beyond the standard model*, *Phys. Rev. D* **63** (2000) 014018 [[hep-ph/0007298](#)] [[INSPIRE](#)].
- [5] Q.-H. Cao, J. Wudka and C.P. Yuan, *Search for new physics via single top production at the LHC*, *Phys. Lett. B* **658** (2007) 50 [[arXiv:0704.2809](#)] [[INSPIRE](#)].
- [6] R.M. Godbole, L. Hartgring, I. Niessen and C.D. White, *Top polarisation studies in H^-t and Wt production*, *JHEP* **01** (2012) 011 [[arXiv:1111.0759](#)] [[INSPIRE](#)].
- [7] C. Zhang and S. Willenbrock, *Effective-field-theory approach to top-quark production and decay*, *Phys. Rev. D* **83** (2011) 034006 [[arXiv:1008.3869](#)] [[INSPIRE](#)].
- [8] J.A. Aguilar-Saavedra, *Single top quark production at LHC with anomalous Wtb couplings*, *Nucl. Phys. B* **804** (2008) 160 [[arXiv:0803.3810](#)] [[INSPIRE](#)].
- [9] J.A. Dror, M. Farina, E. Salvioni and J. Serra, *Strong tW scattering at the LHC*, *JHEP* **01** (2016) 071 [[arXiv:1511.03674](#)] [[INSPIRE](#)].
- [10] M.S. Berger, V.A. Kostelecký and Z. Liu, *Lorentz and CPT violation in top-quark production and decay*, *Phys. Rev. D* **93** (2016) 036005 [[arXiv:1509.08929](#)] [[INSPIRE](#)].
- [11] H.-J. He, T.M.P. Tait and C.P. Yuan, *New top flavor models with seesaw mechanism*, *Phys. Rev. D* **62** (2000) 011702 [[hep-ph/9911266](#)] [[INSPIRE](#)].
- [12] J.A. Aguilar-Saavedra, R. Benbrik, S. Heinemeyer and M. Pérez-Victoria, *Handbook of vectorlike quarks: Mixing and single production*, *Phys. Rev. D* **88** (2013) 094010 [[arXiv:1306.0572](#)] [[INSPIRE](#)].
- [13] G. Durieux, F. Maltoni and C. Zhang, *Global approach to top-quark flavor-changing interactions*, *Phys. Rev. D* **91** (2015) 074017 [[arXiv:1412.7166](#)] [[INSPIRE](#)].
- [14] J. Nutter, R. Schwienhorst, D.G.E. Walker and J.-H. Yu, *Single top production as a probe of B -prime quarks*, *Phys. Rev. D* **86** (2012) 094006 [[arXiv:1207.5179](#)] [[INSPIRE](#)].
- [15] M. Hashemi, *Observability of heavy charged higgs through s -channel single top events at LHC*, *JHEP* **11** (2013) 005 [[arXiv:1310.5209](#)] [[INSPIRE](#)].
- [16] E. Drueke et al., *Single top production as a probe of heavy resonances*, *Phys. Rev. D* **91** (2015) 054020 [[arXiv:1409.7607](#)] [[INSPIRE](#)].
- [17] N. Cabibbo, *Unitary symmetry and leptonic decays*, *Phys. Rev. Lett.* **10** (1963) 531 [[INSPIRE](#)].
- [18] M. Kobayashi and T. Maskawa, *CP violation in the renormalizable theory of weak interaction*, *Prog. Theor. Phys.* **49** (1973) 652 [[INSPIRE](#)].
- [19] PARTICLE DATA GROUP collaboration, *Review of particle physics*, *Phys. Rev. D* **98** (2018) 030001 [[INSPIRE](#)].

- [20] D0 collaboration, *Precision measurement of the ratio $B(t \rightarrow Wb)/B(t \rightarrow Wq)$ and Extraction of V_{tb}* , *Phys. Rev. Lett.* **107** (2011) 121802 [[arXiv:1106.5436](#)] [[INSPIRE](#)].
- [21] CDF collaboration, *Measurement of $R = B(t \rightarrow Wb)/B(t \rightarrow Wq)$ in top-quark-pair decays using lepton+jets events and the full CDF Run II data set*, *Phys. Rev. D* **87** (2013) 111101 [[arXiv:1303.6142](#)] [[INSPIRE](#)].
- [22] CDF collaboration, *Measurement of $B(t \rightarrow Wb)/B(t \rightarrow Wq)$ in top-quark-pair decays using dilepton events and the full CDF Run II data set*, *Phys. Rev. Lett.* **112** (2014) 221801 [[arXiv:1404.3392](#)] [[INSPIRE](#)].
- [23] CMS collaboration, *Measurement of the ratio $B(t \rightarrow Wb)/B(t \rightarrow Wq)$ in pp collisions at $\sqrt{s} = 8$ TeV*, *Phys. Lett. B* **736** (2014) 33 [[arXiv:1404.2292](#)] [[INSPIRE](#)].
- [24] J.A. Aguilar-Saavedra, *A minimal set of top anomalous couplings*, *Nucl. Phys. B* **812** (2009) 181 [[arXiv:0811.3842](#)] [[INSPIRE](#)].
- [25] D0 collaboration, *Combination of searches for anomalous top quark couplings with 5.4 fb⁻¹ of pp collisions*, *Phys. Lett. B* **713** (2012) 165 [[arXiv:1204.2332](#)] [[INSPIRE](#)].
- [26] J. Alwall et al., *Is $V_{tb} \simeq 1$?*, *Eur. Phys. J. C* **49** (2007) 791 [[hep-ph/0607115](#)] [[INSPIRE](#)].
- [27] T.M.P. Tait, *The tW^- mode of single top production*, *Phys. Rev. D* **61** (1999) 034001 [[hep-ph/9909352](#)] [[INSPIRE](#)].
- [28] A. Belyaev and E. Boos, *Single top quark $tW + X$ production at the CERN LHC: a closer look*, *Phys. Rev. D* **63** (2001) 034012 [[hep-ph/0003260](#)] [[INSPIRE](#)].
- [29] Q.-H. Cao and B. Yan, *Determining V_{tb} at electron-positron colliders*, *Phys. Rev. D* **92** (2015) 094018 [[arXiv:1507.06204](#)] [[INSPIRE](#)].
- [30] CDF, D0 collaboration, *Tevatron combination of single-top-quark cross sections and determination of the magnitude of the Cabibbo-Kobayashi-maskawa matrix element V_{tb}* , *Phys. Rev. Lett.* **115** (2015) 152003 [[arXiv:1503.05027](#)] [[INSPIRE](#)].
- [31] R. Frederix, E. Re and P. Torrielli, *Single-top t-channel hadroproduction in the four-flavour scheme with POWHEG and aMC@NLO*, *JHEP* **09** (2012) 130 [[arXiv:1207.5391](#)] [[INSPIRE](#)].
- [32] ATLAS collaboration, *Fiducial, total and differential cross-section measurements of t-channel single top-quark production in pp collisions at 8 TeV using data collected by the ATLAS detector*, *Eur. Phys. J. C* **77** (2017) 531 [[arXiv:1702.02859](#)] [[INSPIRE](#)].
- [33] CMS collaboration, *Measurement of the t-channel single-top-quark production cross section and of the $|V_{tb}|$ CKM matrix element in pp collisions at $\sqrt{s} = 8$ TeV*, *JHEP* **06** (2014) 090 [[arXiv:1403.7366](#)] [[INSPIRE](#)].
- [34] ATLAS collaboration, *Measurement of the production cross-section of a single top quark in association with a W boson at 8 TeV with the ATLAS experiment*, *JHEP* **01** (2016) 064 [[arXiv:1510.03752](#)] [[INSPIRE](#)].
- [35] CMS collaboration, *Observation of the associated production of a single top quark and a W boson in pp collisions at $\sqrt{s} = 8$ TeV*, *Phys. Rev. Lett.* **112** (2014) 231802 [[arXiv:1401.2942](#)] [[INSPIRE](#)].
- [36] CDF, D0 collaboration, *Observation of s-channel production of single top quarks at the Tevatron*, *Phys. Rev. Lett.* **112** (2014) 231803 [[arXiv:1402.5126](#)] [[INSPIRE](#)].

- [37] ATLAS collaboration, *Evidence for single top-quark production in the s-channel in proton-proton collisions at $\sqrt{s} = 8$ TeV with the ATLAS detector using the Matrix Element Method*, *Phys. Lett. B* **756** (2016) 228 [[arXiv:1511.05980](#)] [[INSPIRE](#)].
- [38] J.M. Campbell, R. Frederix, F. Maltoni and F. Tramontano, *Next-to-leading-order predictions for t-channel single-top production at hadron colliders*, *Phys. Rev. Lett.* **102** (2009) 182003 [[arXiv:0903.0005](#)] [[INSPIRE](#)].
- [39] J.M. Campbell, R. Frederix, F. Maltoni and F. Tramontano, *NLO predictions for t-channel production of single top and fourth generation quarks at hadron colliders*, *JHEP* **10** (2009) 042 [[arXiv:0907.3933](#)] [[INSPIRE](#)].
- [40] M. Aliev et al., *HATHOR: HAdronic Top and Heavy quarks crOss section calculator*, *Comput. Phys. Commun.* **182** (2011) 1034 [[arXiv:1007.1327](#)] [[INSPIRE](#)].
- [41] P. Kant et al., *HatHor for single top-quark production: Updated predictions and uncertainty estimates for single top-quark production in hadronic collisions*, *Comput. Phys. Commun.* **191** (2015) 74 [[arXiv:1406.4403](#)] [[INSPIRE](#)].
- [42] M. Botje et al., *The PDF4LHC Working Group Interim Recommendations*, [arXiv:1101.0538](#).
- [43] H.-L. Lai et al., *New parton distributions for collider physics*, *Phys. Rev. D* **82** (2010) 074024 [[arXiv:1007.2241](#)] [[INSPIRE](#)].
- [44] R.D. Ball et al., *Parton distributions with LHC data*, *Nucl. Phys. B* **867** (2013) 244 [[arXiv:1207.1303](#)] [[INSPIRE](#)].
- [45] N. Kidonakis, *NNLL threshold resummation for top-pair and single-top production*, *Phys. Part. Nucl.* **45** (2014) 714 [[arXiv:1210.7813](#)] [[INSPIRE](#)].
- [46] N. Kidonakis, *Next-to-next-to-leading-order collinear and soft gluon corrections for t-channel single top quark production*, *Phys. Rev. D* **83** (2011) 091503 [[arXiv:1103.2792](#)] [[INSPIRE](#)].
- [47] N. Kidonakis, *Two-loop soft anomalous dimensions for single top quark associated production with a W^- or H^-* , *Phys. Rev. D* **82** (2010) 054018 [[arXiv:1005.4451](#)] [[INSPIRE](#)].
- [48] N. Kidonakis, *NNLL resummation for s-channel single top quark production*, *Phys. Rev. D* **81** (2010) 054028 [[arXiv:1001.5034](#)] [[INSPIRE](#)].
- [49] A.D. Martin, W.J. Stirling, R.S. Thorne and G. Watt, *Uncertainties on α_s in global PDF analyses and implications for predicted hadronic cross sections*, *Eur. Phys. J. C* **64** (2009) 653 [[arXiv:0905.3531](#)] [[INSPIRE](#)].
- [50] A.D. Martin, W.J. Stirling, R.S. Thorne and G. Watt, *Parton distributions for the LHC*, *Eur. Phys. J. C* **63** (2009) 189 [[arXiv:0901.0002](#)] [[INSPIRE](#)].
- [51] M. Brucherseifer, F. Caola and K. Melnikov, *On the NNLO QCD corrections to single-top production at the LHC*, *Phys. Lett. B* **736** (2014) 58 [[arXiv:1404.7116](#)] [[INSPIRE](#)].
- [52] S.S.D. Willenbrock and D.A. Dicus, *Production of heavy quarks from W gluon fusion*, *Phys. Rev. D* **34** (1986) 155 [[INSPIRE](#)].
- [53] N. Kidonakis, *Top quark production*, in the proceedings of the *Helmholtz International Summer School on Physics of Heavy Quarks and Hadrons (HQ 2013)*, July 15–28, Dubna, Russia (2013), [arXiv:1311.0283](#).

- [54] F. Demartin et al., *tWH associated production at the LHC*, *Eur. Phys. J. C* **77** (2017) 34 [[arXiv:1607.05862](#)] [[INSPIRE](#)].
- [55] J.M. Campbell and F. Tramontano, *Next-to-leading order corrections to Wt production and decay*, *Nucl. Phys. B* **726** (2005) 109 [[hep-ph/0506289](#)] [[INSPIRE](#)].
- [56] M. Czakon, P. Fiedler and A. Mitov, *Total top-quark pair-production cross section at hadron colliders through $O(\alpha_S^4)$* , *Phys. Rev. Lett.* **110** (2013) 252004 [[arXiv:1303.6254](#)] [[INSPIRE](#)].
- [57] U. Langenfeld, S. Moch and P. Uwer, *New results for $t\bar{t}$ production at hadron colliders*, in the proceedings of the 17th *International Workshop on Deep-Inelastic Scattering and Related Subjects (DIS 2009)*, April 26–30, Madrid, Spain (2009), [[arXiv:0907.2527](#)] [[INSPIRE](#)].
- [58] E. Todesco and J. Wenninger, *Large Hadron Collider momentum calibration and accuracy*, *Phys. Rev. Accel. Beams* **20** (2017) 081003 [[INSPIRE](#)].
- [59] ATLAS collaboration, *Comprehensive measurements of t-channel single top-quark production cross sections at $\sqrt{s} = 7$ TeV with the ATLAS detector*, *Phys. Rev. D* **90** (2014) 112006 [[arXiv:1406.7844](#)] [[INSPIRE](#)].
- [60] CMS collaboration, *Measurement of the single-top-quark t-channel cross section in pp collisions at $\sqrt{s} = 7$ TeV*, *JHEP* **12** (2012) 035 [[arXiv:1209.4533](#)] [[INSPIRE](#)].
- [61] ATLAS collaboration, *Evidence for the associated production of a W boson and a top quark in ATLAS at $\sqrt{s} = 7$ TeV*, *Phys. Lett. B* **716** (2012) 142 [[arXiv:1205.5764](#)] [[INSPIRE](#)].
- [62] CMS collaboration, *Evidence for associated production of a single top quark and W boson in pp collisions at $\sqrt{s} = 7$ TeV*, *Phys. Rev. Lett.* **110** (2013) 022003 [[arXiv:1209.3489](#)] [[INSPIRE](#)].
- [63] CMS collaboration, *Search for s channel single top quark production in pp collisions at $\sqrt{s} = 7$ and 8 TeV*, *JHEP* **09** (2016) 027 [[arXiv:1603.02555](#)] [[INSPIRE](#)].
- [64] Y. Freund and R.E. Schapire, *A decision-theoretic generalization of on-line learning and an application to boosting*, *J. Comput. Syst. Sci.* **55** (1997) 119.
- [65] J.H. Friedman, *Recent advances in predictive (machine) learning*, *J. Classif.* **23** (2006) 175.
- [66] A. Hoecker et al., *TMVA — Toolkit for Multivariate Data Analysis*, [[physics/0703039](#)].
- [67] M. Feindt and U. Kerzel, *The NeuroBayes neural network package*, *Nucl. Instrum. Meth. A* **559** (2006) 190 [[INSPIRE](#)].
- [68] K. Kondo, *Dynamical likelihood method for reconstruction of events with missing momentum. 1: method and toy models*, *J. Phys. Soc. Jap.* **57** (1988) 4126 [[INSPIRE](#)].
- [69] K. Kondo, *Dynamical likelihood method for reconstruction of events with missing momentum. 2: mass spectra for $2 \rightarrow 2$ processes*, *J. Phys. Soc. Jap.* **60** (1991) 836 [[INSPIRE](#)].
- [70] P. Nason, *A new method for combining NLO QCD with shower Monte Carlo algorithms*, *JHEP* **11** (2004) 040 [[hep-ph/0409146](#)] [[INSPIRE](#)].
- [71] S. Frixione, P. Nason and C. Oleari, *Matching NLO QCD computations with Parton Shower simulations: the POWHEG method*, *JHEP* **11** (2007) 070 [[arXiv:0709.2092](#)] [[INSPIRE](#)].
- [72] S. Alioli, P. Nason, C. Oleari and E. Re, *NLO single-top production matched with shower in POWHEG: s- and t-channel contributions*, *JHEP* **09** (2009) 111 [*Erratum ibid.* **02** (2010) 011] [[arXiv:0907.4076](#)] [[INSPIRE](#)].

- [73] S. Alioli, P. Nason, C. Oleari and E. Re, *A general framework for implementing NLO calculations in shower Monte Carlo programs: the POWHEG BOX*, *JHEP* **06** (2010) 043 [[arXiv:1002.2581](#)] [[INSPIRE](#)].
- [74] E. Re, *Single-top Wt -channel production matched with parton showers using the POWHEG method*, *Eur. Phys. J. C* **71** (2011) 1547 [[arXiv:1009.2450](#)] [[INSPIRE](#)].
- [75] J. Alwall et al., *MadGraph 5: going beyond*, *JHEP* **06** (2011) 128 [[arXiv:1106.0522](#)] [[INSPIRE](#)].
- [76] T. Sjöstrand, S. Mrenna and P.Z. Skands, *PYTHIA 6.4 physics and manual*, *JHEP* **05** (2006) 026 [[hep-ph/0603175](#)] [[INSPIRE](#)].
- [77] L. Lyons, D. Gibaut and P. Clifford, *How to combine correlated estimates of a single physical quantity*, *Nucl. Instrum. Meth. A* **270** (1988) 110 [[INSPIRE](#)].
- [78] A. Valassi, *Combining correlated measurements of several different physical quantities*, *Nucl. Instrum. Meth. A* **500** (2003) 391 [[INSPIRE](#)].
- [79] R. Nisius, *On the combination of correlated estimates of a physics observable*, *Eur. Phys. J. C* **74** (2014) 3004 [[arXiv:1402.4016](#)] [[INSPIRE](#)].
- [80] L. Lista, *The bias of the unbiased estimator: a study of the iterative application of the BLUE method*, *Nucl. Instrum. Meth. A* **764** (2014) 82 [*Erratum ibid.* **A 773** (2015) 87] [[arXiv:1405.3425](#)] [[INSPIRE](#)].
- [81] A. Valassi and R. Chierici, *Information and treatment of unknown correlations in the combination of measurements using the BLUE method*, *Eur. Phys. J. C* **74** (2014) 2717 [[arXiv:1307.4003](#)] [[INSPIRE](#)].
- [82] ATLAS collaboration, *Improved luminosity determination in pp collisions at $\sqrt{s} = 7$ TeV using the ATLAS detector at the LHC*, *Eur. Phys. J. C* **73** (2013) 2518 [[arXiv:1302.4393](#)] [[INSPIRE](#)].
- [83] ATLAS collaboration, *Luminosity determination in pp collisions at $\sqrt{s} = 8$ TeV using the ATLAS detector at the LHC*, *Eur. Phys. J. C* **76** (2016) 653 [[arXiv:1608.03953](#)] [[INSPIRE](#)].
- [84] CMS collaboration, *Absolute calibration of the luminosity measurement at CMS: winter 2012 update*, [CMS-PAS-SMP-12-008](#) (2012).
- [85] CMS Collaboration, *CMS luminosity based on pixel cluster counting — Summer 2013 update*, [CMS-PAS-LUM-13-001](#) (2013).
- [86] S. van der Meer, *Calibration of the effective beam height in the ISR*, [CERN-ISR-PO-68-31](#) (1968).
- [87] ATLAS collaboration, *Measurement of $t\bar{t}$ production with a veto on additional central jet activity in pp collisions at $\sqrt{s} = 7$ TeV using the ATLAS detector*, *Eur. Phys. J. C* **72** (2012) 2043 [[arXiv:1203.5015](#)] [[INSPIRE](#)].
- [88] ATLAS collaboration, *Comparison of Monte Carlo generator predictions for gap fraction and jet multiplicity observables in top-antitop events*, [ATL-PHYS-PUB-2014-005](#) (2014).
- [89] M.L. Mangano et al., *ALPGEN, a generator for hard multiparton processes in hadronic collisions*, *JHEP* **07** (2003) 001 [[hep-ph/0206293](#)] [[INSPIRE](#)].
- [90] T. Gleisberg et al., *Event generation with SHERPA 1.1*, *JHEP* **02** (2009) 007 [[arXiv:0811.4622](#)] [[INSPIRE](#)].

- [91] S. Frixione and B.R. Webber, *Matching NLO QCD computations and parton shower simulations*, *JHEP* **06** (2002) 029 [[hep-ph/0204244](#)] [[INSPIRE](#)].
- [92] P.Z. Skands, *Tuning Monte Carlo generators: the Perugia tunes*, *Phys. Rev. D* **82** (2010) 074018 [[arXiv:1005.3457](#)] [[INSPIRE](#)].
- [93] J. Alwall et al., *The automated computation of tree-level and next-to-leading order differential cross sections and their matching to parton shower simulations*, *JHEP* **07** (2014) 079 [[arXiv:1405.0301](#)] [[INSPIRE](#)].
- [94] G. Corcella et al., *HERWIG 6: an event generator for hadron emission reactions with interfering gluons (including supersymmetric processes)*, *JHEP* **01** (2001) 010 [[hep-ph/0011363](#)] [[INSPIRE](#)].
- [95] J.M. Butterworth, J.R. Forshaw and M.H. Seymour, *Multiparton interactions in photoproduction at HERA*, *Z. Phys. C* **72** (1996) 637 [[hep-ph/9601371](#)] [[INSPIRE](#)].
- [96] COMPHEP collaboration, *CompHEP 4.4: automatic computations from Lagrangians to events*, *Nucl. Instrum. Meth. A* **534** (2004) 250 [[hep-ph/0403113](#)] [[INSPIRE](#)].
- [97] A. Pukhov et al., *CompHEP — A package for evaluation of Feynman diagrams and integration over multi-particle phase space*, [hep-ph/9908288](#).
- [98] ATLAS collaboration, *Jet energy measurement with the ATLAS detector in proton-proton collisions at $\sqrt{s} = 7$ TeV*, *Eur. Phys. J. C* **73** (2013) 2304 [[arXiv:1112.6426](#)] [[INSPIRE](#)].
- [99] ATLAS collaboration, *Jet energy measurement and its systematic uncertainty in proton-proton collisions at $\sqrt{s} = 7$ TeV with the ATLAS detector*, *Eur. Phys. J. C* **75** (2015) 17 [[arXiv:1406.0076](#)] [[INSPIRE](#)].
- [100] CMS collaboration, *Determination of jet energy calibration and transverse momentum resolution in CMS*, *2011 JINST* **6** P11002 [[arXiv:1107.4277](#)] [[INSPIRE](#)].
- [101] CMS collaboration, *Jet energy scale and resolution in the CMS experiment in pp collisions at 8 TeV*, *2017 JINST* **12** P02014 [[arXiv:1607.03663](#)] [[INSPIRE](#)].
- [102] ATLAS collaboration, *Performance of b-jet identification in the ATLAS experiment*, *2016 JINST* **11** P04008 [[arXiv:1512.01094](#)] [[INSPIRE](#)].
- [103] ATLAS collaboration, *Calibration of b-tagging using dileptonic top pair events in a combinatorial likelihood approach with the ATLAS experiment*, *ATLAS-CONF-2014-004* (2014).
- [104] ATLAS collaboration, *Calibration of the performance of b-tagging for c and light-flavour jets in the 2012 ATLAS data*, *ATLAS-CONF-2014-046* (2014).
- [105] CMS collaboration, *Identification of b-quark jets with the CMS experiment*, *2013 JINST* **8** P04013 [[arXiv:1211.4462](#)] [[INSPIRE](#)].
- [106] CMS collaboration, *Performance of b tagging at $\sqrt{s} = 8$ TeV in multijet, ttbar and boosted topology events*, *CMS-PAS-BTV-13-001* (2013).
- [107] M.L. Mangano, M. Moretti, F. Piccinini and M. Treccani, *Matching matrix elements and shower evolution for top-quark production in hadronic collisions*, *JHEP* **01** (2007) 013 [[hep-ph/0611129](#)] [[INSPIRE](#)].
- [108] S. Alekhin et al., *The PDF4LHC working group interim report*, [arXiv:1101.0536](#) [[INSPIRE](#)].

- [109] J. Butterworth et al., *PDF₄LHC recommendations for LHC Run II*, *J. Phys. G* **43** (2016) 023001 [[arXiv:1510.03865](#)] [[INSPIRE](#)].
- [110] S. Frixione et al., *Single-top hadroproduction in association with a W boson*, *JHEP* **07** (2008) 029 [[arXiv:0805.3067](#)] [[INSPIRE](#)].
- [111] A.S. Belyaev, E.E. Boos and L.V. Dudko, *Single top quark at future hadron colliders: complete signal and background study*, *Phys. Rev. D* **59** (1999) 075001 [[hep-ph/9806332](#)] [[INSPIRE](#)].
- [112] C.D. White, S. Frixione, E. Laenen and F. Maltoni, *Isolating Wt production at the LHC*, *JHEP* **11** (2009) 074 [[arXiv:0908.0631](#)] [[INSPIRE](#)].
- [113] CMS collaboration, *Measurement of the differential cross section for top quark pair production in pp collisions at $\sqrt{s} = 8$ TeV*, *Eur. Phys. J. C* **75** (2015) 542 [[arXiv:1505.04480](#)] [[INSPIRE](#)].
- [114] M. Czakon, P. Fiedler, D. Heymes and A. Mitov, *NNLO QCD predictions for fully-differential top-quark pair production at the Tevatron*, *JHEP* **05** (2016) 034 [[arXiv:1601.05375](#)] [[INSPIRE](#)].
- [115] ATLAS collaboration, *Measurements of top-quark pair differential cross-sections in the lepton+jets channel in pp collisions at $\sqrt{s} = 8$ TeV using the ATLAS detector*, *Eur. Phys. J. C* **76** (2016) 538 [[arXiv:1511.04716](#)] [[INSPIRE](#)].
- [116] ATLAS collaboration, *Jet energy scale uncertainty correlations between ATLAS and CMS*, *ATL-PHYS-PUB-2014-020* (2014).
- [117] ATLAS and CMS collaborations, *Jet energy scale uncertainty correlations between ATLAS and CMS at $\sqrt{s} = 8$ TeV*, *ATL-PHYS-PUB-2015-049* (2015) [CMS-PAS-JME-15-001].
- [118] ATLAS collaboration, *Measurement of the muon reconstruction performance of the ATLAS detector using 2011 and 2012 LHC proton–proton collision data*, *Eur. Phys. J. C* **74** (2014) 3130 [[arXiv:1407.3935](#)] [[INSPIRE](#)].
- [119] ATLAS collaboration, *Electron and photon energy calibration with the ATLAS detector using LHC Run 1 data*, *Eur. Phys. J. C* **74** (2014) 3071 [[arXiv:1407.5063](#)] [[INSPIRE](#)].
- [120] ATLAS collaboration, *Electron reconstruction and identification efficiency measurements with the ATLAS detector using the 2011 LHC proton–proton collision data*, *Eur. Phys. J. C* **74** (2014) 2941 [[arXiv:1404.2240](#)] [[INSPIRE](#)].
- [121] ATLAS collaboration, *Electron efficiency measurements with the ATLAS detector using 2012 LHC proton–proton collision data*, *Eur. Phys. J. C* **77** (2017) 195 [[arXiv:1612.01456](#)] [[INSPIRE](#)].
- [122] CMS collaboration, *Particle-flow reconstruction and global event description with the CMS detector*, *2017 JINST* **12** P10003 [[arXiv:1706.04965](#)] [[INSPIRE](#)].
- [123] ATLAS collaboration, *Performance of algorithms that reconstruct missing transverse momentum in $\sqrt{s} = 8$ TeV proton–proton collisions in the ATLAS detector*, *Eur. Phys. J. C* **77** (2017) 241 [[arXiv:1609.09324](#)] [[INSPIRE](#)].
- [124] CMS collaboration, *Performance of the CMS missing transverse momentum reconstruction in pp data at $\sqrt{s} = 8$ TeV*, *2015 JINST* **10** P02006 [[arXiv:1411.0511](#)] [[INSPIRE](#)].
- [125] R.J. Barlow and C. Beeston, *Fitting using finite Monte Carlo samples*, *Comput. Phys. Commun.* **77** (1993) 219 [[INSPIRE](#)].

- [126] ATLAS collaboration, *Comparison of Monte Carlo generator predictions to ATLAS measurements of top pair production at 7 TeV*, [ATL-PHYS-PUB-2015-002](#) (2015).
- [127] ATLAS collaboration, *ATLAS computing acknowledgements*, [ATL-GEN-PUB-2016-002](#) (2016).

The ATLAS collaboration

M. Aaboud^{34d}, G. Aad¹⁰⁰, B. Abbott¹²⁶, D.C. Abbott¹⁰¹, O. Abidinov^{13,*}, A. Abed Abud^{69a,69b}, D.K. Abhayasinghe⁹², S.H. Abidi¹⁶⁵, O.S. AbouZeid³⁹, N.L. Abraham¹⁵⁴, H. Abramowicz¹⁵⁹, H. Abreu¹⁵⁸, Y. Abulaiti⁶, B.S. Acharya^{65a,65b,o}, S. Adachi¹⁶¹, L. Adam⁹⁸, L. Adamczyk^{82a}, L. Adamek¹⁶⁵, J. Adelman¹²⁰, M. Adersberger¹¹³, A. Adiguzel^{12c,ah}, S. Adorni⁵³, T. Adye¹⁴², A.A. Affolder¹⁴⁴, Y. Afik¹⁵⁸, C. Agapopoulou¹³⁰, M.N. Agaras³⁷, A. Aggarwal¹¹⁸, C. Agheorghiesei^{27c}, J.A. Aguilar-Saavedra^{138f,138a,ag}, F. Ahmadov⁷⁸, X. Ai^{15a}, G. Aielli^{72a,72b}, S. Akatsuka⁸⁴, T.P.A. Åkesson⁹⁵, E. Akilli⁵³, A.V. Akimov¹⁰⁹, K. Al Houry¹³⁰, G.L. Alberghi^{23b,23a}, J. Albert¹⁷⁴, M.J. Alconada Verzini⁸⁷, S. Alderweireldt¹¹⁸, M. Aleksa³⁵, I.N. Aleksandrov⁷⁸, C. Alexa^{27b}, D. Alexandre¹⁹, T. Alexopoulos¹⁰, A. Alfonsi¹¹⁹, M. Alhroob¹²⁶, B. Ali¹⁴⁰, G. Alimonti^{67a}, J. Alison³⁶, S.P. Alkire¹⁴⁶, C. Allaire¹³⁰, B.M.M. Allbrooke¹⁵⁴, B.W. Allen¹²⁹, P.P. Allport²¹, A. Aloisio^{68a,68b}, A. Alonso³⁹, F. Alonso⁸⁷, C. Alpigiani¹⁴⁶, A.A. Alshehri⁵⁶, M.I. Alstaty¹⁰⁰, M. Alvarez Estevez⁹⁷, B. Alvarez Gonzalez³⁵, D. Álvarez Piqueras¹⁷², M.G. Alviggi^{68a,68b}, Y. Amaral Coutinho^{79b}, A. Ambler¹⁰², L. Ambroz¹³³, C. Amelung²⁶, D. Amidei¹⁰⁴, S.P. Amor Dos Santos^{138a,138c}, S. Amoroso⁴⁵, C.S. Amrouche⁵³, F. An⁷⁷, C. Anastopoulos¹⁴⁷, N. Andari¹⁴³, T. Andeen¹¹, C.F. Anders^{60b}, J.K. Anders²⁰, A. Andreatza^{67a,67b}, V. Andrei^{60a}, C.R. Anelli¹⁷⁴, S. Angelidakis³⁷, I. Angelozzi¹¹⁹, A. Angerami³⁸, A.V. Anisenkov^{121b,121a}, A. Annovi^{70a}, C. Antel^{60a}, M.T. Anthony¹⁴⁷, M. Antonelli⁵⁰, D.J.A. Antrim¹⁶⁹, F. Anulli^{71a}, M. Aoki⁸⁰, J.A. Aparisi Pozo¹⁷², L. Aperio Bella³⁵, G. Arabidze¹⁰⁵, J.P. Araque^{138a}, V. Araujo Ferraz^{79b}, R. Araujo Pereira^{79b}, A.T.H. Arce⁴⁸, F.A. Arduh⁸⁷, J-F. Arguin¹⁰⁸, S. Argyropoulos⁷⁶, J.-H. Arling⁴⁵, A.J. Armbruster³⁵, L.J. Armitage⁹¹, A. Armstrong¹⁶⁹, O. Arnaez¹⁶⁵, H. Arnold¹¹⁹, A. Artamonov^{110,*}, G. Artoni¹³³, S. Artz⁹⁸, S. Asai¹⁶¹, N. Asbah⁵⁸, E.M. Asimakopoulou¹⁷⁰, L. Asquith¹⁵⁴, K. Assamagan²⁹, R. Astalos^{28a}, R.J. Atkin^{32a}, M. Atkinson¹⁷¹, N.B. Atlay¹⁴⁹, H. Atmani¹³⁰, K. Augsten¹⁴⁰, G. Avolio³⁵, R. Avramidou^{59a}, M.K. Ayoub^{15a}, A.M. Azoulay^{166b}, G. Azuelos^{108,av}, A.E. Baas^{60a}, M.J. Baca²¹, H. Bachacou¹⁴³, K. Bachas^{66a,66b}, M. Backes¹³³, F. Backman^{44a,44b}, P. Bagnaia^{71a,71b}, M. Bahmani⁸³, H. Bahrasemani¹⁵⁰, A.J. Bailey¹⁷², V.R. Bailey¹⁷¹, J.T. Baines¹⁴², M. Bajic³⁹, C. Bakalis¹⁰, O.K. Baker¹⁸¹, P.J. Bakker¹¹⁹, D. Bakshi Gupta⁸, S. Balaji¹⁵⁵, E.M. Baldin^{121b,121a}, P. Balek¹⁷⁸, F. Balli¹⁴³, W.K. Balunas¹³³, J. Balz⁹⁸, E. Banas⁸³, A. Bandyopadhyay²⁴, S. Banerjee^{179,k}, A.A.E. Bannoura¹⁸⁰, L. Barak¹⁵⁹, W.M. Barbe³⁷, E.L. Barberio¹⁰³, D. Barberis^{54b,54a}, M. Barbero¹⁰⁰, T. Barillari¹¹⁴, M-S. Barisits³⁵, J. Barkeloo¹²⁹, T. Barklow¹⁵¹, R. Barnea¹⁵⁸, S.L. Barnes^{59c}, B.M. Barnett¹⁴², R.M. Barnett¹⁸, Z. Barnovska-Blenessy^{59a}, A. Baroncelli^{59a}, G. Barone²⁹, A.J. Barr¹³³, L. Barranco Navarro¹⁷², F. Barreiro⁹⁷, J. Barreiro Guimarães da Costa^{15a}, R. Bartoldus¹⁵¹, G. Bartolini¹⁰⁰, A.E. Barton⁸⁸, P. Bartos^{28a}, A. Basalae⁴⁵, A. Bassalat¹³⁰, R.L. Bates⁵⁶, S.J. Batista¹⁶⁵, S. Batlamous^{34e}, J.R. Batley³¹, B. Batool¹⁴⁹, M. Battaglia¹⁴⁴, M. Bauge^{71a,71b}, F. Bauer¹⁴³, K.T. Bauer¹⁶⁹, H.S. Bawa¹⁵¹, J.B. Beacham¹²⁴, T. Beau¹³⁴, P.H. Beauchemin¹⁶⁸, P. Bechtel²⁴, H.C. Beck⁵², H.P. Beck^{20,r}, K. Becker⁵¹, M. Becker⁹⁸, C. Becot⁴⁵, A. Beddall^{12d}, A.J. Beddall^{12a}, V.A. Bednyakov⁷⁸, M. Bedognetti¹¹⁹, C.P. Bee¹⁵³, T.A. Beermann⁷⁵, M. Begalli^{79b}, M. Beger²⁹, A. Behera¹⁵³, J.K. Behr⁴⁵, F. Beisiegel²⁴, A.S. Bell⁹³, G. Bella¹⁵⁹, L. Bellagamba^{23b}, A. Bellerive³³, P. Bellos⁹, K. Beloborodov^{121b,121a}, K. Belotskiy¹¹¹, N.L. Belyaev¹¹¹, O. Benary^{159,*}, D. Benchekroun^{34a}, N. Benekos¹⁰, Y. Benhammou¹⁵⁹, D.P. Benjamin⁶, M. Benoit⁵³, J.R. Bensinger²⁶, S. Bentvelsen¹¹⁹, L. Beresford¹³³, M. Beretta⁵⁰, D. Berge⁴⁵, E. Bergeas Kuutmann¹⁷⁰, N. Berger⁵, B. Bergmann¹⁴⁰, L.J. Bergsten²⁶, J. Beringer¹⁸, S. Berlendis⁷, N.R. Bernard¹⁰¹, G. Bernardi¹³⁴, C. Bernius¹⁵¹, F.U. Bernlochner²⁴, T. Berry⁹², P. Berta⁹⁸, C. Bertella^{15a}, G. Bertoli^{44a,44b}, I.A. Bertram⁸⁸, G.J. Besjes³⁹, O. Bessidskaia Bylund¹⁸⁰, N. Besson¹⁴³, A. Bethani⁹⁹, S. Bethke¹¹⁴, A. Betti²⁴, A.J. Bevan⁹¹,

J. Beyer¹¹⁴, R. Bi¹³⁷, R.M. Bianchi¹³⁷, O. Biebel¹¹³, D. Biedermann¹⁹, R. Bielski³⁵,
 K. Bierwagen⁹⁸, N.V. Biesuz^{70a,70b}, M. Biglietti^{73a}, T.R.V. Billoud¹⁰⁸, M. Bindi⁵², A. Bingul^{12d},
 C. Bini^{71a,71b}, S. Biondi^{23b,23a}, M. Birman¹⁷⁸, T. Bisanz⁵², J.P. Biswal¹⁵⁹, A. Bitadze⁹⁹,
 C. Bittrich⁴⁷, D.M. Bjerggaard⁴⁸, J.E. Black¹⁵¹, K.M. Black²⁵, T. Blazek^{28a}, I. Bloch⁴⁵,
 C. Blocker²⁶, A. Blue⁵⁶, U. Blumenschein⁹¹, G.J. Bobbink¹¹⁹, V.S. Bobrovnikov^{121b,121a},
 S.S. Bocchetta⁹⁵, A. Bocci⁴⁸, D. Boerner⁴⁵, D. Bogavac¹¹³, A.G. Bogdanchikov^{121b,121a},
 C. Bohm^{44a}, V. Boisvert⁹², P. Bokan^{52,170}, T. Bold^{82a}, A.S. Boldyrev¹¹², A.E. Bolz^{60b},
 M. Bomben¹³⁴, M. Bona⁹¹, J.S. Bonilla¹²⁹, M. Boonekamp¹⁴³, H.M. Borecka-Bielska⁸⁹,
 A. Borisov¹²², G. Borissov⁸⁸, J. Bortfeldt³⁵, D. Bortoletto¹³³, V. Bortolotto^{72a,72b},
 D. Boscherini^{23b}, M. Bosman¹⁴, J.D. Bossio Sola³⁰, K. Bouaouda^{34a}, J. Boudreau¹³⁷,
 E.V. Bouhova-Thacker⁸⁸, D. Boumediene³⁷, C. Bourdarios¹³⁰, S.K. Boutle⁵⁶, A. Boveia¹²⁴,
 J. Boyd³⁵, D. Boye^{32b,ap}, I.R. Boyko⁷⁸, A.J. Bozson⁹², J. Bracinik²¹, N. Brahimi¹⁰⁰, G. Brandt¹⁸⁰,
 O. Brandt^{60a}, F. Braren⁴⁵, U. Bratzler¹⁶², B. Brau¹⁰¹, J.E. Brau¹²⁹, W.D. Breaden Madden⁵⁶,
 K. Brendlinger⁴⁵, L. Brenner⁴⁵, R. Brenner¹⁷⁰, S. Bressler¹⁷⁸, B. Brickwedde⁹⁸, D.L. Briglin²¹,
 D. Britton⁵⁶, D. Britzger¹¹⁴, I. Brock²⁴, R. Brock¹⁰⁵, G. Brooijmans³⁸, T. Brooks⁹²,
 W.K. Brooks^{145b}, E. Brost¹²⁰, J.H. Broughton²¹, P.A. Bruckman de Renstrom⁸³, D. Bruncko^{28b},
 A. Bruni^{23b}, G. Bruni^{23b}, L.S. Bruni¹¹⁹, S. Bruno^{72a,72b}, B.H. Brunt³¹, M. Bruschi^{23b},
 N. Bruscinò¹³⁷, P. Bryant³⁶, L. Bryngemark⁹⁵, T. Buanes¹⁷, Q. Buat³⁵, P. Buchholz¹⁴⁹,
 A.G. Buckley⁵⁶, I.A. Budagov⁷⁸, M.K. Bugge¹³², F. Bühner⁵¹, O. Bulekov¹¹¹, T.J. Burch¹²⁰,
 S. Burdin⁸⁹, C.D. Burgard¹¹⁹, A.M. Burger¹²⁷, B. Burghgrave⁸, K. Burka⁸³, J.T.P. Burr⁴⁵,
 V. Büscher⁹⁸, E. Buschmann⁵², P. Bussey⁵⁶, J.M. Butler²⁵, C.M. Buttar⁵⁶, J.M. Butterworth⁹³,
 P. Butti³⁵, W. Buttinger³⁵, A. Buzatu¹⁵⁶, A.R. Buzykaev^{121b,121a}, G. Cabras^{23b,23a},
 S. Cabrera Urbán¹⁷², D. Caforio¹⁴⁰, H. Cai¹⁷¹, V.M.M. Cairo¹⁵¹, O. Cakir^{4a}, N. Calace³⁵,
 P. Calafiura¹⁸, A. Calandri¹⁰⁰, G. Calderini¹³⁴, P. Calfayan⁶⁴, G. Callea⁵⁶, L.P. Caloba^{79b},
 S. Calvente Lopez⁹⁷, D. Calvet³⁷, S. Calvet³⁷, T.P. Calvet¹⁵³, M. Calvetti^{70a,70b},
 R. Camacho Toro¹³⁴, S. Camarda³⁵, D. Camarero Munoz⁹⁷, P. Camarri^{72a,72b}, D. Cameron¹³²,
 R. Caminal Armadans¹⁰¹, C. Camincher³⁵, S. Campana³⁵, M. Campanelli⁹³, A. Camplani³⁹,
 A. Campoverde¹⁴⁹, V. Canale^{68a,68b}, A. Canesse¹⁰², M. Cano Bret^{59c}, J. Cantero¹²⁷, T. Cao¹⁵⁹,
 Y. Cao¹⁷¹, M.D.M. Capeans Garrido³⁵, M. Capua^{40b,40a}, R. Cardarelli^{72a}, F.C. Cardillo¹⁴⁷,
 I. Carli¹⁴¹, T. Carli³⁵, G. Carlino^{68a}, B.T. Carlson¹³⁷, L. Carminati^{67a,67b}, R.M.D. Carney^{44a,44b},
 S. Caron¹¹⁸, E. Carquin^{145b}, S. Carrá^{67a,67b}, J.W.S. Carter¹⁶⁵, M.P. Casado^{14,g}, A.F. Casha¹⁶⁵,
 D.W. Casper¹⁶⁹, R. Castelijm¹¹⁹, F.L. Castillo¹⁷², V. Castillo Gimenez¹⁷², N.F. Castro^{138a,138e},
 A. Catinaccio³⁵, J.R. Catmore¹³², A. Cattai³⁵, J. Caudron²⁴, V. Cavaliere²⁹, E. Cavallaro¹⁴,
 D. Cavalli^{67a}, M. Cavalli-Sforza¹⁴, V. Cavasinni^{70a,70b}, E. Celebi^{12b}, L. Cerda Alberich¹⁷²,
 A.S. Cerqueira^{79a}, A. Cerri¹⁵⁴, L. Cerrito^{72a,72b}, F. Cerutti¹⁸, A. Cervelli^{23b,23a}, S.A. Cetin^{12b},
 A. Chafaq^{34a}, D. Chakraborty¹²⁰, S.K. Chan⁵⁸, W.S. Chan¹¹⁹, W.Y. Chan⁸⁹, J.D. Chapman³¹,
 B. Chargeishvili^{157b}, D.G. Charlton²¹, C.C. Chau³³, C.A. Chavez Barajas¹⁵⁴, S. Che¹²⁴,
 A. Chegwidden¹⁰⁵, S. Chekanov⁶, S.V. Chekulaev^{166a}, G.A. Chelkov^{78,au}, M.A. Chelstowska³⁵,
 B. Chen⁷⁷, C. Chen^{59a}, C.H. Chen⁷⁷, H. Chen²⁹, J. Chen^{59a}, J. Chen³⁸, S. Chen¹³⁵, S.J. Chen^{15c},
 X. Chen^{15b,at}, Y. Chen⁸¹, Y.-H. Chen⁴⁵, H.C. Cheng^{62a}, H.J. Cheng^{15d}, A. Cheplakov⁷⁸,
 E. Cheremushkina¹²², R. Cherkaoui El Moursli^{34e}, E. Cheu⁷, K. Cheung⁶³, T.J.A. Chevaléras¹⁴³,
 L. Chevalier¹⁴³, V. Chiarella⁵⁰, G. Chiarelli^{70a}, G. Chiodini^{66a}, A.S. Chisholm^{35,21}, A. Chitan^{27b},
 I. Chiu¹⁶¹, Y.H. Chiu¹⁷⁴, M.V. Chizhov⁷⁸, K. Choi⁶⁴, A.R. Chomont¹³⁰, S. Chouridou¹⁶⁰,
 Y.S. Chow¹¹⁹, M.C. Chu^{62a}, J. Chudoba¹³⁹, A.J. Chuinard¹⁰², J.J. Chwastowski⁸³, L. Chytka¹²⁸,
 D. Cinca⁴⁶, V. Cindro⁹⁰, I.A. Cioară^{27b}, A. Ciocio¹⁸, F. Ciroto^{68a,68b}, Z.H. Citron¹⁷⁸,
 M. Citterio^{67a}, B.M. Ciungu¹⁶⁵, A. Clark⁵³, M.R. Clark³⁸, P.J. Clark⁴⁹, C. Clement^{44a,44b},
 Y. Coadou¹⁰⁰, M. Cobal^{65a,65c}, A. Coccaro^{54b}, J. Cochran⁷⁷, H. Cohen¹⁵⁹, A.E.C. Coimbra¹⁷⁸,
 L. Colasurdo¹¹⁸, B. Cole³⁸, A.P. Colijn¹¹⁹, J. Collot⁵⁷, P. Conde Muiño^{138a,h}, E. Coniavitis⁵¹,

S.H. Connell^{32b}, I.A. Connelly⁵⁶, S. Constantinescu^{27b}, F. Conventi^{68a,aw}, A.M. Cooper-Sarkar¹³³, F. Cormier¹⁷³, K.J.R. Cormier¹⁶⁵, L.D. Corpe⁹³, M. Corradi^{71a,71b}, E.E. Corrigan⁹⁵, F. Corriveau^{102,ac}, A. Cortes-Gonzalez³⁵, M.J. Costa¹⁷², F. Costanza⁵, D. Costanzo¹⁴⁷, G. Cowan⁹², J.W. Cowley³¹, J. Crane⁹⁹, K. Cranmer¹²³, S.J. Crawley⁵⁶, R.A. Creager¹³⁵, S. Crépé-Renaudin⁵⁷, F. Crescioli¹³⁴, M. Cristinziani²⁴, V. Croft¹¹⁹, G. Crosetti^{40b,40a}, A. Cueto⁵, T. Cuhadar Donszelmann¹⁴⁷, A.R. Cukierman¹⁵¹, S. Czekierda⁸³, P. Czodrowski³⁵, M.J. Da Cunha Sargedas De Sousa^{59b}, J.V. Da Fonseca Pinto^{79b}, C. Da Via⁹⁹, W. Dabrowski^{82a}, T. Dado^{28a}, S. Dahbi^{34e}, T. Dai¹⁰⁴, C. Dallapiccola¹⁰¹, M. Dam³⁹, G. D'amen^{23b,23a}, J. Damp⁹⁸, J.R. Dandoy¹³⁵, M.F. Daneri³⁰, N.P. Dang^{179,k}, N.D. Dann⁹⁹, M. Danninger¹⁷³, V. Dao³⁵, G. Darbo^{54b}, O. Dartsis⁵, A. Dattagupta¹²⁹, T. Daubney⁴⁵, S. D'Auria^{67a,67b}, W. Davey²⁴, C. David⁴⁵, T. Davidek¹⁴¹, D.R. Davis⁴⁸, E. Dawe¹⁰³, I. Dawson¹⁴⁷, K. De⁸, R. De Asmundis^{68a}, A. De Benedetti¹²⁶, M. De Beurs¹¹⁹, S. De Castro^{23b,23a}, S. De Cecco^{71a,71b}, N. De Groot¹¹⁸, P. de Jong¹¹⁹, H. De la Torre¹⁰⁵, A. De Maria^{15c}, D. De Pedis^{71a}, A. De Salvo^{71a}, U. De Sanctis^{72a,72b}, M. De Santis^{72a,72b}, A. De Santo¹⁵⁴, K. De Vasconcelos Corga¹⁰⁰, J.B. De Vivie De Regie¹³⁰, C. Debenedetti¹⁴⁴, D.V. Dedovich⁷⁸, M. Del Gaudio^{40b,40a}, J. Del Peso⁹⁷, Y. Delabat Diaz⁴⁵, D. Delgove¹³⁰, F. Deliot¹⁴³, C.M. Delitzsch⁷, M. Della Pietra^{68a,68b}, D. Della Volpe⁵³, A. Dell'Acqua³⁵, L. Dell'Asta²⁵, M. Delmastro⁵, C. Delporte¹³⁰, P.A. Delsart⁵⁷, D.A. DeMarco¹⁶⁵, S. Demers¹⁸¹, M. Demichev⁷⁸, G. Demontigny¹⁰⁸, S.P. Denisov¹²², D. Denysiuk¹¹⁹, L. D'Eramo¹³⁴, D. Derendarz⁸³, J.E. Derkaoui^{34d}, F. Derue¹³⁴, P. Dervan⁸⁹, K. Desch²⁴, C. Deterre⁴⁵, K. Dette¹⁶⁵, M.R. Devesa³⁰, P.O. Deviveiros³⁵, A. Dewhurst¹⁴², S. Dhaliwal²⁶, F.A. Di Bello⁵³, A. Di Ciaccio^{72a,72b}, L. Di Ciaccio⁵, W.K. Di Clemente¹³⁵, C. Di Donato^{68a,68b}, A. Di Girolamo³⁵, G. Di Gregorio^{70a,70b}, B. Di Micco^{73a,73b}, R. Di Nardo¹⁰¹, K.F. Di Petrillo⁵⁸, R. Di Sipio¹⁶⁵, D. Di Valentino³³, C. Diaconu¹⁰⁰, F.A. Dias³⁹, T. Dias Do Vale^{138a,138e}, M.A. Diaz^{145a}, J. Dickinson¹⁸, E.B. Diehl¹⁰⁴, J. Dietrich¹⁹, S. Díez Cornell⁴⁵, A. Dimitrievska¹⁸, W. Ding^{15b}, J. Dingfelder²⁴, F. Dittus³⁵, F. Djama¹⁰⁰, T. Djobava^{157b}, J.I. Djuvsland¹⁷, M.A.B. Do Vale^{79c}, M. Dobre^{27b}, D. Dodsworth²⁶, C. Doglioni⁹⁵, J. Dolejsi¹⁴¹, Z. Dolezal¹⁴¹, M. Donadelli^{79d}, J. Donini³⁷, A. D'Onofrio⁹¹, M. D'Onofrio⁸⁹, J. Dopke¹⁴², A. Doria^{68a}, M.T. Dova⁸⁷, A.T. Doyle⁵⁶, E. Drechsler¹⁵⁰, E. Dreyer¹⁵⁰, T. Dreyer⁵², Y. Du^{59b}, Y. Duan^{59b}, F. Dubinin¹⁰⁹, M. Dubovsky^{28a}, A. Dubreuil⁵³, E. Duchovni¹⁷⁸, G. Duckeck¹¹³, A. Ducourthial¹³⁴, O.A. Ducu^{108,w}, D. Duda¹¹⁴, A. Dudarev³⁵, A.C. Dudder⁹⁸, E.M. Duffield¹⁸, L. Dufflot¹³⁰, M. Dührssen³⁵, C. Dülsen¹⁸⁰, M. Dumancic¹⁷⁸, A.E. Dumitriu^{27b}, A.K. Duncan⁵⁶, M. Dunford^{60a}, A. Duperrin¹⁰⁰, H. Duran Yildiz^{4a}, M. Düren⁵⁵, A. Durglishvili^{157b}, D. Duschinger⁴⁷, B. Dutta⁴⁵, D. Duvnjak¹, G. Dyckes¹³⁵, M. Dyndal⁴⁵, S. Dysch⁹⁹, B.S. Dziedzic⁸³, K.M. Ecker¹¹⁴, R.C. Edgar¹⁰⁴, T. Eifert³⁵, G. Eigen¹⁷, K. Einsweiler¹⁸, T. Ekelof¹⁷⁰, M. El Kacimi^{34c}, R. El Kosseifi¹⁰⁰, V. Ellajosyula¹⁷⁰, M. Ellert¹⁷⁰, F. Ellinghaus¹⁸⁰, A.A. Elliot⁹¹, N. Ellis³⁵, J. Elmsheuser²⁹, M. Elsing³⁵, D. Emeliyanov¹⁴², A. Emerman³⁸, Y. Enari¹⁶¹, J.S. Ennis¹⁷⁶, M.B. Epland⁴⁸, J. Erdmann⁴⁶, A. Ereditato²⁰, M. Escalier¹³⁰, C. Escobar¹⁷², O. Estrada Pastor¹⁷², A.I. Etienvre¹⁴³, E. Etzion¹⁵⁹, H. Evans⁶⁴, A. Ezhilov¹³⁶, M. Ezzi^{34e}, F. Fabbri⁵⁶, L. Fabbri^{23b,23a}, V. Fabiani¹¹⁸, G. Facini⁹³, R.M. Faisca Rodrigues Pereira^{138a}, R.M. Fakhruddinov¹²², S. Falciano^{71a}, P.J. Falke⁵, S. Falke⁵, J. Faltova¹⁴¹, Y. Fang^{15a}, Y. Fang^{15a}, G. Fanourakis⁴³, M. Fanti^{67a,67b}, A. Farbin⁸, A. Farilla^{73a}, E.M. Farina^{69a,69b}, T. Farooque¹⁰⁵, S. Farrell¹⁸, S.M. Farrington¹⁷⁶, P. Farthouat³⁵, F. Fassi^{34e}, P. Fassnacht³⁵, D. Fassouliotis⁹, M. Faucci Giannelli⁴⁹, W.J. Fawcett³¹, L. Fayard¹³⁰, O.L. Fedin^{136,p}, W. Fedorko¹⁷³, M. Feickert⁴¹, S. Feigl¹³², L. Feligioni¹⁰⁰, A. Fell¹⁴⁷, C. Feng^{59b}, E.J. Feng³⁵, M. Feng⁴⁸, M.J. Fenton⁵⁶, A.B. Fenyuk¹²², J. Ferrando⁴⁵, A. Ferrari¹⁷⁰, P. Ferrari¹¹⁹, R. Ferrari^{69a}, D.E. Ferreira de Lima^{60b}, A. Ferrer¹⁷², D. Ferrere⁵³, C. Ferretti¹⁰⁴, F. Fiedler⁹⁸, A. Filipčić⁹⁰, F. Filthaut¹¹⁸, K.D. Finelli²⁵, M.C.N. Fiolhais^{138a,a}, L. Fiorini¹⁷², C. Fischer¹⁴,

F. Fischer¹¹³, W.C. Fisher¹⁰⁵, I. Fleck¹⁴⁹, P. Fleischmann¹⁰⁴, R.R.M. Fletcher¹³⁵, T. Flick¹⁸⁰, B.M. Flierl¹¹³, L.M. Flores¹³⁵, L.R. Flores Castillo^{62a}, F.M. Follega^{74a,74b}, N. Fomin¹⁷, G.T. Forcolin^{74a,74b}, A. Formica¹⁴³, F.A. Förster¹⁴, A.C. Forti⁹⁹, A.G. Foster²¹, D. Fournier¹³⁰, H. Fox⁸⁸, S. Fracchia¹⁴⁷, P. Francavilla^{70a,70b}, M. Franchini^{23b,23a}, S. Franchino^{60a}, D. Francis³⁵, L. Franconi²⁰, M. Franklin⁵⁸, M. Frate¹⁶⁹, A.N. Fray⁹¹, B. Freund¹⁰⁸, W.S. Freund^{79b}, E.M. Freundlich⁴⁶, D.C. Frizzell¹²⁶, D. Froidevaux³⁵, J.A. Frost¹³³, C. Fukunaga¹⁶², E. Fullana Torregrosa¹⁷², E. Fumagalli^{54b,54a}, T. Fusayasu¹¹⁵, J. Fuster¹⁷², A. Gabrielli^{23b,23a}, A. Gabrielli¹⁸, G.P. Gach^{82a}, S. Gadatsch⁵³, P. Gadow¹¹⁴, G. Gagliardi^{54b,54a}, L.G. Gagnon¹⁰⁸, C. Galea^{27b}, B. Galhardo^{138a,138c}, E.J. Gallas¹³³, B.J. Gallop¹⁴², P. Gallus¹⁴⁰, G. Galster³⁹, R. Gamboa Goni⁹¹, K.K. Gan¹²⁴, S. Ganguly¹⁷⁸, J. Gao^{59a}, Y. Gao⁸⁹, Y.S. Gao^{151,m}, C. García¹⁷², J.E. García Navarro¹⁷², J.A. García Pascual^{15a}, C. Garcia-Argos⁵¹, M. Garcia-Sciveres¹⁸, R.W. Gardner³⁶, N. Garelli¹⁵¹, S. Gargiulo⁵¹, V. Garonne¹³², A. Gaudiello^{54b,54a}, G. Gaudio^{69a}, I.L. Gavrilenko¹⁰⁹, A. Gavriluk¹¹⁰, C. Gay¹⁷³, G. Gaycken²⁴, E.N. Gazis¹⁰, C.N.P. Gee¹⁴², J. Geisen⁵², M. Geisen⁹⁸, M.P. Geisler^{60a}, C. Gemme^{54b}, M.H. Genest⁵⁷, C. Geng¹⁰⁴, S. Gentile^{71a,71b}, S. George⁹², T. Gerialis⁴³, D. Gerbaudo¹⁴, L.O. Gerlach⁵², G. Gessner⁴⁶, S. Ghasemi¹⁴⁹, M. Ghasemi Bostanabad¹⁷⁴, M. Ghneimat²⁴, A. Ghosh⁷⁶, B. Giacobbe^{23b}, S. Giagu^{71a,71b}, N. Giangiacomi^{23b,23a}, P. Giannetti^{70a}, A. Giannini^{68a,68b}, S.M. Gibson⁹², M. Gignac¹⁴⁴, D. Gillberg³³, G. Gilles¹⁸⁰, D.M. Gingrich^{3,av}, M.P. Giordani^{65a,65c}, F.M. Giorgi^{23b}, P.F. Giraud¹⁴³, G. Giugliarelli^{65a,65c}, D. Giugni^{67a}, F. Giuli¹³³, M. Giulini^{60b}, S. Gkaitatzis¹⁶⁰, I. Gkialas^{9,j}, E.L. Gkoukousis¹⁴, P. Gkoutoumis¹⁰, L.K. Gladilin¹¹², C. Glasman⁹⁷, J. Glatzer¹⁴, P.C.F. Glaysheer⁴⁵, A. Glazov⁴⁵, M. Goblirsch-Kolb²⁶, S. Goldfarb¹⁰³, T. Golling⁵³, D. Golubkov¹²², A. Gomes^{138a,138b}, R. Goncalves Gama⁵², R. Gonçalo^{138a,138b}, G. Gonella⁵¹, L. Gonella²¹, A. Gongadze⁷⁸, F. Gonnella²¹, J.L. Gonski⁵⁸, S. González de la Hoz¹⁷², S. Gonzalez-Sevilla⁵³, G.R. Gonzalvo Rodriguez¹⁷², L. Goossens³⁵, P.A. Gorbounov¹¹⁰, H.A. Gordon²⁹, B. Gorini³⁵, E. Gorini^{66a,66b}, A. Gorišek⁹⁰, A.T. Goshaw⁴⁸, C. Gössling⁴⁶, M.I. Gostkin⁷⁸, C.A. Gottardo²⁴, C.R. Goudet¹³⁰, M. Gouighri^{34a}, D. Goujdami^{34c}, A.G. Goussiou¹⁴⁶, N. Govender^{32b,c}, C. Goy⁵, E. Gozani¹⁵⁸, I. Grabowska-Bold^{82a}, P.O.J. Gradin¹⁷⁰, E.C. Graham⁸⁹, J. Gramling¹⁶⁹, E. Gramstad¹³², S. Grancagnolo¹⁹, M. Grandi¹⁵⁴, V. Gratchev¹³⁶, P.M. Gravila^{27f}, F.G. Gravili^{66a,66b}, C. Gray⁵⁶, H.M. Gray¹⁸, C. Grefe²⁴, K. Gregersen⁹⁵, I.M. Gregor⁴⁵, P. Grenier¹⁵¹, K. Grevtsov⁴⁵, N.A. Grieser¹²⁶, J. Griffiths⁸, A.A. Grillo¹⁴⁴, K. Grimm^{151,b}, S. Grinstein^{14,x}, J.-F. Grivaz¹³⁰, S. Groh⁹⁸, E. Gross¹⁷⁸, J. Grosse-Knetter⁵², Z.J. Grout⁹³, C. Grud¹⁰⁴, A. Grummer¹¹⁷, L. Guan¹⁰⁴, W. Guan¹⁷⁹, J. Guenther³⁵, A. Guerguichon¹³⁰, F. Guescini^{166a}, D. Guest¹⁶⁹, R. Gugel⁵¹, B. Gui¹²⁴, T. Guillemin⁵, S. Guindon³⁵, U. Gul⁵⁶, J. Guo^{59c}, W. Guo¹⁰⁴, Y. Guo^{59a,s}, Z. Guo¹⁰⁰, R. Gupta⁴⁵, S. Gurbuz^{12c}, G. Gustavino¹²⁶, P. Gutierrez¹²⁶, C. Gutsche⁹³, C. Guyot¹⁴³, M.P. Guzik^{82a}, C. Gwenlan¹³³, C.B. Gwilliam⁸⁹, A. Haas¹²³, C. Haber¹⁸, H.K. Hadavand⁸, N. Haddad^{34e}, A. Hadeef^{59a}, S. Hageböck³⁵, M. Hagihara¹⁶⁷, M. Haleem¹⁷⁵, J. Haley¹²⁷, G. Halladjian¹⁰⁵, G.D. Hallewell¹⁰⁰, K. Hamacher¹⁸⁰, P. Hamal¹²⁸, K. Hamano¹⁷⁴, H. Hamdaoui^{34e}, G.N. Hamity¹⁴⁷, K. Han^{59a,aj}, L. Han^{59a}, S. Han^{15d}, K. Hanagaki^{80,u}, M. Hance¹⁴⁴, D.M. Handl¹¹³, B. Haney¹³⁵, R. Hankache¹³⁴, P. Hanke^{60a}, E. Hansen⁹⁵, J.B. Hansen³⁹, J.D. Hansen³⁹, M.C. Hansen²⁴, P.H. Hansen³⁹, E.C. Hanson⁹⁹, K. Hara¹⁶⁷, A.S. Hard¹⁷⁹, T. Harenberg¹⁸⁰, S. Harkusha¹⁰⁶, P.F. Harrison¹⁷⁶, N.M. Hartmann¹¹³, Y. Hasegawa¹⁴⁸, A. Hasib⁴⁹, S. Hassani¹⁴³, S. Haug²⁰, R. Hauser¹⁰⁵, L. Hauswald⁴⁷, L.B. Havener³⁸, M. Havranek¹⁴⁰, C.M. Hawkes²¹, R.J. Hawkins³⁵, D. Hayden¹⁰⁵, C. Hayes¹⁵³, R.L. Hayes¹⁷³, C.P. Hays¹³³, J.M. Hays⁹¹, H.S. Hayward⁸⁹, S.J. Haywood¹⁴², F. He^{59a}, M.P. Heath⁴⁹, V. Hedberg⁹⁵, L. Heelan⁸, S. Heer²⁴, K.K. Heidegger⁵¹, J. Heilman³³, S. Heim⁴⁵, T. Heim¹⁸, B. Heinemann^{45,aq}, J.J. Heinrich¹²⁹, L. Heinrich³⁵, C. Heinz⁵⁵, J. Hejbal¹³⁹, L. Helary^{60b}, A. Held¹⁷³, S. Hellesund¹³², C.M. Helling¹⁴⁴, S. Hellman^{44a,44b},

C. Helsens³⁵, R.C.W. Henderson⁸⁸, Y. Heng¹⁷⁹, S. Henkelmann¹⁷³, A.M. Henriques Correia³⁵, G.H. Herbert¹⁹, H. Herde²⁶, V. Herget¹⁷⁵, Y. Hernández Jiménez^{32c}, H. Herr⁹⁸, M.G. Herrmann¹¹³, T. Herrmann⁴⁷, G. Herten⁵¹, R. Hertenberger¹¹³, L. Hervas³⁵, T.C. Herwig¹³⁵, G.G. Hesketh⁹³, N.P. Hessey^{166a}, A. Higashida¹⁶¹, S. Higashino⁸⁰, E. Higón-Rodríguez¹⁷², K. Hildebrand³⁶, E. Hill¹⁷⁴, J.C. Hill³¹, K.K. Hill²⁹, K.H. Hiller⁴⁵, S.J. Hillier²¹, M. Hils⁴⁷, I. Hinchliffe¹⁸, F. Hinterkeuser²⁴, M. Hirose¹³¹, S. Hirose⁵¹, D. Hirschbuehl¹⁸⁰, B. Hiti⁹⁰, O. Hladik¹³⁹, D.R. Hlaluku^{32c}, X. Hoad⁴⁹, J. Hobbs¹⁵³, N. Hod¹⁷⁸, M.C. Hodgkinson¹⁴⁷, A. Hoecker³⁵, F. Hoenig¹¹³, D. Hohn⁵¹, D. Hohov¹³⁰, T.R. Holmes³⁶, M. Holzbock¹¹³, L.B.A.H. Hommels³¹, S. Honda¹⁶⁷, T. Honda⁸⁰, T.M. Hong¹³⁷, A. Hönle¹¹⁴, B.H. Hooberman¹⁷¹, W.H. Hopkins⁶, Y. Horii¹¹⁶, P. Horn⁴⁷, A.J. Horton¹⁵⁰, L.A. Horyn³⁶, J.-Y. Hostachy⁵⁷, A. Hostiuc¹⁴⁶, S. Hou¹⁵⁶, A. Hoummada^{34a}, J. Howarth⁹⁹, J. Hoya⁸⁷, M. Hrabovsky¹²⁸, J. Hrdinka⁷⁵, I. Hristova¹⁹, J. Hrivnac¹³⁰, A. Hrynevich¹⁰⁷, T. Hryn'ova⁵, P.J. Hsu⁶³, S.-C. Hsu¹⁴⁶, Q. Hu²⁹, S. Hu^{59c}, Y. Huang^{15a}, Z. Hubacek¹⁴⁰, F. Hubaut¹⁰⁰, M. Huebner²⁴, F. Huegging²⁴, T.B. Huffman¹³³, M. Huhtinen³⁵, R.F.H. Hunter³³, P. Huo¹⁵³, A.M. Hupe³³, N. Huseynov^{78,ae}, J. Huston¹⁰⁵, J. Huth⁵⁸, R. Hyneman¹⁰⁴, S. Hyrych^{28a}, G. Iacobucci⁵³, G. Iakovidis²⁹, I. Ibragimov¹⁴⁹, L. Iconomidou-Fayard¹³⁰, Z. Idrissi^{34e}, P. Iengo³⁵, R. Ignazzi³⁹, O. Igonkina^{119,z}, R. Iguchi¹⁶¹, T. Iizawa⁵³, Y. Ikegami⁸⁰, M. Ikeno⁸⁰, D. Iliadis¹⁶⁰, N. Ilic¹¹⁸, F. Iltzsche⁴⁷, G. Introzzi^{69a,69b}, M. Iodice^{73a}, K. Iordanidou³⁸, V. Ippolito^{71a,71b}, M.F. Isacson¹⁷⁰, N. Ishijima¹³¹, M. Ishino¹⁶¹, M. Ishitsuka¹⁶³, W. Islam¹²⁷, C. Issever¹³³, S. Istin¹⁵⁸, F. Ito¹⁶⁷, J.M. Iturbe Ponce^{62a}, R. Iuppa^{74a,74b}, A. Ivina¹⁷⁸, H. Iwasaki⁸⁰, J.M. Izen⁴², V. Izzo^{68a}, P. Jacka¹³⁹, P. Jackson¹, R.M. Jacobs²⁴, V. Jain², G. Jäkel¹⁸⁰, K.B. Jakobi⁹⁸, K. Jakobs⁵¹, S. Jakobsen⁷⁵, T. Jakoubek¹³⁹, J. Jamieson⁵⁶, D.O. Jamin¹²⁷, R. Jansky⁵³, J. Janssen²⁴, M. Janus⁵², P.A. Janus^{82a}, G. Jarlskog⁹⁵, N. Javadov^{78,ae}, T. Javůrek³⁵, M. Javurkova⁵¹, F. Jeanneau¹⁴³, L. Jeanty¹²⁹, J. Jejelava^{157a,af}, A. Jelinskas¹⁷⁶, P. Jenni^{51,d}, J. Jeong⁴⁵, N. Jeong⁴⁵, S. Jézéquel⁵, H. Ji¹⁷⁹, J. Jia¹⁵³, H. Jiang⁷⁷, Y. Jiang^{59a}, Z. Jiang^{151,q}, S. Jiggins⁵¹, F.A. Jimenez Morales³⁷, J. Jimenez Pena¹⁷², S. Jin^{15c}, A. Jinaru^{27b}, O. Jinnouchi¹⁶³, H. Jivan^{32c}, P. Johansson¹⁴⁷, K.A. Johns⁷, C.A. Johnson⁶⁴, K. Jon-And^{44a,44b}, R.W.L. Jones⁸⁸, S.D. Jones¹⁵⁴, S. Jones⁷, T.J. Jones⁸⁹, J. Jongmanns^{60a}, P.M. Jorge^{138a,138b}, J. Jovicevic^{166a}, X. Ju¹⁸, J.J. Junggeburth¹¹⁴, A. Juste Rozas^{14,x}, A. Kaczmarska⁸³, M. Kado¹³⁰, H. Kagan¹²⁴, M. Kagan¹⁵¹, T. Kaji¹⁷⁷, E. Kajomovitz¹⁵⁸, C.W. Kalderon⁹⁵, A. Kaluza⁹⁸, A. Kamenshchikov¹²², L. Kanjir⁹⁰, Y. Kano¹⁶¹, V.A. Kantserov¹¹¹, J. Kanzaki⁸⁰, L.S. Kaplan¹⁷⁹, D. Kar^{32c}, M.J. Kareem^{166b}, E. Karentzos¹⁰, S.N. Karpov⁷⁸, Z.M. Karpova⁷⁸, V. Kartvelishvili⁸⁸, A.N. Karyukhin¹²², L. Kashif¹⁷⁹, R.D. Kass¹²⁴, A. Kastanas^{44a,44b}, Y. Kataoka¹⁶¹, C. Kato^{59d,59c}, J. Katzy⁴⁵, K. Kawade⁸¹, K. Kawagoe⁸⁶, T. Kawaguchi¹¹⁶, T. Kawamoto¹⁶¹, G. Kawamura⁵², E.F. Kay¹⁷⁴, V.F. Kazanin^{121b,121a}, R. Keeler¹⁷⁴, R. Kehoe⁴¹, J.S. Keller³³, E. Kellermann⁹⁵, J.J. Kempster²¹, J. Kendrick²¹, O. Kepka¹³⁹, S. Kersten¹⁸⁰, B.P. Kerševan⁹⁰, S. Ketabchi Haghighat¹⁶⁵, R.A. Keyes¹⁰², M. Khader¹⁷¹, F. Khalil-Zada¹³, A. Khanov¹²⁷, A.G. Kharlamov^{121b,121a}, T. Kharlamova^{121b,121a}, E.E. Khoda¹⁷³, A. Khodinov¹⁶⁴, T.J. Khoo⁵³, E. Khramov⁷⁸, J. Khubua^{157b}, S. Kido⁸¹, M. Kiehn⁵³, C.R. Kilby⁹², Y.K. Kim³⁶, N. Kimura^{65a,65c}, O.M. Kind¹⁹, B.T. King⁸⁹, D. Kirchmeier⁴⁷, J. Kirk¹⁴², A.E. Kiryunin¹¹⁴, T. Kishimoto¹⁶¹, V. Kitali⁴⁵, O. Kivernyk⁵, E. Kladiva^{28b,*}, T. Klapdor-Kleingrothaus⁵¹, M.H. Klein¹⁰⁴, M. Klein⁸⁹, U. Klein⁸⁹, K. Kleinknecht⁹⁸, P. Klimek¹²⁰, A. Klimentov²⁹, T. Klingl²⁴, T. Klioutchnikova³⁵, F.F. Klitzner¹¹³, P. Kluit¹¹⁹, S. Kluth¹¹⁴, E. Kneringer⁷⁵, E.B.F.G. Knoops¹⁰⁰, A. Knue⁵¹, D. Kobayashi⁸⁶, T. Kobayashi¹⁶¹, M. Kobel⁴⁷, M. Kocian¹⁵¹, P. Kodys¹⁴¹, P.T. Koenig²⁴, T. Koffas³³, N.M. Köhler¹¹⁴, T. Koi¹⁵¹, M. Kolb^{60b}, I. Koletsou⁵, T. Kondo⁸⁰, N. Kondrashova^{59c}, K. Köneke⁵¹, A.C. König¹¹⁸, T. Kono⁸⁰, R. Konoplich^{123,am}, V. Konstantinides⁹³, N. Konstantinidis⁹³, B. Konya⁹⁵, R. Kopeliansky⁶⁴, S. Koperny^{82a}, K. Korcyl⁸³, K. Kordas¹⁶⁰, G. Koren¹⁵⁹, A. Korn⁹³, I. Korolkov¹⁴, E.V. Korolkova¹⁴⁷,

N. Korotkova¹¹², O. Kortner¹¹⁴, S. Kortner¹¹⁴, T. Kosek¹⁴¹, V.V. Kostyukhin²⁴, A. Kotwal⁴⁸,
 A. Koulouris¹⁰, A. Kourkoumeli-Charalampidi^{69a,69b}, C. Kourkoumelis⁹, E. Kourlitis¹⁴⁷,
 V. Kouskoura²⁹, A.B. Kowalewska⁸³, R. Kowalewski¹⁷⁴, C. Kozakai¹⁶¹, W. Kozanecki¹⁴³,
 A.S. Kozhin¹²², V.A. Kramarenko¹¹², G. Kramberger⁹⁰, D. Krasnopevtsev^{59a}, M.W. Krasny¹³⁴,
 A. Krasznahorkay³⁵, D. Krauss¹¹⁴, J.A. Kremer^{82a}, J. Kretzschmar⁸⁹, P. Krieger¹⁶⁵,
 A. Krishnan^{60b}, K. Krizka¹⁸, K. Kroeninger⁴⁶, H. Kroha¹¹⁴, J. Kroll¹³⁹, J. Kroll¹³⁵, J. Krstic¹⁶,
 U. Kruchonak⁷⁸, H. Krüger²⁴, N. Krumnack⁷⁷, M.C. Kruse⁴⁸, T. Kubota¹⁰³, S. Kuday^{4b},
 J.T. Kuechler⁴⁵, S. Kuehn³⁵, A. Kugel^{60a}, T. Kuhl⁴⁵, V. Kukhtin⁷⁸, R. Kukla¹⁰⁰,
 Y. Kulchitsky^{106,ai}, S. Kuleshov^{145b}, Y.P. Kulinich¹⁷¹, M. Kuna⁵⁷, T. Kunigo⁸⁴, A. Kupco¹³⁹,
 T. Kupfer⁴⁶, O. Kuprash⁵¹, H. Kurashige⁸¹, L.L. Kurchaninov^{166a}, Y.A. Kurochkin¹⁰⁶,
 A. Kurova¹¹¹, M.G. Kurth^{15d}, E.S. Kuwertz³⁵, M. Kuze¹⁶³, A.K. Kvam¹⁴⁶, J. Kvita¹²⁸,
 T. Kwan¹⁰², A. La Rosa¹¹⁴, J.L. La Rosa Navarro^{79d}, L. La Rotonda^{40b,40a}, F. La Ruffa^{40b,40a},
 C. Lacasta¹⁷², F. Lacava^{71a,71b}, D.P.J. Lack⁹⁹, H. Lacker¹⁹, D. Lacour¹³⁴, E. Ladygin⁷⁸,
 R. Lafaye⁵, B. Laforge¹³⁴, T. Lagouri^{32c}, S. Lai⁵², S. Lammers⁶⁴, W. Lampl⁷, E. Lançon²⁹,
 U. Landgraf⁵¹, M.P.J. Landon⁹¹, M.C. Lanfermann⁵³, V.S. Lang⁴⁵, J.C. Lange⁵²,
 R.J. Langenberg³⁵, A.J. Lankford¹⁶⁹, F. Lanni²⁹, K. Lantzsch²⁴, A. Lanza^{69a}, A. Lapertosa^{54b,54a},
 S. Laplace¹³⁴, J.F. Laporte¹⁴³, T. Lari^{67a}, F. Lasagni Manghi^{23b,23a}, M. Lassnig³⁵, T.S. Lau^{62a},
 A. Laudrain¹³⁰, A. Laurier³³, M. Lavorgna^{68a,68b}, M. Lazzaroni^{67a,67b}, B. Le¹⁰³, O. Le Dortz¹³⁴,
 E. Le Guirriec¹⁰⁰, M. LeBlanc⁷, T. LeCompte⁶, F. Ledroit-Guillon⁵⁷, C.A. Lee²⁹, G.R. Lee^{145a},
 L. Lee⁵⁸, S.C. Lee¹⁵⁶, S.J. Lee³³, B. Lefebvre^{166a}, M. Lefebvre¹⁷⁴, F. Legger¹¹³, C. Leggett¹⁸,
 K. Lehmann¹⁵⁰, N. Lehmann¹⁸⁰, G. Lehmann Miotto³⁵, W.A. Leight⁴⁵, A. Leisos^{160,v},
 M.A.L. Leite^{79d}, R. Leitner¹⁴¹, D. Lellouch¹⁷⁸, K.J.C. Leney⁴¹, T. Lenz²⁴, B. Lenzi³⁵, R. Leone⁷,
 S. Leone^{70a}, C. Leonidopoulos⁴⁹, A. Leopold¹³⁴, G. Lerner¹⁵⁴, C. Leroy¹⁰⁸, R. Les¹⁶⁵,
 C.G. Lester³¹, M. Levchenko¹³⁶, J. Levêque⁵, D. Levin¹⁰⁴, L.J. Levinson¹⁷⁸, D.J. Lewis²¹,
 B. Li^{15b}, B. Li¹⁰⁴, C-Q. Li^{59a,al}, F. Li^{59c}, H. Li^{59a}, H. Li^{59b}, J. Li^{59c}, K. Li¹⁵¹, L. Li^{59c}, M. Li^{15a},
 Q. Li^{15d}, Q.Y. Li^{59a}, S. Li^{59d,59c}, X. Li⁴⁵, Y. Li⁴⁵, Z. Liang^{15a}, B. Liberti^{72a}, A. Liblong¹⁶⁵,
 K. Lie^{62c}, S. Liem¹¹⁹, C.Y. Lin³¹, K. Lin¹⁰⁵, T.H. Lin⁹⁸, R.A. Linck⁶⁴, J.H. Lindon²¹,
 A.L. Lioni⁵³, E. Lipeles¹³⁵, A. Lipniacka¹⁷, M. Lisovsky^{60b}, T.M. Liss^{171,as}, A. Lister¹⁷³,
 A.M. Litke¹⁴⁴, J.D. Little⁸, B. Liu⁷⁷, B.L. Liu⁶, H.B. Liu²⁹, H. Liu¹⁰⁴, J.B. Liu^{59a}, J.K.K. Liu¹³³,
 K. Liu¹³⁴, M. Liu^{59a}, P. Liu¹⁸, Y. Liu^{15d}, Y.L. Liu¹⁰⁴, Y.W. Liu^{59a}, M. Livan^{69a,69b}, A. Lleres⁵⁷,
 J. Llorente Merino^{15a}, S.L. Lloyd⁹¹, C.Y. Lo^{62b}, F. Lo Sterzo⁴¹, E.M. Lobodzinska⁴⁵, P. Loch⁷,
 S. Loffredo^{72a,72b}, T. Lohse¹⁹, K. Lohwasser¹⁴⁷, M. Lokajicek¹³⁹, J.D. Long¹⁷¹, R.E. Long⁸⁸,
 L. Longo³⁵, K.A. Looper¹²⁴, J.A. Lopez^{145b}, I. Lopez Paz⁹⁹, A. Lopez Solis¹⁴⁷, J. Lorenz¹¹³,
 N. Lorenzo Martinez⁵, M. Losada²², P.J. Lösel¹¹³, A. Lösle⁵¹, X. Lou⁴⁵, X. Lou^{15a}, A. Lounis¹³⁰,
 J. Love⁶, P.A. Love⁸⁸, J.J. Lozano Bahilo¹⁷², H. Lu^{62a}, M. Lu^{59a}, Y.J. Lu⁶³, H.J. Lubatti¹⁴⁶,
 C. Luci^{71a,71b}, A. Lucotte⁵⁷, C. Luedtke⁵¹, F. Luehring⁶⁴, I. Luise¹³⁴, L. Luminari^{71a},
 B. Lund-Jensen¹⁵², M.S. Lutz¹⁰¹, D. Lynn²⁹, R. Lysak¹³⁹, E. Lytken⁹⁵, F. Lyu^{15a},
 V. Lyubushkin⁷⁸, T. Lyubushkina⁷⁸, H. Ma²⁹, L.L. Ma^{59b}, Y. Ma^{59b}, G. Maccarrone⁵⁰,
 A. Macchiolo¹¹⁴, C.M. Macdonald¹⁴⁷, J. Machado Miguens^{135,138b}, D. Madaffari¹⁷², R. Madar³⁷,
 W.F. Mader⁴⁷, N. Madysa⁴⁷, J. Maeda⁸¹, K. Maekawa¹⁶¹, S. Maeland¹⁷, T. Maeno²⁹,
 M. Maerker⁴⁷, A.S. Maevskiy¹¹², V. Magerl⁵¹, N. Magini⁷⁷, D.J. Mahon³⁸, C. Maidantchik^{79b},
 T. Maier¹¹³, A. Maio^{138a,138b,138d}, O. Majersky^{28a}, S. Majewski¹²⁹, Y. Makida⁸⁰, N. Makovec¹³⁰,
 B. Malaescu¹³⁴, Pa. Malecki⁸³, V.P. Maleev¹³⁶, F. Malek⁵⁷, U. Mallik⁷⁶, D. Malon⁶, C. Malone³¹,
 S. Maltezos¹⁰, S. Malyukov³⁵, J. Mamuzic¹⁷², G. Mancini⁵⁰, I. Mandić⁹⁰,
 L. Manhaes de Andrade Filho^{79a}, I.M. Maniatis¹⁶⁰, J. Manjarres Ramos⁴⁷, K.H. Mankinen⁹⁵,
 A. Mann¹¹³, A. Manousos⁷⁵, B. Mansoulie¹⁴³, I. Manthos¹⁶⁰, S. Manzoni¹¹⁹, A. Marantis¹⁶⁰,
 G. Marceca³⁰, L. Marchese¹³³, G. Marchiori¹³⁴, M. Marcisovsky¹³⁹, C. Marcon⁹⁵,
 C.A. Marin Tobon³⁵, M. Marjanovic³⁷, F. Marroquim^{79b}, Z. Marshall¹⁸, M.U.F. Martensson¹⁷⁰,

S. Marti-Garcia¹⁷², C.B. Martin¹²⁴, T.A. Martin¹⁷⁶, V.J. Martin⁴⁹, B. Martin dit Latour¹⁷, M. Martinez^{14,x}, V.I. Martinez Outschoorn¹⁰¹, S. Martin-Haugh¹⁴², V.S. Martoio^{27b}, A.C. Martyniuk⁹³, A. Marzin³⁵, L. Masetti⁹⁸, T. Mashimo¹⁶¹, R. Mashinistov¹⁰⁹, J. Masik⁹⁹, A.L. Maslennikov^{121b,121a}, L.H. Mason¹⁰³, L. Massa^{72a,72b}, P. Massarotti^{68a,68b}, P. Mastrandrea^{70a,70b}, A. Mastroberardino^{40b,40a}, T. Masubuchi¹⁶¹, A. Matic¹¹³, P. Mättig²⁴, J. Maurer^{27b}, B. Maček⁹⁰, S.J. Maxfield⁸⁹, D.A. Maximov^{121b,121a}, R. Mazini¹⁵⁶, I. Maznas¹⁶⁰, S.M. Mazza¹⁴⁴, S.P. Mc Kee¹⁰⁴, A. McCarn, Deiana⁴¹, T.G. McCarthy¹¹⁴, L.I. McClymont⁹³, W.P. McCormack¹⁸, E.F. McDonald¹⁰³, J.A. Mcfayden³⁵, G. Mchedlidze⁵², M.A. McKay⁴¹, K.D. McLean¹⁷⁴, S.J. McMahon¹⁴², P.C. McNamara¹⁰³, C.J. McNicol¹⁷⁶, R.A. McPherson^{174,ac}, J.E. Mdhluli^{32c}, Z.A. Meadows¹⁰¹, S. Meehan¹⁴⁶, T.M. Megy⁵¹, S. Mehlhase¹¹³, A. Mehta⁸⁹, T. Meideck⁵⁷, B. Meirose⁴², D. Melini¹⁷², B.R. Mellado Garcia^{32c}, J.D. Mellenthin⁵², M. Melo^{28a}, F. Meloni⁴⁵, A. Melzer²⁴, S.B. Menary⁹⁹, E.D. Mendes Gouveia^{138a,138e}, L. Meng³⁵, X.T. Meng¹⁰⁴, S. Menke¹¹⁴, E. Meoni^{40b,40a}, S. Mergelmeyer¹⁹, S.A.M. Merkt¹³⁷, C. Merlassino²⁰, P. Mermod⁵³, L. Merola^{68a,68b}, C. Meroni^{67a}, O. Meshkov¹¹², J.K.R. Meshreki¹⁴⁹, A. Messina^{71a,71b}, J. Metcalfe⁶, A.S. Mete¹⁶⁹, C. Meyer⁶⁴, J. Meyer¹⁵⁸, J-P. Meyer¹⁴³, H. Meyer Zu Theenhausen^{60a}, F. Miano¹⁵⁴, R.P. Middleton¹⁴², L. Mijović⁴⁹, G. Mikenberg¹⁷⁸, M. Mikesikova¹³⁹, M. Mikuz⁹⁰, H. Mildner¹⁴⁷, M. Milesi¹⁰³, A. Milic¹⁶⁵, D.A. Millar⁹¹, D.W. Miller³⁶, A. Milov¹⁷⁸, D.A. Milstead^{44a,44b}, R.A. Mina^{151,q}, A.A. Minaenko¹²², M. Miñano Moya¹⁷², I.A. Minashvili^{157b}, A.I. Mincer¹²³, B. Mindur^{82a}, M. Mineev⁷⁸, Y. Minegishi¹⁶¹, Y. Ming¹⁷⁹, L.M. Mir¹⁴, A. Mirto^{66a,66b}, K.P. Mistry¹³⁵, T. Mitani¹⁷⁷, J. Mitrevski¹¹³, V.A. Mitsou¹⁷², M. Mittal^{59c}, A. Miucci²⁰, P.S. Miyagawa¹⁴⁷, A. Mizukami⁸⁰, J.U. Mjörnmark⁹⁵, T. Mkrtchyan¹⁸², M. Mlynarikova¹⁴¹, T. Moa^{44a,44b}, K. Mochizuki¹⁰⁸, P. Mogg⁵¹, S. Mohapatra³⁸, R. Moles-Valls²⁴, M.C. Mondragon¹⁰⁵, K. Mönig⁴⁵, J. Monk³⁹, E. Monnier¹⁰⁰, A. Montalbano¹⁵⁰, J. Montejo Berlingen³⁵, M. Montella⁹³, F. Monticelli⁸⁷, S. Monzani^{67a}, N. Morange¹³⁰, D. Moreno²², M. Moreno Llácer³⁵, P. Morettini^{54b}, M. Morgenstern¹¹⁹, S. Morgenstern⁴⁷, D. Mori¹⁵⁰, M. Morii⁵⁸, M. Morinaga¹⁷⁷, V. Morisbak¹³², A.K. Morley³⁵, G. Mornacchi³⁵, A.P. Morris⁹³, L. Morvaj¹⁵³, P. Moschovakos¹⁰, B. Moser¹¹⁹, M. Mosidze^{157b}, H.J. Moss¹⁴⁷, J. Moss^{151,n}, K. Motohashi¹⁶³, E. Mountricha³⁵, E.J.W. Moyse¹⁰¹, S. Muanza¹⁰⁰, F. Mueller¹¹⁴, J. Mueller¹³⁷, R.S.P. Mueller¹¹³, D. Muenstermann⁸⁸, G.A. Mullier⁹⁵, J.L. Munoz Martinez¹⁴, F.J. Munoz Sanchez⁹⁹, P. Murin^{28b}, W.J. Murray^{176,142}, A. Murrone^{67a,67b}, M. Muškinja¹⁸, C. Mwewa^{32a}, A.G. Myagkov^{122,an}, J. Myers¹²⁹, M. Myska¹⁴⁰, B.P. Nachman¹⁸, O. Nackenhorst⁴⁶, A.Nag Nag⁴⁷, K. Nagai¹³³, K. Nagano⁸⁰, Y. Nagasaka⁶¹, M. Nagel⁵¹, E. Nagy¹⁰⁰, A.M. Nairz³⁵, Y. Nakahama¹¹⁶, K. Nakamura⁸⁰, T. Nakamura¹⁶¹, I. Nakano¹²⁵, H. Nanjo¹³¹, F. Napolitano^{60a}, R.F. Naranjo Garcia⁴⁵, R. Narayan¹¹, D.I. Narrias Villar^{60a}, I. Naryshkin¹³⁶, T. Naumann⁴⁵, G. Navarro²², H.A. Neal^{104,*}, P.Y. Nechaeva¹⁰⁹, F. Nechansky⁴⁵, T.J. Neep²¹, A. Negri^{69a,69b}, M. Negrini^{23b}, S. Nektarijevic¹¹⁸, C. Nellist⁵², M.E. Nelson¹³³, S. Nemecek¹³⁹, P. Nemethy¹²³, M. Nessi^{35,f}, M.S. Neubauer¹⁷¹, M. Neumann¹⁸⁰, P.R. Newman²¹, T.Y. Ng^{62c}, Y.S. Ng¹⁹, Y.W.Y. Ng¹⁶⁹, H.D.N. Nguyen¹⁰⁰, T. Nguyen Manh¹⁰⁸, E. Nibigira³⁷, R.B. Nickerson¹³³, R. Nicolaidou¹⁴³, D.S. Nielsen³⁹, J. Nielsen¹⁴⁴, N. Nikiforou¹¹, V. Nikolaenko^{122,an}, I. Nikolic-Audit¹³⁴, K. Nikolopoulos²¹, P. Nilsson²⁹, H.R. Nindhito⁵³, Y. Ninomiya⁸⁰, A. Nisati^{71a}, N. Nishu^{59c}, R. Nisius¹¹⁴, I. Nitsche⁴⁶, T. Nitta¹⁷⁷, T. Nobe¹⁶¹, Y. Noguchi⁸⁴, M. Nomachi¹³¹, I. Nomidis¹³⁴, M.A. Nomura²⁹, M. Nordberg³⁵, N. Norjoharuddeen¹³³, T. Novak⁹⁰, O. Novgorodova⁴⁷, R. Novotny¹⁴⁰, L. Nozka¹²⁸, K. Ntekas¹⁶⁹, E. Nurse⁹³, F. Nuti¹⁰³, F.G. Oakham^{33,av}, H. Oberlack¹¹⁴, J. Ocariz¹³⁴, A. Ochi⁸¹, I. Ochoa³⁸, J.P. Ochoa-Ricoux^{145a}, K. O'Connor²⁶, S. Oda⁸⁶, S. Odaka⁸⁰, S. Oerdek⁵², A. Ogrodnik^{82a}, A. Oh⁹⁹, S.H. Oh⁴⁸, C.C. Ohm¹⁵², H. Oide^{54b,54a}, M.L. Ojeda¹⁶⁵, H. Okawa¹⁶⁷, Y. Okazaki⁸⁴, Y. Okumura¹⁶¹, T. Okuyama⁸⁰, A. Olariu^{27b}, L.F. Oleiro Seabra^{138a}, S.A. Olivares Pino^{145a}, D. Oliveira Damazio²⁹, J.L. Oliver¹, M.J.R. Olsson¹⁶⁹, A. Olszewski⁸³,

J. Olszowska⁸³, D.C. O’Neil¹⁵⁰, A. Onofre^{138a,138e}, K. Onogi¹¹⁶, P.U.E. Onyisi¹¹, H. Oppen¹³²,
 M.J. Oreglia³⁶, G.E. Orellana⁸⁷, Y. Oren¹⁵⁹, D. Orestano^{73a,73b}, N. Orlando¹⁴, R.S. Orr¹⁶⁵,
 B. Osculati^{54b,54a,*}, V. O’Shea⁵⁶, R. Ospanov^{59a}, G. Otero y Garzon³⁰, H. Otono⁸⁶,
 M. Ouchrif^{34d}, F. Ould-Saada¹³², A. Ouraou¹⁴³, Q. Ouyang^{15a}, M. Owen⁵⁶, R.E. Owen²¹,
 V.E. Ozcan^{12c}, N. Ozturk⁸, J. Pacalt¹²⁸, H.A. Pacey³¹, K. Pachal⁴⁸, A. Pacheco Pages¹⁴,
 C. Padilla Aranda¹⁴, S. Pagan Griso¹⁸, M. Paganini¹⁸¹, G. Palacino⁶⁴, S. Palazzo⁴⁹, S. Palestini³⁵,
 M. Palka^{82b}, D. Pallin³⁷, I. Panagoulas¹⁰, C.E. Pandini³⁵, J.G. Panduro Vazquez⁹², P. Pani⁴⁵,
 G. Panizzo^{65a,65c}, L. Paolozzi⁵³, C. Papadatos¹⁰⁸, K. Papageorgiou^{9,j}, A. Paramonov⁶,
 D. Paredes Hernandez^{62b}, S.R. Paredes Saenz¹³³, B. Parida¹⁶⁴, T.H. Park¹⁶⁵, A.J. Parker⁸⁸,
 M.A. Parker³¹, F. Parodi^{54b,54a}, E.W.P. Parrish¹²⁰, J.A. Parsons³⁸, U. Parzefall⁵¹,
 L. Pascual Dominguez¹³⁴, V.R. Pascuzzi¹⁶⁵, J.M.P. Pasner¹⁴⁴, E. Pasqualucci^{71a}, S. Passaggio^{54b},
 F. Pastore⁹², P. Pasuwan^{44a,44b}, S. Patariaia⁹⁸, J.R. Pater⁹⁹, A. Pathak^{179,k}, T. Pauly³⁵,
 B. Pearson¹¹⁴, M. Pedersen¹³², L. Pedraza Diaz¹¹⁸, R. Pedro^{138a,138b}, S.V. Peleganchuk^{121b,121a},
 O. Penc¹³⁹, C. Peng^{15a}, H. Peng^{59a}, B.S. Peralva^{79a}, M.M. Perego¹³⁰,
 A.P. Pereira Peixoto^{138a,138e}, D.V. Perepelitsa²⁹, F. Peri¹⁹, L. Perini^{67a,67b}, H. Pernegger³⁵,
 S. Perrella^{68a,68b}, V.D. Peshekhonov^{78,*}, K. Peters⁴⁵, R.F.Y. Peters⁹⁹, B.A. Petersen³⁵,
 T.C. Petersen³⁹, E. Petit⁵⁷, A. Petridis¹, C. Petridou¹⁶⁰, P. Petroff¹³⁰, M. Petrov¹³³,
 F. Petrucci^{73a,73b}, M. Pettee¹⁸¹, N.E. Pettersson¹⁰¹, K. Petukhova¹⁴¹, A. Peyaud¹⁴³, R. Pezoa^{145b},
 T. Pham¹⁰³, F.H. Phillips¹⁰⁵, P.W. Phillips¹⁴², M.W. Phipps¹⁷¹, G. Piacquadio¹⁵³, E. Pianori¹⁸,
 A. Picazio¹⁰¹, R.H. Pickles⁹⁹, R. Piegaiia³⁰, D. Pietreanu^{27b}, J.E. Pilcher³⁶, A.D. Pilkington⁹⁹,
 M. Pinamonti^{72a,72b}, J.L. Pinfold³, M. Pitt¹⁷⁸, L. Pizzimento^{72a,72b}, M.-A. Pleier²⁹, V. Pleskot¹⁴¹,
 E. Plotnikova⁷⁸, D. Pluth⁷⁷, P. Podberezko^{121b,121a}, R. Poettgen⁹⁵, R. Poggi⁵³, L. Poggioli¹³⁰,
 I. Pogrebnyak¹⁰⁵, D. Pohl²⁴, I. Pokharel⁵², G. Polesello^{69a}, A. Poley¹⁸, A. Policicchio^{71a,71b},
 R. Polifka³⁵, A. Polini^{23b}, C.S. Pollard⁴⁵, V. Polychronakos²⁹, D. Ponomarenko¹¹¹,
 L. Pontecorvo³⁵, S. Popa^{27a}, G.A. Popeneciu^{27d}, D.M. Portillo Quintero¹³⁴, S. Pospisil¹⁴⁰,
 K. Potamianos⁴⁵, I.N. Potrap⁷⁸, C.J. Potter³¹, H. Potti¹¹, T. Poulsen⁹⁵, J. Poveda³⁵,
 T.D. Powell¹⁴⁷, G. Pownall⁴⁵, M.E. Pozo Astigarraga³⁵, P. Pralavorio¹⁰⁰, S. Prell⁷⁷, D. Price⁹⁹,
 M. Primavera^{66a}, S. Prince¹⁰², M.L. Proffitt¹⁴⁶, N. Proklova¹¹¹, K. Prokofiev^{62c}, F. Prokoshin^{145b},
 S. Protopopescu²⁹, J. Proudfoot⁶, M. Przybycien^{82a}, A. Puri¹⁷¹, P. Puzo¹³⁰, J. Qian¹⁰⁴, Y. Qin⁹⁹,
 A. Quadt⁵², M. Queitsch-Maitland⁴⁵, A. Qureshi¹, P. Rados¹⁰³, F. Ragusa^{67a,67b}, G. Rahal⁹⁶,
 J.A. Raine⁵³, S. Rajagopalan²⁹, A. Ramirez Morales⁹¹, K. Ran^{15d}, T. Rashid¹³⁰, S. Raspopov⁵,
 M.G. Ratti^{67a,67b}, D.M. Rauch⁴⁵, F. Rauscher¹¹³, S. Rave⁹⁸, B. Ravina¹⁴⁷, I. Ravinovich¹⁷⁸,
 J.H. Rawling⁹⁹, M. Raymond³⁵, A.L. Read¹³², N.P. Readioff⁵⁷, M. Reale^{66a,66b},
 D.M. Rebuzzi^{69a,69b}, A. Redelbach¹⁷⁵, G. Redlinger²⁹, R.G. Reed^{32c}, K. Reeves⁴², L. Rehnisch¹⁹,
 J. Reichert¹³⁵, D. Reikher¹⁵⁹, A. Reiss⁹⁸, A. Rej¹⁴⁹, C. Rembser³⁵, H. Ren^{15a}, M. Rescigno^{71a},
 S. Resconi^{67a}, E.D. Resseguie¹³⁵, S. Rettie¹⁷³, E. Reynolds²¹, O.L. Rezanova^{121b,121a},
 P. Reznicek¹⁴¹, E. Ricci^{74a,74b}, R. Richter¹¹⁴, S. Richter⁴⁵, E. Richter-Was^{82b}, O. Ricken²⁴,
 M. Ridel¹³⁴, P. Rieck¹¹⁴, C.J. Riegel¹⁸⁰, O. Rifki⁴⁵, M. Rijssenbeek¹⁵³, A. Rimoldi^{69a,69b},
 M. Rimoldi²⁰, L. Rinaldi^{23b}, G. Ripellino¹⁵², B. Ristić⁸⁸, E. Ritsch³⁵, I. Riu¹⁴,
 J.C. Rivera Vergara^{145a}, F. Rizatdinova¹²⁷, E. Rizvi⁹¹, C. Rizzi³⁵, R.T. Roberts⁹⁹,
 S.H. Robertson^{102,ac}, M. Robin⁴⁵, D. Robinson³¹, J.E.M. Robinson⁴⁵, A. Robson⁵⁶, E. Rocco⁹⁸,
 C. Roda^{70a,70b}, Y. Rodina¹⁰⁰, S. Rodriguez Bosca¹⁷², A. Rodriguez Perez¹⁴,
 D. Rodriguez Rodriguez¹⁷², A.M. Rodríguez Vera^{166b}, S. Roe³⁵, O. Røhne¹³², R. Röhrig¹¹⁴,
 C.P.A. Roland⁶⁴, J. Roloff⁵⁸, A. Romaniouk¹¹¹, M. Romano^{23b,23a}, N. Rompotis⁸⁹,
 M. Ronzani¹²³, L. Roos¹³⁴, S. Rosati^{71a}, K. Rosbach⁵¹, N-A. Rosien⁵², G. Rosin¹⁰¹,
 B.J. Rosser¹³⁵, E. Rossi⁴⁵, E. Rossi^{73a,73b}, E. Rossi^{68a,68b}, L.P. Rossi^{54b}, L. Rossini^{67a,67b},
 J.H.N. Rosten³¹, R. Rosten¹⁴, M. Rotaru^{27b}, J. Rothberg¹⁴⁶, D. Rousseau¹³⁰, D. Roy^{32c},
 A. Rozanov¹⁰⁰, Y. Rozen¹⁵⁸, X. Ruan^{32c}, F. Rubbo¹⁵¹, F. Rühr⁵¹, A. Ruiz-Martinez¹⁷²,

A. Rummeler³⁵, Z. Rurikova⁵¹, N.A. Rusakovich⁷⁸, H.L. Russell¹⁰², L. Rustige^{37,46},
 J.P. Rutherford⁷, E.M. Rüttinger^{45,1}, Y.F. Ryabov¹³⁶, M. Rybar³⁸, G. Rybkin¹³⁰, A. Ryzhov¹²²,
 G.F. Rzehorz⁵², P. Sabatini⁵², G. Sabato¹¹⁹, S. Sacerdoti¹³⁰, H.F.-W. Sadrozinski¹⁴⁴,
 R. Sadykov⁷⁸, F. Safai Tehrani^{71a}, P. Saha¹²⁰, S. Saha¹⁰², M. Sahinsoy^{60a}, A. Sahu¹⁸⁰,
 M. Saimpert⁴⁵, M. Saito¹⁶¹, T. Saito¹⁶¹, H. Sakamoto¹⁶¹, A. Sakharov^{123,am}, D. Salamani⁵³,
 G. Salamanna^{73a,73b}, J.E. Salazar Loyola^{145b}, P.H. Sales De Bruin¹⁷⁰, D. Salihagic^{114,*},
 A. Salnikov¹⁵¹, J. Salt¹⁷², D. Salvatore^{40b,40a}, F. Salvatore¹⁵⁴, A. Salvucci^{62a,62b,62c},
 A. Salzburger³⁵, J. Samarati³⁵, D. Sammel⁵¹, D. Sampsonidis¹⁶⁰, D. Sampsonidou¹⁶⁰,
 J. Sánchez¹⁷², A. Sanchez Pineda^{65a,65c}, H. Sandaker¹³², C.O. Sander⁴⁵, M. Sandhoff¹⁸⁰,
 C. Sandoval²², D.P.C. Sankey¹⁴², M. Sannino^{54b,54a}, Y. Sano¹¹⁶, A. Sansoni⁵⁰, C. Santoni³⁷,
 H. Santos^{138a,138b}, S.N. Santpur¹⁸, A. Santra¹⁷², A. Sapronov⁷⁸, J.G. Saraiva^{138a,138d},
 O. Sasaki⁸⁰, K. Sato¹⁶⁷, E. Sauvan⁵, P. Savard^{165,av}, N. Savic¹¹⁴, R. Sawada¹⁶¹, C. Sawyer¹⁴²,
 L. Sawyer^{94,ak}, C. Sbarra^{23b}, A. Sbrizzi^{23a}, T. Scanlon⁹³, J. Schaarschmidt¹⁴⁶, P. Schacht¹¹⁴,
 B.M. Schachtner¹¹³, D. Schaefer³⁶, L. Schaefer¹³⁵, J. Schaeffer⁹⁸, S. Schaepe³⁵, U. Schäfer⁹⁸,
 A.C. Schaffer¹³⁰, D. Schaile¹¹³, R.D. Schamberger¹⁵³, N. Scharmberg⁹⁹, V.A. Schegelsky¹³⁶,
 D. Scheirich¹⁴¹, F. Schenck¹⁹, M. Schernau¹⁶⁹, C. Schiavi^{54b,54a}, S. Schier¹⁴⁴, L.K. Schildgen²⁴,
 Z.M. Schillaci²⁶, E.J. Schioppa³⁵, M. Schioppa^{40b,40a}, K.E. Schleicher⁵¹, S. Schlenker³⁵,
 K.R. Schmidt-Sommerfeld¹¹⁴, K. Schmieden³⁵, C. Schmitt⁹⁸, S. Schmitt⁴⁵, S. Schmitz⁹⁸,
 J.C. Schmoeckel⁴⁵, U. Schnoor⁵¹, L. Schoeffel¹⁴³, A. Schoening^{60b}, E. Schopf¹³³, M. Schott⁹⁸,
 J.F.P. Schouwenberg¹¹⁸, J. Schovancova³⁵, S. Schramm⁵³, F. Schroeder¹⁸⁰, A. Schulte⁹⁸,
 H.-C. Schultz-Coulon^{60a}, M. Schumacher⁵¹, B.A. Schumm¹⁴⁴, Ph. Schune¹⁴³, A. Schwartzman¹⁵¹,
 T.A. Schwarz¹⁰⁴, Ph. Schwemling¹⁴³, R. Schwienhorst¹⁰⁵, A. Sciandra²⁴, G. Sciolla²⁶,
 M. Scornajenghi^{40b,40a}, F. Scuri^{70a}, F. Scutti¹⁰³, L.M. Scyboz¹¹⁴, C.D. Sebastiani^{71a,71b},
 P. Seema¹⁹, S.C. Seidel¹¹⁷, A. Seiden¹⁴⁴, T. Seiss³⁶, J.M. Seixas^{79b}, G. Sekhniaidze^{68a},
 K. Sekhon¹⁰⁴, S.J. Sekula⁴¹, N. Semprini-Cesari^{23b,23a}, S. Sen⁴⁸, S. Senkin³⁷, C. Serfon⁷⁵,
 L. Serin¹³⁰, L. Serkin^{65a,65b}, M. Sessa^{59a}, H. Severini¹²⁶, F. Sforza¹⁶⁸, A. Sfyrla⁵³, E. Shabalina⁵²,
 J.D. Shahinian¹⁴⁴, N.W. Shaikh^{44a,44b}, D. Shaked Renous¹⁷⁸, L.Y. Shan^{15a}, R. Shang¹⁷¹,
 J.T. Shank²⁵, M. Shapiro¹⁸, A.S. Sharma¹, A. Sharma¹³³, P.B. Shatalov¹¹⁰, K. Shaw¹⁵⁴,
 S.M. Shaw⁹⁹, A. Shcherbakova¹³⁶, Y. Shen¹²⁶, N. Sherafati³³, A.D. Sherman²⁵, P. Sherwood⁹³,
 L. Shi^{156,ar}, S. Shimizu⁸⁰, C.O. Shimmin¹⁸¹, Y. Shimogama¹⁷⁷, M. Shimojima¹¹⁵,
 I.P.J. Shipsey¹³³, S. Shirabe⁸⁶, M. Shiyakova^{78,aa}, J. Shlomi¹⁷⁸, A. Shmeleva¹⁰⁹, M.J. Shochet³⁶,
 S. Shojaii¹⁰³, D.R. Shope¹²⁶, S. Shrestha¹²⁴, E. Shulga¹¹¹, P. Sicho¹³⁹, A.M. Sickles¹⁷¹,
 P.E. Sidebo¹⁵², E. Sideras Haddad^{32c}, O. Sidiropoulou³⁵, A. Sidoti^{23b,23a}, F. Siegert⁴⁷,
 Dj. Sijacki¹⁶, M. Silva Jr.¹⁷⁹, M.V. Silva Oliveira^{79a}, S.B. Silverstein^{44a}, S. Simion¹³⁰,
 E. Simioni⁹⁸, M. Simon⁹⁸, R. Simoniello⁹⁸, P. Sinervo¹⁶⁵, N.B. Sinev¹²⁹, M. Sioli^{23b,23a}, I. Siral¹⁰⁴,
 S.Yu. Sivoklov¹¹², J. Sjölin^{44a,44b}, E. Skorda⁹⁵, P. Skubic¹²⁶, M. Slawinska⁸³, K. Sliwa¹⁶⁸,
 R. Slovak¹⁴¹, V. Smakhtin¹⁷⁸, B.H. Smart¹⁴², J. Smiesko^{28a}, N. Smirnov¹¹¹, S.Yu. Smirnov¹¹¹,
 Y. Smirnov¹¹¹, L.N. Smirnova¹¹², O. Smirnova⁹⁵, J.W. Smith⁵², M. Smizanska⁸⁸, K. Smolek¹⁴⁰,
 A. Smykiewicz⁸³, A.A. Snesev¹⁰⁹, I.M. Snyder¹²⁹, S. Snyder²⁹, R. Sobie^{174,ac}, A.M. Soffa¹⁶⁹,
 A. Soffer¹⁵⁹, A. Sogaard⁴⁹, F. Sohns⁵², G. Sokhrannyi⁹⁰, C.A. Solans Sanchez³⁵,
 E.Yu. Soldatov¹¹¹, U. Soldevila¹⁷², A.A. Solodkov¹²², A. Soloshenko⁷⁸, O.V. Solovyanov¹²²,
 V. Solovyev¹³⁶, P. Sommer¹⁴⁷, H. Son¹⁶⁸, W. Song¹⁴², W.Y. Song^{166b}, A. Sopczak¹⁴⁰,
 F. Sopkova^{28b}, C.L. Sotiropoulou^{70a,70b}, S. Sottocornola^{69a,69b}, R. Soualah^{65a,65c,i},
 A.M. Soukharev^{121b,121a}, D. South⁴⁵, S. Spagnolo^{66a,66b}, M. Spalla¹¹⁴, M. Spangenberg¹⁷⁶,
 F. Spanò⁹², D. Sperlich¹⁹, T.M. Spieker^{60a}, R. Spighi^{23b}, G. Spigo³⁵, L.A. Spiller¹⁰³, M. Spina¹⁵⁴,
 D.P. Spiteri⁵⁶, M. Spousta¹⁴¹, A. Stabile^{67a,67b}, B.L. Stamas¹²⁰, R. Stamen^{60a},
 M. Stamenkovic¹¹⁹, S. Stamm¹⁹, E. Stanecka⁸³, R.W. Stanek⁶, B. Stanislaus¹³³,
 M.M. Stanitzki⁴⁵, M. Stankaityte¹³³, B. Stapf¹¹⁹, E.A. Starchenko¹²², G.H. Stark¹⁴⁴, J. Stark⁵⁷,

S.H Stark³⁹, P. Staroba¹³⁹, P. Starovoitov^{60a}, S. Stärz¹⁰², R. Staszewski⁸³, G. Stavropoulos⁴³, M. Stegler⁴⁵, P. Steinberg²⁹, B. Stelzer¹⁵⁰, H.J. Stelzer³⁵, O. Stelzer-Chilton^{166a}, H. Stenzel⁵⁵, T.J. Stevenson¹⁵⁴, G.A. Stewart³⁵, M.C. Stockton³⁵, G. Stoicea^{27b}, M. Stolarski^{138a}, P. Stolte⁵², S. Stonjek¹¹⁴, A. Straessner⁴⁷, J. Strandberg¹⁵², S. Strandberg^{44a,44b}, M. Strauss¹²⁶, P. Strizenec^{28b}, R. Ströhmer¹⁷⁵, D.M. Strom¹²⁹, R. Stroynowski⁴¹, A. Strubig⁴⁹, S.A. Stucci²⁹, B. Stugu¹⁷, J. Stupak¹²⁶, N.A. Styles⁴⁵, D. Su¹⁵¹, S. Suchek^{60a}, Y. Sugaya¹³¹, V.V. Sulim¹⁰⁹, M.J. Sullivan⁸⁹, D.M.S. Sultan⁵³, S. Sultansoy^{4c}, T. Sumida⁸⁴, S. Sun¹⁰⁴, X. Sun³, K. Suruliz¹⁵⁴, C.J.E. Suster¹⁵⁵, M.R. Sutton¹⁵⁴, S. Suzuki⁸⁰, M. Svatos¹³⁹, M. Swiatlowski³⁶, S.P. Swift², A. Sydorenko⁹⁸, I. Sykora^{28a}, M. Sykora¹⁴¹, T. Sykora¹⁴¹, D. Ta⁹⁸, K. Tackmann^{45,y}, J. Taenzer¹⁵⁹, A. Taffard¹⁶⁹, R. Tafirout^{166a}, E. Tahirovic⁹¹, H. Takai²⁹, R. Takashima⁸⁵, K. Takeda⁸¹, T. Takeshita¹⁴⁸, E.P. Takeva⁴⁹, Y. Takubo⁸⁰, M. Talby¹⁰⁰, A.A. Talyshev^{121b,121a}, N.M. Tamir¹⁵⁹, J. Tanaka¹⁶¹, M. Tanaka¹⁶³, R. Tanaka¹³⁰, B.B. Tannenwald¹²⁴, S. Tapia Araya¹⁷¹, S. Tapprogge⁹⁸, A. Tarek Abouelfadl Mohamed¹³⁴, S. Tarem¹⁵⁸, G. Tarna^{27b,e}, G.F. Tartarelli^{67a}, P. Tas¹⁴¹, M. Tasevsky¹³⁹, T. Tashiro⁸⁴, E. Tassi^{40b,40a}, A. Tavares Delgado^{138a,138b}, Y. Tayalati^{34e}, A.J. Taylor⁴⁹, G.N. Taylor¹⁰³, P.T.E. Taylor¹⁰³, W. Taylor^{166b}, A.S. Tee⁸⁸, R. Teixeira De Lima¹⁵¹, P. Teixeira-Dias⁹², H. Ten Kate³⁵, J.J. Teoh¹¹⁹, S. Terada⁸⁰, K. Terashi¹⁶¹, J. Terron⁹⁷, S. Terzo¹⁴, M. Testa⁵⁰, R.J. Teuscher^{165,ac}, S.J. Thais¹⁸¹, T. Theveneaux-Pelzer⁴⁵, F. Thiele³⁹, D.W. Thomas⁹², J.O. Thomas⁴¹, J.P. Thomas²¹, A.S. Thompson⁵⁶, P.D. Thompson²¹, L.A. Thomsen¹⁸¹, E. Thomson¹³⁵, Y. Tian³⁸, R.E. Ticse Torres⁵², V.O. Tikhomirov^{109,ao}, Yu.A. Tikhonov^{121b,121a}, S. Timoshenko¹¹¹, P. Tipton¹⁸¹, S. Tisserant¹⁰⁰, K. Todome^{23b,23a}, S. Todorova-Nova⁵, S. Todt⁴⁷, J. Tojo⁸⁶, S. Tokár^{28a}, K. Tokushuku⁸⁰, E. Tolley¹²⁴, K.G. Tomiwa^{32c}, M. Tomoto¹¹⁶, L. Tompkins^{151,q}, K. Toms¹¹⁷, B. Tong⁵⁸, P. Tornambe¹⁰¹, E. Torrence¹²⁹, H. Torres⁴⁷, E. Torró Pastor¹⁴⁶, C. Toscirì¹³³, J. Toth^{100,ab}, D.R. Tovey¹⁴⁷, C.J. Treado¹²³, T. Trefzger¹⁷⁵, F. Tresoldi¹⁵⁴, A. Tricoli²⁹, I.M. Trigger^{166a}, S. Trincaz-Duvoid¹³⁴, W. Trischuk¹⁶⁵, B. Trocmé⁵⁷, A. Trofymov¹³⁰, C. Troncon^{67a}, M. Trovatelli¹⁷⁴, F. Trovato¹⁵⁴, L. Truong^{32b}, M. Trzebinski⁸³, A. Trzupek⁸³, F. Tsai⁴⁵, J.C.-L. Tseng¹³³, P.V. Tsiareshka^{106,ai}, A. Tsirigotis¹⁶⁰, N. Tsirintanis⁹, V. Tsiskaridze¹⁵³, E.G. Tskhadadze^{157a}, M. Tsopoulou¹⁶⁰, I.I. Tsukerman¹¹⁰, V. Tsulaia¹⁸, S. Tsuno⁸⁰, D. Tsybychev^{153,164}, Y. Tu^{62b}, A. Tudorache^{27b}, V. Tudorache^{27b}, T.T. Tumbure^{27a}, A.N. Tuna⁵⁸, S. Turchikhin⁷⁸, D. Turgeman¹⁷⁸, I. Turk Cakir^{4b,t}, R.J. Turner²¹, R.T. Turra^{67a}, P.M. Tuts³⁸, S. Tzamarias¹⁶⁰, E. Tzovara⁹⁸, G. Uchielli⁴⁶, I. Ueda⁸⁰, M. Ughetto^{44a,44b}, F. Ukegawa¹⁶⁷, G. Unal³⁵, A. Undrus²⁹, G. Unel¹⁶⁹, F.C. Ungaro¹⁰³, Y. Unno⁸⁰, K. Uno¹⁶¹, J. Urban^{28b}, P. Urquijo¹⁰³, G. Usai⁸, J. Usui⁸⁰, L. Vacavant¹⁰⁰, V. Vacek¹⁴⁰, B. Vachon¹⁰², K.O.H. Vadla¹³², A. Vaidya⁹³, C. Valderanis¹¹³, E. Valdes Santurio^{44a,44b}, M. Valente⁵³, S. Valentini^{23b,23a}, A. Valero¹⁷², L. Valéry⁴⁵, R.A. Vallance²¹, A. Vallier³⁵, J.A. Valls Ferrer¹⁷², T.R. Van Daalen¹⁴, P. Van Gemmeren⁶, I. Van Vulpen¹¹⁹, M. Vanadia^{72a,72b}, W. Vandelli³⁵, A. Vaniachine¹⁶⁴, R. Vari^{71a}, E.W. Varnes⁷, C. Varni^{54b,54a}, T. Varol⁴¹, D. Varouchas¹³⁰, K.E. Varvell¹⁵⁵, M.E. Vasile^{27b}, G.A. Vasquez¹⁷⁴, J.G. Vasquez¹⁸¹, F. Vazeille³⁷, D. Vazquez Furelos¹⁴, T. Vazquez Schroeder³⁵, J. Veatch⁵², V. Vecchio^{73a,73b}, L.M. Veloce¹⁶⁵, F. Veloso^{138a,138c}, S. Veneziano^{71a}, A. Ventura^{66a,66b}, N. Venturi³⁵, A. Verbytskyi¹¹⁴, V. Vercesi^{69a}, M. Verducci^{73a,73b}, C.M. Vergel Infante⁷⁷, C. Vergis²⁴, W. Verkerke¹¹⁹, A.T. Vermeulen¹¹⁹, J.C. Vermeulen¹¹⁹, M.C. Vetterli^{150,av}, N. Viaux Maira^{145b}, M. Vicente Barreto Pinto⁵³, I. Vichou^{171,*}, T. Vickey¹⁴⁷, O.E. Vickey Boeriu¹⁴⁷, G.H.A. Viehhauser¹³³, L. Vigani¹³³, M. Villa^{23b,23a}, M. Villaplana Perez^{67a,67b}, E. Vilucchi⁵⁰, M.G. Vincter³³, V.B. Vinogradov⁷⁸, A. Vishwakarma⁴⁵, C. Vittori^{23b,23a}, I. Vivarelli¹⁵⁴, M. Vogel¹⁸⁰, P. Vokac¹⁴⁰, G. Volpi¹⁴, S.E. von Buddenbrock^{32c}, E. Von Toerne²⁴, V. Vorobel¹⁴¹, K. Vorobev¹¹¹, M. Vos¹⁷², J.H. Vosseveld⁸⁹, N. Vranjes¹⁶, M. Vranjes Milosavljevic¹⁶, V. Vrba¹⁴⁰, M. Vreeswijk¹¹⁹, T. Šfiligoj⁹⁰, R. Vuillermet³⁵, I. Vukotic³⁶, T. Ženiš^{28a}, L. Živković¹⁶,

P. Wagner²⁴, W. Wagner¹⁸⁰, J. Wagner-Kuhr¹¹³, H. Wahlberg⁸⁷, S. Wahrmond⁴⁷,
 K. Wakamiya⁸¹, V.M. Walbrecht¹¹⁴, J. Walder⁸⁸, R. Walker¹¹³, S.D. Walker⁹², W. Walkowiak¹⁴⁹,
 V. Wallangen^{44a,44b}, A.M. Wang⁵⁸, C. Wang^{59b}, F. Wang¹⁷⁹, H. Wang¹⁸, H. Wang³, J. Wang¹⁵⁵,
 J. Wang^{60b}, P. Wang⁴¹, Q. Wang¹²⁶, R.-J. Wang¹³⁴, R. Wang^{59a}, R. Wang⁶, S.M. Wang¹⁵⁶,
 W.T. Wang^{59a}, W. Wang^{15c,ad}, W.X. Wang^{59a,ad}, Y. Wang^{59a,al}, Z. Wang^{59c}, C. Wanotayaroj⁴⁵,
 A. Warburton¹⁰², C.P. Ward³¹, D.R. Wardrope⁹³, A. Washbrook⁴⁹, A.T. Watson²¹,
 M.F. Watson²¹, G. Watts¹⁴⁶, B.M. Waugh⁹³, A.F. Webb¹¹, S. Webb⁹⁸, C. Weber¹⁸¹,
 M.S. Weber²⁰, S.A. Weber³³, S.M. Weber^{60a}, A.R. Weidberg¹³³, J. Weingarten⁴⁶, M. Weirich⁹⁸,
 C. Weiser⁵¹, P.S. Wells³⁵, T. Wenaus²⁹, T. Wengler³⁵, S. Wenig³⁵, N. Vermes²⁴, M.D. Werner⁷⁷,
 P. Werner³⁵, M. Wessels^{60a}, T.D. Weston²⁰, K. Whalen¹²⁹, N.L. Whallon¹⁴⁶, A.M. Wharton⁸⁸,
 A.S. White¹⁰⁴, A. White⁸, M.J. White¹, R. White^{145b}, D. Whiteson¹⁶⁹, B.W. Whitmore⁸⁸,
 F.J. Wickens¹⁴², W. Wiedenmann¹⁷⁹, M. Wielers¹⁴², C. Wiglesworth³⁹, L.A.M. Wiik-Fuchs⁵¹,
 F. Wilk⁹⁹, H.G. Wilkens³⁵, L.J. Wilkins⁹², H.H. Williams¹³⁵, S. Williams³¹, C. Willis¹⁰⁵,
 S. Willocq¹⁰¹, J.A. Wilson²¹, I. Wingerter-Seez⁵, E. Winkels¹⁵⁴, F. Winklmeier¹²⁹,
 O.J. Winston¹⁵⁴, B.T. Winter⁵¹, M. Wittgen¹⁵¹, M. Wobisch⁹⁴, A. Wolf⁹⁸, T.M.H. Wolf¹¹⁹,
 R. Wolff¹⁰⁰, R.W. Wölker¹³³, J. Wollrath⁵¹, M.W. Wolter⁸³, H. Wolters^{138a,138c}, V.W.S. Wong¹⁷³,
 N.L. Woods¹⁴⁴, S.D. Worm²¹, B.K. Wosiek⁸³, K.W. Woźniak⁸³, K. Wraight⁵⁶, S.L. Wu¹⁷⁹,
 X. Wu⁵³, Y. Wu^{59a}, T.R. Wyatt⁹⁹, B.M. Wynne⁴⁹, S. Xella³⁹, Z. Xi¹⁰⁴, L. Xia¹⁷⁶, D. Xu^{15a},
 H. Xu^{59a,e}, L. Xu²⁹, T. Xu¹⁴³, W. Xu¹⁰⁴, Z. Xu^{59b}, Z. Xu¹⁵¹, B. Yabsley¹⁵⁵, S. Yacoub^{32a},
 K. Yajima¹³¹, D.P. Yallup⁹³, D. Yamaguchi¹⁶³, Y. Yamaguchi¹⁶³, A. Yamamoto⁸⁰,
 T. Yamanaka¹⁶¹, F. Yamane⁸¹, M. Yamatani¹⁶¹, T. Yamazaki¹⁶¹, Y. Yamazaki⁸¹, Z. Yan²⁵,
 H.J. Yang^{59c,59d}, H.T. Yang¹⁸, S. Yang⁷⁶, X. Yang^{59b,57}, Y. Yang¹⁶¹, Z. Yang¹⁷, W.-M. Yao¹⁸,
 Y.C. Yap⁴⁵, Y. Yasu⁸⁰, E. Yatsenko^{59c,59d}, J. Ye⁴¹, S. Ye²⁹, I. Yeletsikh⁷⁸, E. Yigitbasi²⁵,
 E. Yildirim⁹⁸, K. Yorita¹⁷⁷, K. Yoshihara¹³⁵, C.J.S. Young³⁵, C. Young¹⁵¹, J. Yu⁷⁷, X. Yue^{60a},
 S.P.Y. Yuen²⁴, B. Zabinski⁸³, G. Zacharis¹⁰, E. Zaffaroni⁵³, J. Zahreddine¹³⁴, R. Zaidan¹⁴,
 A.M. Zaitsev^{122,an}, T. Zakareishvili^{157b}, N. Zakharchuk³³, S. Zambito⁵⁸, D. Zanzi³⁵,
 D.R. Zaripovas⁵⁶, S.V. Zeiβner⁴⁶, C. Zeitnitz¹⁸⁰, G. Zemaityte¹³³, J.C. Zeng¹⁷¹, O. Zenin¹²²,
 D. Zerwas¹³⁰, M. Zgubič¹³³, D.F. Zhang^{15b}, F. Zhang¹⁷⁹, G. Zhang^{59a}, G. Zhang^{15b}, H. Zhang^{15c},
 J. Zhang⁶, L. Zhang^{15c}, L. Zhang^{59a}, M. Zhang¹⁷¹, R. Zhang^{59a}, R. Zhang²⁴, X. Zhang^{59b},
 Y. Zhang^{15d}, Z. Zhang^{62a}, Z. Zhang¹³⁰, P. Zhao⁴⁸, Y. Zhao^{59b}, Z. Zhao^{59a}, A. Zhemchugov⁷⁸,
 Z. Zheng¹⁰⁴, D. Zhong¹⁷¹, B. Zhou¹⁰⁴, C. Zhou¹⁷⁹, M.S. Zhou^{15d}, M. Zhou¹⁵³, N. Zhou^{59c},
 Y. Zhou⁷, C.G. Zhu^{59b}, H.L. Zhu^{59a}, H. Zhu^{15a}, J. Zhu¹⁰⁴, Y. Zhu^{59a}, X. Zhuang^{15a},
 K. Zhukov¹⁰⁹, V. Zhulanov^{121b,121a}, D. Ziemska⁶⁴, N.I. Zimine⁷⁸, S. Zimmermann⁵¹,
 Z. Zinonos¹¹⁴, M. Ziolkowski¹⁴⁹, G. Zoernig¹⁷⁹, A. Zoccoli^{23b,23a}, K. Zoch⁵², T.G. Zorbas¹⁴⁷,
 R. Zou³⁶, L. Zwalinski³⁵

¹ Department of Physics, University of Adelaide, Adelaide; Australia

² Physics Department, SUNY Albany, Albany NY; United States of America

³ Department of Physics, University of Alberta, Edmonton AB; Canada

⁴ Department of Physics^(a), Ankara University, Ankara; Istanbul Aydin University^(b), Istanbul;
 Division of Physics^(c), TOBB University of Economics and Technology, Ankara; Turkey

⁵ LAPP, Université Grenoble Alpes, Université Savoie Mont Blanc, CNRS/IN2P3, Annecy; France

⁶ High Energy Physics Division, Argonne National Laboratory, Argonne IL; United States of America

⁷ Department of Physics, University of Arizona, Tucson AZ; United States of America

⁸ Department of Physics, University of Texas at Arlington, Arlington TX; United States of America

⁹ Physics Department, National and Kapodistrian University of Athens, Athens; Greece

¹⁰ Physics Department, National Technical University of Athens, Zografou; Greece

¹¹ Department of Physics, University of Texas at Austin, Austin TX; United States of America

- ¹² Bahcesehir University^(a), Faculty of Engineering and Natural Sciences, Istanbul; Istanbul Bilgi University^(b), Faculty of Engineering and Natural Sciences, Istanbul; Department of Physics^(c), Bogazici University, Istanbul; Department of Physics Engineering^(d), Gaziantep University, Gaziantep; Turkey
- ¹³ Institute of Physics, Azerbaijan Academy of Sciences, Baku; Azerbaijan
- ¹⁴ Institut de Física d'Altes Energies (IFAE), Barcelona Institute of Science and Technology, Barcelona; Spain
- ¹⁵ Institute of High Energy Physics^(a), Chinese Academy of Sciences, Beijing; Physics Department^(b), Tsinghua University, Beijing; Department of Physics^(c), Nanjing University, Nanjing; University of Chinese Academy of Science (UCAS)^(d), Beijing; China
- ¹⁶ Institute of Physics, University of Belgrade, Belgrade; Serbia
- ¹⁷ Department for Physics and Technology, University of Bergen, Bergen; Norway
- ¹⁸ Physics Division, Lawrence Berkeley National Laboratory and University of California, Berkeley CA; United States of America
- ¹⁹ Institut für Physik, Humboldt Universität zu Berlin, Berlin; Germany
- ²⁰ Albert Einstein Center for Fundamental Physics and Laboratory for High Energy Physics, University of Bern, Bern; Switzerland
- ²¹ School of Physics and Astronomy, University of Birmingham, Birmingham; United Kingdom
- ²² Facultad de Ciencias y Centro de Investigaciones, Universidad Antonio Nariño, Bogota; Colombia
- ²³ INFN Bologna and Università di Bologna^(a), Dipartimento di Fisica; INFN Sezione di Bologna^(b); Italy
- ²⁴ Physikalisches Institut, Universität Bonn, Bonn; Germany
- ²⁵ Department of Physics, Boston University, Boston MA; United States of America
- ²⁶ Department of Physics, Brandeis University, Waltham MA; United States of America
- ²⁷ Transilvania University of Brasov^(a), Brasov; Horia Hulubei National Institute of Physics and Nuclear Engineering^(b), Bucharest; Department of Physics^(c), Alexandru Ioan Cuza University of Iasi, Iasi; National Institute for Research and Development of Isotopic and Molecular Technologies^(d), Physics Department, Cluj-Napoca; University Politehnica Bucharest^(e), Bucharest; West University in Timisoara^(f), Timisoara; Romania
- ²⁸ Faculty of Mathematics^(a), Physics and Informatics, Comenius University, Bratislava; Department of Subnuclear Physics^(b), Institute of Experimental Physics of the Slovak Academy of Sciences, Kosice; Slovak Republic
- ²⁹ Physics Department, Brookhaven National Laboratory, Upton NY; United States of America
- ³⁰ Departamento de Física, Universidad de Buenos Aires, Buenos Aires; Argentina
- ³¹ Cavendish Laboratory, University of Cambridge, Cambridge; United Kingdom
- ³² Department of Physics^(a), University of Cape Town, Cape Town; Department of Mechanical Engineering Science^(b), University of Johannesburg, Johannesburg; School of Physics^(c), University of the Witwatersrand, Johannesburg; South Africa
- ³³ Department of Physics, Carleton University, Ottawa ON; Canada
- ³⁴ Faculté des Sciences Ain Chock^(a), Réseau Universitaire de Physique des Hautes Energies — Université Hassan II, Casablanca; Centre National de l'Energie des Sciences Techniques Nucleaires (CNESTEN)^(b), Rabat; Faculté des Sciences Semlalia^(c), Université Cadi Ayyad, LPHEA-Marrakech; Faculté des Sciences^(d), Université Mohamed Premier and LPTPM, Oujda; Faculté des sciences^(e), Université Mohammed V, Rabat; Morocco
- ³⁵ CERN, Geneva; Switzerland
- ³⁶ Enrico Fermi Institute, University of Chicago, Chicago IL; United States of America
- ³⁷ LPC, Université Clermont Auvergne, CNRS/IN2P3, Clermont-Ferrand; France
- ³⁸ Nevis Laboratory, Columbia University, Irvington NY; United States of America
- ³⁹ Niels Bohr Institute, University of Copenhagen, Copenhagen; Denmark
- ⁴⁰ Dipartimento di Fisica^(a), Università della Calabria, Rende; INFN Gruppo Collegato di Cosenza^(b), Laboratori Nazionali di Frascati; Italy
- ⁴¹ Physics Department, Southern Methodist University, Dallas TX; United States of America
- ⁴² Physics Department, University of Texas at Dallas, Richardson TX; United States of America

- 43 National Centre for Scientific Research “Demokritos”, Agia Paraskevi; Greece
- 44 Department of Physics^(a), Stockholm University; Oskar Klein Centre^(b), Stockholm; Sweden
- 45 Deutsches Elektronen-Synchrotron DESY, Hamburg and Zeuthen; Germany
- 46 Lehrstuhl für Experimentelle Physik IV, Technische Universität Dortmund, Dortmund; Germany
- 47 Institut für Kern- und Teilchenphysik, Technische Universität Dresden, Dresden; Germany
- 48 Department of Physics, Duke University, Durham NC; United States of America
- 49 SUPA — School of Physics and Astronomy, University of Edinburgh, Edinburgh; United Kingdom
- 50 INFN e Laboratori Nazionali di Frascati, Frascati; Italy
- 51 Physikalisches Institut, Albert-Ludwigs-Universität Freiburg, Freiburg; Germany
- 52 II. Physikalisches Institut, Georg-August-Universität Göttingen, Göttingen; Germany
- 53 Département de Physique Nucléaire et Corpusculaire, Université de Genève, Genève; Switzerland
- 54 Dipartimento di Fisica^(a), Università di Genova, Genova; INFN Sezione di Genova^(b); Italy
- 55 II. Physikalisches Institut, Justus-Liebig-Universität Giessen, Giessen; Germany
- 56 SUPA — School of Physics and Astronomy, University of Glasgow, Glasgow; United Kingdom
- 57 LPSC, Université Grenoble Alpes, CNRS/IN2P3, Grenoble INP, Grenoble; France
- 58 Laboratory for Particle Physics and Cosmology, Harvard University, Cambridge MA; United States of America
- 59 Department of Modern Physics and State Key Laboratory of Particle Detection and Electronics^(a), University of Science and Technology of China, Hefei; Institute of Frontier and Interdisciplinary Science and Key Laboratory of Particle Physics and Particle Irradiation (MOE)^(b), Shandong University, Qingdao; School of Physics and Astronomy^(c), Shanghai Jiao Tong University, KLPPAC-MoE, SKLPPC, Shanghai; Tsung-Dao Lee Institute^(d), Shanghai; China
- 60 Kirchhoff-Institut für Physik^(a), Ruprecht-Karls-Universität Heidelberg, Heidelberg; Physikalisches Institut^(b), Ruprecht-Karls-Universität Heidelberg, Heidelberg; Germany
- 61 Faculty of Applied Information Science, Hiroshima Institute of Technology, Hiroshima; Japan
- 62 Department of Physics^(a), Chinese University of Hong Kong, Shatin, N.T., Hong Kong; Department of Physics^(b), University of Hong Kong, Hong Kong; Department of Physics and Institute for Advanced Study^(c), Hong Kong University of Science and Technology, Clear Water Bay, Kowloon, Hong Kong; China
- 63 Department of Physics, National Tsing Hua University, Hsinchu; Taiwan
- 64 Department of Physics, Indiana University, Bloomington IN; United States of America
- 65 INFN Gruppo Collegato di Udine^(a), Sezione di Trieste, Udine; ICTP^(b), Trieste; Dipartimento Politecnico di Ingegneria e Architettura^(c), Università di Udine, Udine; Italy
- 66 INFN Sezione di Lecce^(a); Dipartimento di Matematica e Fisica^(b), Università del Salento, Lecce; Italy
- 67 INFN Sezione di Milano^(a); Dipartimento di Fisica^(b), Università di Milano, Milano; Italy
- 68 INFN Sezione di Napoli^(a); Dipartimento di Fisica^(b), Università di Napoli, Napoli; Italy
- 69 INFN Sezione di Pavia^(a); Dipartimento di Fisica^(b), Università di Pavia, Pavia; Italy
- 70 INFN Sezione di Pisa^(a); Dipartimento di Fisica E. Fermi^(b), Università di Pisa, Pisa; Italy
- 71 INFN Sezione di Roma^(a); Dipartimento di Fisica^(b), Sapienza Università di Roma, Roma; Italy
- 72 INFN Sezione di Roma Tor Vergata^(a); Dipartimento di Fisica^(b), Università di Roma Tor Vergata, Roma; Italy
- 73 INFN Sezione di Roma Tre^(a); Dipartimento di Matematica e Fisica^(b), Università Roma Tre, Roma; Italy
- 74 INFN-TIFPA^(a); Università degli Studi di Trento^(b), Trento; Italy
- 75 Institut für Astro- und Teilchenphysik, Leopold-Franzens-Universität, Innsbruck; Austria
- 76 University of Iowa, Iowa City IA; United States of America
- 77 Department of Physics and Astronomy, Iowa State University, Ames IA; United States of America
- 78 Joint Institute for Nuclear Research, Dubna; Russia
- 79 Departamento de Engenharia Elétrica^(a), Universidade Federal de Juiz de Fora (UFJF), Juiz de Fora; Universidade Federal do Rio De Janeiro COPPE/EE/IF^(b), Rio de Janeiro; Universidade Federal de São João del Rei (UFSJ)^(c), São João del Rei; Instituto de Física^(d), Universidade de São Paulo, São Paulo; Brazil

- 80 KEK, High Energy Accelerator Research Organization, Tsukuba; Japan
- 81 Graduate School of Science, Kobe University, Kobe; Japan
- 82 AGH University of Science and Technology^(a), Faculty of Physics and Applied Computer Science, Krakow; Marian Smoluchowski Institute of Physics^(b), Jagiellonian University, Krakow; Poland
- 83 Institute of Nuclear Physics Polish Academy of Sciences, Krakow; Poland
- 84 Faculty of Science, Kyoto University, Kyoto; Japan
- 85 Kyoto University of Education, Kyoto; Japan
- 86 Research Center for Advanced Particle Physics and Department of Physics, Kyushu University, Fukuoka; Japan
- 87 Instituto de Física La Plata, Universidad Nacional de La Plata and CONICET, La Plata; Argentina
- 88 Physics Department, Lancaster University, Lancaster; United Kingdom
- 89 Oliver Lodge Laboratory, University of Liverpool, Liverpool; United Kingdom
- 90 Department of Experimental Particle Physics, Jožef Stefan Institute and Department of Physics, University of Ljubljana, Ljubljana; Slovenia
- 91 School of Physics and Astronomy, Queen Mary University of London, London; United Kingdom
- 92 Department of Physics, Royal Holloway University of London, Egham; United Kingdom
- 93 Department of Physics and Astronomy, University College London, London; United Kingdom
- 94 Louisiana Tech University, Ruston LA; United States of America
- 95 Fysiska institutionen, Lunds universitet, Lund; Sweden
- 96 Centre de Calcul de l'Institut National de Physique Nucléaire et de Physique des Particules (IN2P3), Villeurbanne; France
- 97 Departamento de Física Teórica C-15 and CIAFF, Universidad Autónoma de Madrid, Madrid; Spain
- 98 Institut für Physik, Universität Mainz, Mainz; Germany
- 99 School of Physics and Astronomy, University of Manchester, Manchester; United Kingdom
- 100 CPPM, Aix-Marseille Université, CNRS/IN2P3, Marseille; France
- 101 Department of Physics, University of Massachusetts, Amherst MA; United States of America
- 102 Department of Physics, McGill University, Montreal QC; Canada
- 103 School of Physics, University of Melbourne, Victoria; Australia
- 104 Department of Physics, University of Michigan, Ann Arbor MI; United States of America
- 105 Department of Physics and Astronomy, Michigan State University, East Lansing MI; United States of America
- 106 B.I. Stepanov Institute of Physics, National Academy of Sciences of Belarus, Minsk; Belarus
- 107 Research Institute for Nuclear Problems of Byelorussian State University, Minsk; Belarus
- 108 Group of Particle Physics, University of Montreal, Montreal QC; Canada
- 109 P.N. Lebedev Physical Institute of the Russian Academy of Sciences, Moscow; Russia
- 110 Institute for Theoretical and Experimental Physics of the National Research Centre Kurchatov Institute, Moscow; Russia
- 111 National Research Nuclear University MEPhI, Moscow; Russia
- 112 D.V. Skobeltsyn Institute of Nuclear Physics, M.V. Lomonosov Moscow State University, Moscow; Russia
- 113 Fakultät für Physik, Ludwig-Maximilians-Universität München, München; Germany
- 114 Max-Planck-Institut für Physik (Werner-Heisenberg-Institut), München; Germany
- 115 Nagasaki Institute of Applied Science, Nagasaki; Japan
- 116 Graduate School of Science and Kobayashi-Maskawa Institute, Nagoya University, Nagoya; Japan
- 117 Department of Physics and Astronomy, University of New Mexico, Albuquerque NM; United States of America
- 118 Institute for Mathematics, Astrophysics and Particle Physics, Radboud University Nijmegen/Nikhef, Nijmegen; Netherlands
- 119 Nikhef National Institute for Subatomic Physics and University of Amsterdam, Amsterdam; Netherlands
- 120 Department of Physics, Northern Illinois University, DeKalb IL; United States of America

- 121 *Budker Institute of Nuclear Physics and NSU^(a), SB RAS, Novosibirsk; Novosibirsk State University Novosibirsk^(b); Russia*
- 122 *Institute for High Energy Physics of the National Research Centre Kurchatov Institute, Protvino; Russia*
- 123 *Department of Physics, New York University, New York NY; United States of America*
- 124 *Ohio State University, Columbus OH; United States of America*
- 125 *Faculty of Science, Okayama University, Okayama; Japan*
- 126 *Homer L. Dodge Department of Physics and Astronomy, University of Oklahoma, Norman OK; United States of America*
- 127 *Department of Physics, Oklahoma State University, Stillwater OK; United States of America*
- 128 *Palacký University, RCPTM, Joint Laboratory of Optics, Olomouc; Czech Republic*
- 129 *Center for High Energy Physics, University of Oregon, Eugene OR; United States of America*
- 130 *LAL, Université Paris-Sud, CNRS/IN2P3, Université Paris-Saclay, Orsay; France*
- 131 *Graduate School of Science, Osaka University, Osaka; Japan*
- 132 *Department of Physics, University of Oslo, Oslo; Norway*
- 133 *Department of Physics, Oxford University, Oxford; United Kingdom*
- 134 *LPNHE, Sorbonne Université, Paris Diderot Sorbonne Paris Cité, CNRS/IN2P3, Paris; France*
- 135 *Department of Physics, University of Pennsylvania, Philadelphia PA; United States of America*
- 136 *Konstantinov Nuclear Physics Institute of National Research Centre “Kurchatov Institute”, PNPI, St. Petersburg; Russia*
- 137 *Department of Physics and Astronomy, University of Pittsburgh, Pittsburgh PA; United States of America*
- 138 *Laboratório de Instrumentação e Física Experimental de Partículas — LIP^(a); Departamento de Física^(b), Faculdade de Ciências, Universidade de Lisboa, Lisboa; Departamento de Física^(c), Universidade de Coimbra, Coimbra; Centro de Física Nuclear da Universidade de Lisboa^(d), Lisboa; Departamento de Física^(e), Universidade do Minho, Braga; Universidad de Granada^(f), Granada (Spain); Dep Física and CEFITEC of Faculdade de Ciências e Tecnologia^(g), Universidade Nova de Lisboa, Caparica; Portugal*
- 139 *Institute of Physics of the Czech Academy of Sciences, Prague; Czech Republic*
- 140 *Czech Technical University in Prague, Prague; Czech Republic*
- 141 *Charles University, Faculty of Mathematics and Physics, Prague; Czech Republic*
- 142 *Particle Physics Department, Rutherford Appleton Laboratory, Didcot; United Kingdom*
- 143 *IRFU, CEA, Université Paris-Saclay, Gif-sur-Yvette; France*
- 144 *Santa Cruz Institute for Particle Physics, University of California Santa Cruz, Santa Cruz CA; United States of America*
- 145 *Departamento de Física^(a), Pontificia Universidad Católica de Chile, Santiago; Departamento de Física^(b), Universidad Técnica Federico Santa María, Valparaíso; Chile*
- 146 *Department of Physics, University of Washington, Seattle WA; United States of America*
- 147 *Department of Physics and Astronomy, University of Sheffield, Sheffield; United Kingdom*
- 148 *Department of Physics, Shinshu University, Nagano; Japan*
- 149 *Department Physik, Universität Siegen, Siegen; Germany*
- 150 *Department of Physics, Simon Fraser University, Burnaby BC; Canada*
- 151 *SLAC National Accelerator Laboratory, Stanford CA; United States of America*
- 152 *Physics Department, Royal Institute of Technology, Stockholm; Sweden*
- 153 *Departments of Physics and Astronomy, Stony Brook University, Stony Brook NY; United States of America*
- 154 *Department of Physics and Astronomy, University of Sussex, Brighton; United Kingdom*
- 155 *School of Physics, University of Sydney, Sydney; Australia*
- 156 *Institute of Physics, Academia Sinica, Taipei; Taiwan*
- 157 *E. Andronikashvili Institute of Physics^(a), Iv. Javakishvili Tbilisi State University, Tbilisi; High Energy Physics Institute^(b), Tbilisi State University, Tbilisi; Georgia*
- 158 *Department of Physics, Technion, Israel Institute of Technology, Haifa; Israel*

- 159 *Raymond and Beverly Sackler School of Physics and Astronomy, Tel Aviv University, Tel Aviv; Israel*
- 160 *Department of Physics, Aristotle University of Thessaloniki, Thessaloniki; Greece*
- 161 *International Center for Elementary Particle Physics and Department of Physics, University of Tokyo, Tokyo; Japan*
- 162 *Graduate School of Science and Technology, Tokyo Metropolitan University, Tokyo; Japan*
- 163 *Department of Physics, Tokyo Institute of Technology, Tokyo; Japan*
- 164 *Tomsk State University, Tomsk; Russia*
- 165 *Department of Physics, University of Toronto, Toronto ON; Canada*
- 166 *TRIUMF^(a), Vancouver BC; Department of Physics and Astronomy^(b), York University, Toronto ON; Canada*
- 167 *Division of Physics and Tomonaga Center for the History of the Universe, Faculty of Pure and Applied Sciences, University of Tsukuba, Tsukuba; Japan*
- 168 *Department of Physics and Astronomy, Tufts University, Medford MA; United States of America*
- 169 *Department of Physics and Astronomy, University of California Irvine, Irvine CA; United States of America*
- 170 *Department of Physics and Astronomy, University of Uppsala, Uppsala; Sweden*
- 171 *Department of Physics, University of Illinois, Urbana IL; United States of America*
- 172 *Instituto de Física Corpuscular (IFIC), Centro Mixto Universidad de Valencia — CSIC, Valencia; Spain*
- 173 *Department of Physics, University of British Columbia, Vancouver BC; Canada*
- 174 *Department of Physics and Astronomy, University of Victoria, Victoria BC; Canada*
- 175 *Fakultät für Physik und Astronomie, Julius-Maximilians-Universität Würzburg, Würzburg; Germany*
- 176 *Department of Physics, University of Warwick, Coventry; United Kingdom*
- 177 *Waseda University, Tokyo; Japan*
- 178 *Department of Particle Physics, Weizmann Institute of Science, Rehovot; Israel*
- 179 *Department of Physics, University of Wisconsin, Madison WI; United States of America*
- 180 *Fakultät für Mathematik und Naturwissenschaften, Fachgruppe Physik, Bergische Universität Wuppertal, Wuppertal; Germany*
- 181 *Department of Physics, Yale University, New Haven CT; United States of America*
- 182 *Yerevan Physics Institute, Yerevan; Armenia*
- ^a *Also at Borough of Manhattan Community College, City University of New York, NY; United States of America*
- ^b *Also at California State University, East Bay; United States of America*
- ^c *Also at Centre for High Performance Computing, CSIR Campus, Rosebank, Cape Town; South Africa*
- ^d *Also at CERN, Geneva; Switzerland*
- ^e *Also at CPPM, Aix-Marseille Université, CNRS/IN2P3, Marseille; France*
- ^f *Also at Département de Physique Nucléaire et Corpusculaire, Université de Genève, Genève; Switzerland*
- ^g *Also at Departament de Física de la Universitat Autònoma de Barcelona, Barcelona; Spain*
- ^h *Also at Departamento de Física, Instituto Superior Técnico, Universidade de Lisboa, Lisboa; Portugal*
- ⁱ *Also at Department of Applied Physics and Astronomy, University of Sharjah, Sharjah; United Arab Emirates*
- ^j *Also at Department of Financial and Management Engineering, University of the Aegean, Chios; Greece*
- ^k *Also at Department of Physics and Astronomy, University of Louisville, Louisville, KY; United States of America*
- ^l *Also at Department of Physics and Astronomy, University of Sheffield, Sheffield; United Kingdom*

- ^m Also at Department of Physics, California State University, Fresno CA; United States of America
- ⁿ Also at Department of Physics, California State University, Sacramento CA; United States of America
- ^o Also at Department of Physics, King's College London, London; United Kingdom
- ^p Also at Department of Physics, St. Petersburg State Polytechnical University, St. Petersburg; Russia
- ^q Also at Department of Physics, Stanford University, Stanford CA; United States of America
- ^r Also at Department of Physics, University of Fribourg, Fribourg; Switzerland
- ^s Also at Department of Physics, University of Michigan, Ann Arbor MI; United States of America
- ^t Also at Giresun University, Faculty of Engineering, Giresun; Turkey
- ^u Also at Graduate School of Science, Osaka University, Osaka; Japan
- ^v Also at Hellenic Open University, Patras; Greece
- ^w Also at Horia Hulubei National Institute of Physics and Nuclear Engineering, Bucharest; Romania
- ^x Also at Institutio Catalana de Recerca i Estudis Avancats, ICREA, Barcelona; Spain
- ^y Also at Institut für Experimentalphysik, Universität Hamburg, Hamburg; Germany
- ^z Also at Institute for Mathematics, Astrophysics and Particle Physics, Radboud University Nijmegen/Nikhef, Nijmegen; Netherlands
- ^{aa} Also at Institute for Nuclear Research and Nuclear Energy (INRNE) of the Bulgarian Academy of Sciences, Sofia; Bulgaria
- ^{ab} Also at Institute for Particle and Nuclear Physics, Wigner Research Centre for Physics, Budapest; Hungary
- ^{ac} Also at Institute of Particle Physics (IPP); Canada
- ^{ad} Also at Institute of Physics, Academia Sinica, Taipei; Taiwan
- ^{ae} Also at Institute of Physics, Azerbaijan Academy of Sciences, Baku; Azerbaijan
- ^{af} Also at Institute of Theoretical Physics, Ili State University, Tbilisi; Georgia
- ^{ag} Also at Instituto de Física Teórica de la Universidad Autónoma de Madrid; Spain
- ^{ah} Also at Istanbul University, Dept. of Physics, Istanbul; Turkey
- ^{ai} Also at Joint Institute for Nuclear Research, Dubna; Russia
- ^{aj} Also at LAL, Université Paris-Sud, CNRS/IN2P3, Université Paris-Saclay, Orsay; France
- ^{ak} Also at Louisiana Tech University, Ruston LA; United States of America
- ^{al} Also at LPNHE, Sorbonne Université, Paris Diderot Sorbonne Paris Cité, CNRS/IN2P3, Paris; France
- ^{am} Also at Manhattan College, New York NY; United States of America
- ^{an} Also at Moscow Institute of Physics and Technology State University, Dolgoprudny; Russia
- ^{ao} Also at National Research Nuclear University MEPhI, Moscow; Russia
- ^{ap} Also at Physics Dept, University of South Africa, Pretoria; South Africa
- ^{aq} Also at Physikalisches Institut, Albert-Ludwigs-Universität Freiburg, Freiburg; Germany
- ^{ar} Also at School of Physics, Sun Yat-sen University, Guangzhou; China
- ^{as} Also at The City College of New York, New York NY; United States of America
- ^{at} Also at The Collaborative Innovation Center of Quantum Matter (CICQM), Beijing; China
- ^{au} Also at Tomsk State University, Tomsk, and Moscow Institute of Physics and Technology State University, Dolgoprudny; Russia
- ^{av} Also at TRIUMF, Vancouver BC; Canada
- ^{aw} Also at Università di Napoli Parthenope, Napoli; Italy
- * Deceased

The CMS collaboration**Yerevan Physics Institute, Yerevan, Armenia**

A.M. Sirunyan, A. Tumasyan

Institut für Hochenergiephysik, Wien, Austria

W. Adam, F. Ambrogio, E. Asilar, T. Bergauer, J. Brandstetter, M. Dragicevic, J. Erö, A. Escalante Del Valle, M. Flechl, R. Frühwirth¹, V.M. Ghete, J. Hrubec, M. Jeitler¹, N. Krammer, I. Krätschmer, D. Liko, T. Madlener, I. Mikulec, N. Rad, H. Rohringer, J. Schieck¹, R. Schöfbeck, M. Spanring, D. Spitzbart, W. Waltenberger, J. Wittmann, C.-E. Wulz¹, M. Zarucki

Institute for Nuclear Problems, Minsk, Belarus

V. Chekhovsky, V. Mossolov, J. Suarez Gonzalez

Universiteit Antwerpen, Antwerpen, Belgium

E.A. De Wolf, D. Di Croce, X. Janssen, J. Lauwers, A. Lelek, M. Pieters, H. Van Haevermaet, P. Van Mechelen, N. Van Remortel

Vrije Universiteit Brussel, Brussel, Belgium

F. Blekman, J. D'Hondt, J. De Clercq, K. Deroover, G. Flouris, D. Lontkovskyi, S. Lowette, I. Marchesini, S. Moortgat, L. Moreels, Q. Python, K. Skovpen, S. Tavernier, W. Van Doninck, P. Van Mulders, I. Van Parijs

Université Libre de Bruxelles, Bruxelles, Belgium

D. Beghin, B. Bilin, H. Brun, B. Clerbaux, G. De Lentdecker, H. Delannoy, B. Dorney, G. Fasanella, L. Favart, A. Grebenyuk, A.K. Kalsi, J. Luetic, A. Popov², N. Postiau, E. Starling, L. Thomas, C. Vander Velde, P. Vanlaer, D. Vannerom, Q. Wang

Ghent University, Ghent, Belgium

T. Cornelis, D. Dobur, A. Fagot, M. Gul, I. Khvastunov³, C. Roskas, D. Trocino, M. Tytgat, W. Verbeke, B. Vermassen, M. Vit, N. Zaganidis

Université Catholique de Louvain, Louvain-la-Neuve, Belgium

H. Bakhshiansohi, O. Bondu, G. Bruno, C. Caputo, P. David, C. Delaere, M. Delcourt, A. Giammanco, G. Krintiras, V. Lemaitre, A. Magitteri, K. Piotrkowski, A. Saggio, M. Vidal Marono, P. Vischia, J. Zobec

Centro Brasileiro de Pesquisas Fisicas, Rio de Janeiro, Brazil

F.L. Alves, G.A. Alves, G. Correia Silva, C. Hensel, A. Moraes, M.E. Pol, P. Rebello Teles

Universidade do Estado do Rio de Janeiro, Rio de Janeiro, Brazil

E. Belchior Batista Das Chagas, W. Carvalho, J. Chinellato⁴, E. Coelho, E.M. Da Costa, G.G. Da Silveira⁵, D. De Jesus Damiao, C. De Oliveira Martins, S. Fonseca De Souza, L.M. Huertas Guativa, H. Malbouisson, D. Matos Figueiredo, M. Melo De Almeida, C. Mora Herrera, L. Mundim, H. Nogima, W.L. Prado Da Silva, L.J. Sanchez Rosas, A. Santoro, A. Sznajder, M. Thiel, E.J. Tonelli Manganote⁴, F. Torres Da Silva De Araujo, A. Vilela Pereira

Universidade Estadual Paulista^a, Universidade Federal do ABC^b, São Paulo, Brazil

S. Ahuja^a, C.A. Bernardes^a, L. Calligaris^a, T.R. Fernandez Perez Tomei^a, E.M. Gregores^b, P.G. Mercadante^b, S.F. Novaes^a, SandraS. Padula^a

Institute for Nuclear Research and Nuclear Energy, Bulgarian Academy of Sciences, Sofia, Bulgaria

A. Aleksandrov, R. Hadjiiska, P. Iaydjiev, A. Marinov, M. Misheva, M. Rodozov, M. Shopova, G. Sultanov

University of Sofia, Sofia, Bulgaria

A. Dimitrov, L. Litov, B. Pavlov, P. Petkov

Beihang University, Beijing, China

W. Fang⁶, X. Gao⁶, L. Yuan

Institute of High Energy Physics, Beijing, China

M. Ahmad, J.G. Bian, G.M. Chen, H.S. Chen, M. Chen, Y. Chen, C.H. Jiang, D. Leggat, H. Liao, Z. Liu, S.M. Shaheen⁷, A. Spiezia, J. Tao, E. Yazgan, H. Zhang, S. Zhang⁷, J. Zhao

State Key Laboratory of Nuclear Physics and Technology, Peking University, Beijing, China

Y. Ban, G. Chen, A. Levin, J. Li, L. Li, Q. Li, Y. Mao, S.J. Qian, D. Wang

Tsinghua University, Beijing, China

Y. Wang

Universidad de Los Andes, Bogota, Colombia

C. Avila, A. Cabrera, C.A. Carrillo Montoya, L.F. Chaparro Sierra, C. Florez, C.F. González Hernández, M.A. Segura Delgado

University of Split, Faculty of Electrical Engineering, Mechanical Engineering and Naval Architecture, Split, Croatia

N. Godinovic, D. Lelas, I. Puljak, T. Sculac

University of Split, Faculty of Science, Split, Croatia

Z. Antunovic, M. Kovac

Institute Rudjer Boskovic, Zagreb, Croatia

V. Brigljevic, D. Ferencek, K. Kadija, B. Mesic, M. Roguljic, A. Starodumov⁸, T. Susa

University of Cyprus, Nicosia, Cyprus

M.W. Ather, A. Attikis, M. Kolosova, G. Mavromanolakis, J. Mousa, C. Nicolaou, F. Ptochos, P.A. Razis, H. Rykaczewski

Charles University, Prague, Czech Republic

M. Finger⁹, M. Finger Jr.⁹

Escuela Politecnica Nacional, Quito, Ecuador

E. Ayala

Universidad San Francisco de Quito, Quito, Ecuador

E. Carrera Jarrin

**Academy of Scientific Research and Technology of the Arab Republic of Egypt,
Egyptian Network of High Energy Physics, Cairo, Egypt**H. Abdalla¹⁰, Y. Assran^{11,12}, A. Mohamed¹³**National Institute of Chemical Physics and Biophysics, Tallinn, Estonia**S. Bhowmik, A. Carvalho Antunes De Oliveira, R.K. Dewanjee, K. Ehataht, M. Kadastik,
M. Raidal, C. Veelken**Department of Physics, University of Helsinki, Helsinki, Finland**

P. Eerola, H. Kirschenmann, J. Pekkanen, M. Voutilainen

Helsinki Institute of Physics, Helsinki, FinlandJ. Havukainen, J.K. Heikkilä, T. Järvinen, V. Karimäki, R. Kinnunen, T. Lampén,
K. Lassila-Perini, S. Laurila, S. Lehti, T. Lindén, P. Luukka, T. Mäenpää, H. Siikonen,
E. Tuominen, J. Tuominiemi**Lappeenranta University of Technology, Lappeenranta, Finland**

T. Tuuva

IRFU, CEA, Université Paris-Saclay, Gif-sur-Yvette, FranceM. Besancon, F. Couderc, M. Dejardin, D. Denegri, J.L. Faure, F. Ferri, S. Ganjour,
A. Givernaud, P. Gras, G. Hamel de Monchenault, P. Jarry, C. Leloup, E. Locci, J. Malcles,
G. Negro, J. Rander, A. Rosowsky, M.Ö. Sahin, A. Savoy-Navarro¹⁴, M. Titov**Laboratoire Leprince-Ringuet, Ecole polytechnique, CNRS/IN2P3, Université
Paris-Saclay, Palaiseau, France**C. Amendola, F. Beaudette, P. Busson, C. Charlot, B. Diab, R. Granier de Cassagnac,
I. Kucher, A. Lobanov, J. Martin Blanco, C. Martin Perez, M. Nguyen, C. Ochando,
G. Ortona, P. Paganini, J. Rembser, R. Salerno, J.B. Sauvan, Y. Sirois, A.G. Stahl Leiton,
A. Zabi, A. Zghiche**Université de Strasbourg, CNRS, IPHC UMR 7178, Strasbourg, France**J.-L. Agram¹⁵, J. Andrea, D. Bloch, G. Bourgatte, J.-M. Brom, E.C. Chabert,
V. Cherepanov, C. Collard, E. Conte¹⁵, J.-C. Fontaine¹⁵, D. Gelé, U. Goerlach, M. Jansová,
A.-C. Le Bihan, N. Tonon, P. Van Hove**Centre de Calcul de l'Institut National de Physique Nucleaire et de Physique
des Particules, CNRS/IN2P3, Villeurbanne, France**

S. Gadrat

**Université de Lyon, Université Claude Bernard Lyon 1, CNRS-IN2P3, Institut
de Physique Nucléaire de Lyon, Villeurbanne, France**S. Beauceron, C. Bernet, G. Boudoul, N. Chanon, R. Chierici, D. Contardo, P. Depasse,
H. El Mamouni, J. Fay, S. Gascon, M. Gouzevitch, G. Grenier, B. Ille, F. Lagarde,
I.B. Laktineh, H. Lattaud, M. Lethuillier, L. Mirabito, S. Perries, V. Sordini, G. Touquet,
M. Vander Donckt, S. Viret

Georgian Technical University, Tbilisi, GeorgiaT. Toriashvili¹⁶**Tbilisi State University, Tbilisi, Georgia**Z. Tsamalaidze⁹**RWTH Aachen University, I. Physikalisches Institut, Aachen, Germany**

C. Autermann, L. Feld, M.K. Kiesel, K. Klein, M. Lipinski, M. Preuten, M.P. Rauch, C. Schomakers, J. Schulz, M. Teroerde, B. Wittmer

RWTH Aachen University, III. Physikalisches Institut A, Aachen, Germany

A. Albert, M. Erdmann, S. Erdweg, T. Esch, R. Fischer, S. Ghosh, T. Hebbeker, C. Heidemann, K. Hoepfner, H. Keller, L. Mastrolorenzo, M. Merschmeyer, A. Meyer, P. Millet, S. Mukherjee, A. Novak, T. Pook, A. Pozdnyakov, M. Radziej, H. Reithler, M. Rieger, A. Schmidt, D. Teyssier, S. Thüer

RWTH Aachen University, III. Physikalisches Institut B, Aachen, GermanyG. Flügge, O. Hlushchenko, T. Kress, T. Müller, A. Nehr Korn, A. Nowack, C. Pistone, O. Pooth, D. Roy, H. Sert, A. Stahl¹⁷**Deutsches Elektronen-Synchrotron, Hamburg, Germany**M. Aldaya Martin, T. Arndt, C. Asawatangtrakuldee, I. Babounikau, K. Beernaert, O. Behnke, U. Behrens, A. Bermúdez Martínez, D. Bertsche, A.A. Bin Anuar, K. Borras¹⁸, V. Botta, A. Campbell, P. Connor, C. Contreras-Campana, V. Danilov, A. De Wit, M.M. Defranchis, C. Diez Pardos, D. Domínguez Damiani, G. Eckerlin, T. Eichhorn, A. Elwood, E. Eren, E. Gallo¹⁹, A. Geiser, J.M. Grados Luyando, A. Grohsjean, M. Guthoff, M. Haranko, A. Harb, N.Z. Jomhari, H. Jung, M. Kasemann, J. Keaveney, C. Kleinwort, J. Knolle, D. Krücker, W. Lange, T. Lenz, J. Leonard, K. Lipka, W. Lohmann²⁰, R. Mankel, I.-A. Melzer-Pellmann, A.B. Meyer, M. Meyer, M. Missiroli, G. Mittag, J. Mnich, V. Myronenko, S.K. Pflitsch, D. Pitzl, A. Raspereza, A. Saibel, M. Savitskyi, P. Saxena, P. Schütze, C. Schwanenberger, R. Shevchenko, A. Singh, H. Tholen, O. Turkot, A. Vagnerini, M. Van De Klundert, G.P. Van Onsem, R. Walsh, Y. Wen, K. Wichmann, C. Wissing, O. Zenaiev**University of Hamburg, Hamburg, Germany**

R. Aggleton, S. Bein, L. Benato, A. Benecke, V. Blobel, T. Dreyer, A. Ebrahimi, E. Garutti, D. Gonzalez, P. Gunnellini, J. Haller, A. Hinzmann, A. Karavdina, G. Kasieczka, R. Klanner, R. Kogler, N. Kovalchuk, S. Kurz, V. Kutzner, J. Lange, D. Marconi, J. Multhaupt, M. Niedziela, C.E.N. Niemeyer, D. Nowatschin, A. Perieanu, A. Reimers, O. Rieger, C. Scharf, P. Schleper, S. Schumann, J. Schwandt, J. Sonneveld, H. Stadie, G. Steinbrück, F.M. Stober, M. Stöver, B. Vormwald, I. Zoi

Karlsruher Institut fuer Technologie, Karlsruhe, GermanyM. Akbiyik, C. Barth, M. Baselga, S. Baur, T. Berger, E. Butz, R. Caspart, T. Chwalek, W. De Boer, A. Dierlamm, K. El Morabit, N. Faltermann, M. Giffels, M.A. Harrendorf, F. Hartmann¹⁷, U. Husemann, I. Katkov², S. Kudella, S. Mitra, M.U. Mozer, Th. Müller,

M. Musich, G. Quast, K. Rabbertz, M. Schröder, I. Shvetsov, H.J. Simonis, R. Ulrich, M. Weber, C. Wöhrmann, R. Wolf

Institute of Nuclear and Particle Physics (INPP), NCSR Demokritos, Aghia Paraskevi, Greece

G. Anagnostou, G. Daskalakis, T. Gerasis, A. Kyriakis, D. Loukas, G. Paspalaki

National and Kapodistrian University of Athens, Athens, Greece

A. Agapitos, G. Karathanasis, P. Kontaxakis, A. Panagiotou, I. Papavergou, N. Saoulidou, K. Vellidis

National Technical University of Athens, Athens, Greece

G. Bakas, K. Kousouris, I. Papakrivopoulos, G. Tsipolitis

University of Ioánnina, Ioánnina, Greece

I. Evangelou, C. Foudas, P. Giannelis, P. Katsoulis, P. Kokkas, S. Mallios, K. Manitaras, N. Manthos, I. Papadopoulos, E. Paradas, J. Strologas, F.A. Triantis, D. Tsitsonis

MTA-ELTE Lendület CMS Particle and Nuclear Physics Group, Eötvös Loránd University, Budapest, Hungary

M. Bartók²¹, M. Csanad, N. Filipovic, P. Major, K. Mandal, A. Mehta, M.I. Nagy, G. Pasztor, O. Surányi, G.I. Veres

Wigner Research Centre for Physics, Budapest, Hungary

G. Bencze, C. Hajdu, D. Horvath²², Á. Hunyadi, F. Sikler, T.Á. Vámi, V. Veszpremi, G. Vesztergombi[†]

Institute of Nuclear Research ATOMKI, Debrecen, Hungary

N. Beni, S. Czellar, J. Karanicsi²¹, A. Makovec, J. Molnar, Z. Szillasi

Institute of Physics, University of Debrecen, Debrecen, Hungary

P. Raics, Z.L. Trocsanyi, B. Ujvari

Indian Institute of Science (IISc), Bangalore, India

S. Choudhury, J.R. Komaragiri, P.C. Tiwari

National Institute of Science Education and Research, HBNI, Bhubaneswar, India

S. Bahinipati²⁴, C. Kar, P. Mal, A. Nayak²⁵, S. Roy Chowdhury, D.K. Sahoo²⁴, S.K. Swain

Panjab University, Chandigarh, India

S. Bansal, S.B. Beri, V. Bhatnagar, S. Chauhan, R. Chawla, N. Dhingra, R. Gupta, A. Kaur, M. Kaur, S. Kaur, P. Kumari, M. Lohan, M. Meena, K. Sandeep, S. Sharma, J.B. Singh, A.K. Viridi, G. Walia

University of Delhi, Delhi, India

A. Bhardwaj, B.C. Choudhary, R.B. Garg, M. Gola, S. Keshri, Ashok Kumar, S. Malhotra, M. Naimuddin, P. Priyanka, K. Ranjan, Aashaq Shah, R. Sharma

Saha Institute of Nuclear Physics, HBNI, Kolkata, India

R. Bhardwaj²⁶, M. Bharti²⁶, R. Bhattacharya, S. Bhattacharya, U. Bhawandeep²⁶, D. Bhowmik, S. Dey, S. Dutt²⁶, S. Dutta, S. Ghosh, M. Maity²⁷, K. Mondal, S. Nandan, A. Purohit, P.K. Rout, A. Roy, G. Saha, S. Sarkar, T. Sarkar²⁷, M. Sharan, B. Singh²⁶, S. Thakur²⁶

Indian Institute of Technology Madras, Madras, India

P.K. Behera, A. Muhammad

Bhabha Atomic Research Centre, Mumbai, India

R. Chudasama, D. Dutta, V. Jha, V. Kumar, D.K. Mishra, P.K. Netrakanti, L.M. Pant, P. Shukla, P. Suggisetti

Tata Institute of Fundamental Research-A, Mumbai, India

T. Aziz, M.A. Bhat, S. Dugad, G.B. Mohanty, N. Sur, RavindraKumar Verma

Tata Institute of Fundamental Research-B, Mumbai, India

S. Banerjee, S. Bhattacharya, S. Chatterjee, P. Das, M. Guchait, Sa. Jain, S. Karmakar, S. Kumar, G. Majumder, K. Mazumdar, N. Sahoo, S. Sawant

Indian Institute of Science Education and Research (IISER), Pune, India

S. Chauhan, S. Dube, V. Hegde, A. Kapoor, K. Kotheekar, S. Pandey, A. Rane, A. Rastogi, S. Sharma

Institute for Research in Fundamental Sciences (IPM), Tehran, Iran

S. Chenarani²⁸, E. Eskandari Tadavani, S.M. Etesami²⁸, M. Khakzad, M. Mohammadi Najafabadi, M. Naseri, F. Rezaei Hosseinabadi, B. Safarzadeh²⁹, M. Zeinali

University College Dublin, Dublin, Ireland

M. Felcini, M. Grunewald

INFN Sezione di Bari^a, Università di Bari^b, Politecnico di Bari^c, Bari, Italy

M. Abbrescia^{a,b}, C. Calabria^{a,b}, A. Colaleo^a, D. Creanza^{a,c}, L. Cristella^{a,b}, N. De Filippis^{a,c}, M. De Palma^{a,b}, A. Di Florio^{a,b}, F. Errico^{a,b}, L. Fiore^a, A. Gelmi^{a,b}, G. Iaselli^{a,c}, M. Ince^{a,b}, S. Lezki^{a,b}, G. Maggi^{a,c}, M. Maggi^a, G. Miniello^{a,b}, S. My^{a,b}, S. Nuzzo^{a,b}, A. Pompili^{a,b}, G. Pugliese^{a,c}, R. Radogna^a, A. Ranieri^a, G. Selvaggi^{a,b}, A. Sharma^a, L. Silvestris^a, R. Venditti^a, P. Verwilligen^a

INFN Sezione di Bologna^a, Università di Bologna^b, Bologna, Italy

G. Abbiendi^a, C. Battilana^{a,b}, D. Bonacorsi^{a,b}, L. Borgonovi^{a,b}, S. Braibant-Giacomelli^{a,b}, R. Campanini^{a,b}, P. Capiluppi^{a,b}, A. Castro^{a,b}, F.R. Cavallo^a, S.S. Chhibra^{a,b}, G. Codispoti^{a,b}, M. Cuffiani^{a,b}, G.M. Dallavalle^a, F. Fabbri^a, A. Fanfani^{a,b}, E. Fontanesi, P. Giacomelli^a, C. Grandi^a, L. Guiducci^{a,b}, F. Iemmi^{a,b}, S. Lo Meo^{a,30}, S. Marcellini^a, G. Masetti^a, A. Montanari^a, F.L. Navarria^{a,b}, A. Perrotta^a, F. Primavera^{a,b}, A.M. Rossi^{a,b}, T. Rovelli^{a,b}, G.P. Siroli^{a,b}, N. Tosi^a

INFN Sezione di Catania^a, Università di Catania^b, Catania, Italy

S. Albergo^{a,b,31}, A. Di Mattia^a, R. Potenza^{a,b}, A. Tricomi^{a,b,31}, C. Tuve^{a,b}

INFN Sezione di Firenze^a, Università di Firenze^b, Firenze, Italy

G. Barbagli^a, K. Chatterjee^{a,b}, V. Ciulli^{a,b}, C. Civinini^a, R. D'Alessandro^{a,b}, E. Focardi^{a,b}, G. Latino, P. Lenzi^{a,b}, M. Meschini^a, S. Paoletti^a, L. Russo^{a,32}, G. Sguazzoni^a, D. Strom^a, L. Viliani^a

INFN Laboratori Nazionali di Frascati, Frascati, Italy

L. Benussi, S. Bianco, F. Fabbri, D. Piccolo

INFN Sezione di Genova^a, Università di Genova^b, Genova, Italy

F. Ferro^a, R. Mulargia^{a,b}, E. Robutti^a, S. Tosi^{a,b}

INFN Sezione di Milano-Bicocca^a, Università di Milano-Bicocca^b, Milano, Italy

A. Benaglia^a, A. Beschi^b, F. Brivio^{a,b}, V. Ciriolo^{a,b,17}, S. Di Guida^{a,b,17}, M.E. Dinardo^{a,b}, S. Fiorendi^{a,b}, S. Gennai^a, A. Ghezzi^{a,b}, P. Govoni^{a,b}, M. Malberti^{a,b}, S. Malvezzi^a, D. Menasce^a, F. Monti, L. Moroni^a, M. Paganoni^{a,b}, D. Pedrini^a, S. Ragazzi^{a,b}, T. Tabarelli de Fatis^{a,b}, D. Zuolo^{a,b}

INFN Sezione di Napoli^a, Università di Napoli 'Federico II'^b, Napoli, Italy, Università della Basilicata^c, Potenza, Italy, Università G. Marconi^d, Roma, Italy

S. Buontempo^a, N. Cavallo^{a,c}, A. De Iorio^{a,b}, A. Di Crescenzo^{a,b}, F. Fabozzi^{a,c}, F. Fienga^a, G. Galati^a, A.O.M. Iorio^{a,b}, L. Lista^a, S. Meola^{a,d,17}, P. Paolucci^{a,17}, C. Sciacca^{a,b}, E. Voevodina^{a,b}

INFN Sezione di Padova^a, Università di Padova^b, Padova, Italy, Università di Trento^c, Trento, Italy

P. Azzi^a, N. Bacchetta^a, D. Bisello^{a,b}, A. Boletti^{a,b}, A. Bragagnolo, R. Carlin^{a,b}, P. Checchia^a, M. Dall'Osso^{a,b}, P. De Castro Manzano^a, T. Dorigo^a, U. Dosselli^a, F. Gasparini^{a,b}, U. Gasparini^{a,b}, A. Gozzelino^a, S.Y. Hoh, S. Lacaprara^a, P. Lujan, M. Margoni^{a,b}, A.T. Meneguzzo^{a,b}, J. Pazzini^{a,b}, M. Presilla^b, P. Ronchese^{a,b}, R. Rossin^{a,b}, F. Simonetto^{a,b}, A. Tiko, E. Torassa^a, M. Tosi^{a,b}, M. Zanetti^{a,b}, P. Zotto^{a,b}, G. Zumerle^{a,b}

INFN Sezione di Pavia^a, Università di Pavia^b, Pavia, Italy

A. Braghieri^a, A. Magnani^a, P. Montagna^{a,b}, S.P. Ratti^{a,b}, V. Re^a, M. Ressegotti^{a,b}, C. Riccardi^{a,b}, P. Salvini^a, I. Vai^{a,b}, P. Vitulo^{a,b}

INFN Sezione di Perugia^a, Università di Perugia^b, Perugia, Italy

M. Biasini^{a,b}, G.M. Bilei^a, C. Cecchi^{a,b}, D. Ciangottini^{a,b}, L. Fanò^{a,b}, P. Lariccia^{a,b}, R. Leonardi^{a,b}, E. Manoni^a, G. Mantovani^{a,b}, V. Mariani^{a,b}, M. Menichelli^a, A. Rossi^{a,b}, A. Santocchia^{a,b}, D. Spiga^a

INFN Sezione di Pisa^a, Università di Pisa^b, Scuola Normale Superiore di Pisa^c, Pisa, Italy

K. Androsov^a, P. Azzurri^a, G. Bagliesi^a, L. Bianchini^a, T. Boccali^a, L. Borrello, R. Castaldi^a, M.A. Ciocci^{a,b}, R. Dell'Orso^a, G. Fedi^a, F. Fiori^{a,c}, L. Giannini^{a,c}, A. Giassi^a, M.T. Grippo^a, F. Ligabue^{a,c}, E. Manca^{a,c}, G. Mandorli^{a,c}, A. Messineo^{a,b}, F. Palla^a, A. Rizzi^{a,b}, G. Rolandi³³, P. Spagnolo^a, R. Tenchini^a, G. Tonelli^{a,b}, A. Venturi^a, P.G. Verdini^a

INFN Sezione di Roma^a, Sapienza Università di Roma^b, Rome, Italy

L. Barone^{a,b}, F. Cavallari^a, M. Cipriani^{a,b}, D. Del Re^{a,b}, E. Di Marco^{a,b},
 M. Diemoz^a, S. Gelli^{a,b}, E. Longo^{a,b}, B. Marzocchi^{a,b}, P. Meridiani^a, G. Organtini^{a,b},
 F. Pandolfi^a, R. Paramatti^{a,b}, F. Preiato^{a,b}, C. Quaranta^{a,b}, S. Rahatlou^{a,b}, C. Rovelli^a,
 F. Santanastasio^{a,b}

INFN Sezione di Torino^a, Università di Torino^b, Torino, Italy, Università del Piemonte Orientale^c, Novara, Italy

N. Amapane^{a,b}, R. Arcidiacono^{a,c}, S. Argiro^{a,b}, M. Arneodo^{a,c}, N. Bartosik^a, R. Bellan^{a,b},
 C. Biino^a, A. Cappati^{a,b}, N. Cartiglia^a, F. Cenna^{a,b}, S. Cometti^a, M. Costa^{a,b},
 R. Covarelli^{a,b}, N. Demaria^a, B. Kiani^{a,b}, C. Mariotti^a, S. Maselli^a, E. Migliore^{a,b},
 V. Monaco^{a,b}, E. Monteil^{a,b}, M. Monteno^a, M.M. Obertino^{a,b}, L. Pacher^{a,b}, N. Pastrone^a,
 M. Pelliccioni^a, G.L. Pinna Angioni^{a,b}, A. Romero^{a,b}, M. Ruspa^{a,c}, R. Sacchi^{a,b},
 R. Salvatico^{a,b}, K. Shchelina^{a,b}, V. Sola^a, A. Solano^{a,b}, D. Soldi^{a,b}, A. Staiano^a

INFN Sezione di Trieste^a, Università di Trieste^b, Trieste, Italy

S. Belforte^a, V. Candelise^{a,b}, M. Casarsa^a, F. Cossutti^a, A. Da Rold^{a,b}, G. Della Ricca^{a,b},
 F. Vazzoler^{a,b}, A. Zanetti^a

Kyungpook National University, Daegu, Korea

D.H. Kim, G.N. Kim, M.S. Kim, J. Lee, S.W. Lee, C.S. Moon, Y.D. Oh, S.I. Pak,
 S. Sekmen, D.C. Son, Y.C. Yang

Chonnam National University, Institute for Universe and Elementary Particles, Kwangju, Korea

H. Kim, D.H. Moon, G. Oh

Hanyang University, Seoul, Korea

B. Francois, J. Goh³⁴, T.J. Kim

Korea University, Seoul, Korea

S. Cho, S. Choi, Y. Go, D. Gyun, S. Ha, B. Hong, Y. Jo, K. Lee, K.S. Lee, S. Lee, J. Lim,
 S.K. Park, Y. Roh

Sejong University, Seoul, Korea

H.S. Kim

Seoul National University, Seoul, Korea

J. Almond, J. Kim, J.S. Kim, H. Lee, K. Lee, S. Lee, K. Nam, S.B. Oh, B.C. Radburn-Smith,
 S.h. Seo, U.K. Yang, H.D. Yoo, G.B. Yu

University of Seoul, Seoul, Korea

D. Jeon, H. Kim, J.H. Kim, J.S.H. Lee, I.C. Park

Sungkyunkwan University, Suwon, Korea

Y. Choi, C. Hwang, J. Lee, I. Yu

Riga Technical University, Riga, Latvia

V. Veckalns³⁵

Vilnius University, Vilnius, Lithuania

V. Dudenas, A. Juodagalvis, J. Vaitkus

National Centre for Particle Physics, Universiti Malaya, Kuala Lumpur, MalaysiaZ.A. Ibrahim, M.A.B. Md Ali³⁶, F. Mohamad Idris³⁷, W.A.T. Wan Abdullah, M.N. Yusli, Z. Zolkapli**Universidad de Sonora (UNISON), Hermosillo, Mexico**

J.F. Benitez, A. Castaneda Hernandez, J.A. Murillo Quijada

Centro de Investigacion y de Estudios Avanzados del IPN, Mexico City, MexicoH. Castilla-Valdez, E. De La Cruz-Burelo, M.C. Duran-Osuna, I. Heredia-De La Cruz³⁸, R. Lopez-Fernandez, J. Mejia Guisao, R.I. Rabadan-Trejo, G. Ramirez-Sanchez, R. Reyes-Almanza, A. Sanchez-Hernandez**Universidad Iberoamericana, Mexico City, Mexico**

S. Carrillo Moreno, C. Oropeza Barrera, M. Ramirez-Garcia, F. Vazquez Valencia

Benemerita Universidad Autonoma de Puebla, Puebla, Mexico

J. Eysermans, I. Pedraza, H.A. Salazar Ibarguen, C. Uribe Estrada

Universidad Autónoma de San Luis Potosí, San Luis Potosí, Mexico

A. Morelos Pineda

University of Montenegro, Podgorica, Montenegro

N. Raicevic

University of Auckland, Auckland, New Zealand

D. Krofcheck

University of Canterbury, Christchurch, New Zealand

S. Bheesette, P.H. Butler

National Centre for Physics, Quaid-I-Azam University, Islamabad, Pakistan

A. Ahmad, M. Ahmad, M.I. Asghar, Q. Hassan, H.R. Hoorani, W.A. Khan, M.A. Shah, M. Shoaib, M. Waqas

National Centre for Nuclear Research, Swierk, Poland

H. Bialkowska, M. Bluj, B. Boimska, T. Frueboes, M. Górski, M. Kazana, M. Szeleper, P. Traczyk, P. Zalewski

Institute of Experimental Physics, Faculty of Physics, University of Warsaw, Warsaw, PolandK. Bunkowski, A. Byszuk³⁹, K. Doroba, A. Kalinowski, M. Konecki, J. Krolikowski, M. Misiura, M. Olszewski, A. Pyskir, M. Walczak

Laboratório de Instrumentação e Física Experimental de Partículas, Lisboa, Portugal

M. Araujo, P. Bargassa, C. Beirão Da Cruz E Silva, A. Di Francesco, P. Faccioli, B. Galinhas, M. Gallinaro, J. Hollar, N. Leonardo, J. Seixas, G. Strong, O. Toldaiev, J. Varela

Joint Institute for Nuclear Research, Dubna, Russia

S. Afanasiev, P. Bunin, M. Gavrilenko, I. Golutvin, I. Gorbunov, A. Kamenev, V. Karjavine, A. Lanev, A. Malakhov, V. Matveev^{40,41}, P. Moisenz, V. Palichik, V. Perelygin, S. Shmatov, S. Shulha, N. Skatchkov, V. Smirnov, N. Voytishin, A. Zarubin

Petersburg Nuclear Physics Institute, Gatchina (St. Petersburg), Russia

V. Golovtsov, Y. Ivanov, V. Kim⁴², E. Kuznetsova⁴³, P. Levchenko, V. Murzin, V. Oreshkin, I. Smirnov, D. Sosnov, V. Sulimov, L. Uvarov, S. Vavilov, A. Vorobyev

Institute for Nuclear Research, Moscow, Russia

Yu. Andreev, A. Dermenev, S. Gninenko, N. Golubev, A. Karneyeu, M. Kirsanov, N. Krasnikov, A. Pashenkov, A. Shabanov, D. Tlisov, A. Toropin

Institute for Theoretical and Experimental Physics, Moscow, Russia

V. Epshteyn, V. Gavrilov, N. Lychkovskaya, V. Popov, I. Pozdnyakov, G. Safronov, A. Spiridonov, A. Stepenov, V. Stolin, M. Toms, E. Vlasov, A. Zhokin

Moscow Institute of Physics and Technology, Moscow, Russia

T. Aushev

National Research Nuclear University ‘Moscow Engineering Physics Institute’ (MEPhI), Moscow, Russia

M. Chadeeva⁴⁴, S. Polikarpov⁴⁴, E. Popova, V. Rusinov

P.N. Lebedev Physical Institute, Moscow, Russia

V. Andreev, M. Azarkin, I. Dremin⁴¹, M. Kirakosyan, A. Terkulov

Skobeltsyn Institute of Nuclear Physics, Lomonosov Moscow State University, Moscow, Russia

A. Belyaev, E. Boos, V. Bunichev, M. Dubinin⁴⁵, L. Dudko, A. Gribushin, V. Klyukhin, N. Korneeva, I. Lokhtin, S. Obraztsov, M. Perfilov, V. Savrin, P. Volkov

Novosibirsk State University (NSU), Novosibirsk, Russia

A. Barnyakov⁴⁶, V. Blinov⁴⁶, T. Dimova⁴⁶, L. Kardapoltsev⁴⁶, Y. Skovpen⁴⁶

Institute for High Energy Physics of National Research Centre ‘Kurchatov Institute’, Protvino, Russia

I. Azhgirey, I. Bayshev, S. Bitioukov, V. Kachanov, A. Kalinin, D. Konstantinov, P. Mandrik, V. Petrov, R. Ryutin, S. Slabospitskii, A. Sobol, S. Troshin, N. Tyurin, A. Uzunian, A. Volkov

National Research Tomsk Polytechnic University, Tomsk, Russia

A. Babaev, S. Baidali, V. Okhotnikov

University of Belgrade: Faculty of Physics and VINCA Institute of Nuclear Sciences

P. Adzic⁴⁷, P. Cirkovic, D. Devetak, M. Dordevic, P. Milenovic⁴⁸, J. Milosevic

Centro de Investigaciones Energéticas Medioambientales y Tecnológicas (CIEMAT), Madrid, Spain

J. Alcaraz Maestre, A. Álvarez Fernández, I. Bachiller, M. Barrio Luna, J.A. Brochero Cifuentes, M. Cerrada, N. Colino, B. De La Cruz, A. Delgado Peris, C. Fernandez Bedoya, J.P. Fernández Ramos, J. Flix, M.C. Fouz, O. Gonzalez Lopez, S. Goy Lopez, J.M. Hernandez, M.I. Josa, D. Moran, A. Pérez-Calero Yzquierdo, J. Puerta Pelayo, I. Redondo, L. Romero, S. Sánchez Navas, M.S. Soares, A. Triossi

Universidad Autónoma de Madrid, Madrid, Spain

C. Albajar, J.F. de Trocóniz

Universidad de Oviedo, Oviedo, Spain

J. Cuevas, C. Erice, J. Fernandez Menendez, S. Folgueras, I. Gonzalez Caballero, J.R. González Fernández, E. Palencia Cortezon, V. Rodríguez Bouza, S. Sanchez Cruz, J.M. Vizán García

Instituto de Física de Cantabria (IFCA), CSIC-Universidad de Cantabria, Santander, Spain

I.J. Cabrillo, A. Calderon, B. Chazin Quero, J. Duarte Campderros, M. Fernandez, P.J. Fernández Manteca, A. García Alonso, J. Garcia-Ferrero, G. Gomez, A. Lopez Virto, J. Marco, C. Martinez Rivero, P. Martinez Ruiz del Arbol, F. Matorras, J. Piedra Gomez, C. Prieels, T. Rodrigo, A. Ruiz-Jimeno, L. Scodellaro, N. Trevisani, I. Vila, R. Villar Cortabitarte

University of Ruhuna, Department of Physics, Matara, Sri Lanka

N. Wickramage

CERN, European Organization for Nuclear Research, Geneva, Switzerland

D. Abbaneo, B. Akgun, E. Auffray, G. Auzinger, P. Baillon, A.H. Ball, D. Barney, J. Bendavid, M. Bianco, A. Bocci, C. Botta, E. Brondolin, T. Camporesi, M. Cepeda, G. Cerminara, E. Chapon, Y. Chen, G. Cucciati, D. d'Enterria, A. Dabrowski, N. Daci, V. Daponte, A. David, A. De Roeck, N. Deelen, M. Dobson, M. Dünser, N. Dupont, A. Elliott-Peisert, F. Fallavollita⁴⁹, D. Fasanella, G. Franzoni, J. Fulcher, W. Funk, D. Gigi, A. Gilbert, K. Gill, F. Glege, M. Gruchala, M. Guilbaud, D. Gulhan, J. Hegeman, C. Heidegger, Y. Iiyama, V. Innocente, G.M. Innocenti, A. Jafari, P. Janot, O. Karacheban²⁰, J. Kieseler, A. Kornmayer, M. Krammer¹, C. Lange, P. Lecoq, C. Lourenço, L. Malgeri, M. Mannelli, A. Massironi, F. Meijers, J.A. Merlin, S. Mersi, E. Meschi, F. Moortgat, M. Mulders, J. Ngadiuba, S. Nourbakhsh, S. Orfanelli, L. Orsini, F. Pantaleo¹⁷, L. Pape, E. Perez, M. Peruzzi, A. Petrilli, G. Petrucciani, A. Pfeiffer, M. Pierini, F.M. Pitters, D. Rabady, A. Racz, M. Rovere, H. Sakulin, C. Schäfer, C. Schwick, M. Selvaggi, A. Sharma, P. Silva, P. Sphicas⁵⁰, A. Stakia, J. Steggemann, D. Treille, A. Tsiros, A. Vartak, M. Verzetti, W.D. Zeuner

Paul Scherrer Institut, Villigen, Switzerland

L. Caminada⁵¹, K. Deiters, W. Erdmann, R. Horisberger, Q. Ingram, H.C. Kaestli, D. Kotlinski, U. Langenegger, T. Rohe, S.A. Wiederkehr

ETH Zurich — Institute for Particle Physics and Astrophysics (IPA), Zurich, Switzerland

M. Backhaus, P. Berger, N. Chernyavskaya, G. Dissertori, M. Dittmar, M. Donegà, C. Dorfer, T.A. Gómez Espinosa, C. Grab, D. Hits, T. Klijnsma, W. Luster, R.A. Manzoni, M. Marionneau, M.T. Meinhard, F. Micheli, P. Musella, F. Nessi-Tedaldi, F. Pauss, G. Perrin, L. Perrozzi, S. Pigazzini, M. Reichmann, C. Reissel, T. Reitenspiess, D. Ruini, D.A. Sanz Becerra, M. Schönenberger, L. Shchutska, V.R. Tavolaro, K. Theofilatos, M.L. Vesterbacka Olsson, R. Wallny, D.H. Zhu

Universität Zürich, Zurich, Switzerland

T.K. Aarrestad, C. AMSler⁵², D. Brzhechko, M.F. Canelli, A. De Cosa, R. Del Burgo, S. Donato, C. Galloni, T. Hreus, B. Kilminster, S. Leontsinis, V.M. Mikuni, I. Neutelings, G. Rauco, P. Robmann, D. Salerno, K. Schweiger, C. Seitz, Y. Takahashi, S. Wertz, A. Zucchetta

National Central University, Chung-Li, Taiwan

T.H. Doan, C.M. Kuo, W. Lin, S.S. Yu

National Taiwan University (NTU), Taipei, Taiwan

P. Chang, Y. Chao, K.F. Chen, P.H. Chen, W.-S. Hou, Y.F. Liu, R.-S. Lu, E. Paganis, A. Psallidas, A. Steen

Chulalongkorn University, Faculty of Science, Department of Physics, Bangkok, Thailand

B. Asavapibhop, N. Srimanobhas, N. Suwonjandee

Çukurova University, Physics Department, Science and Art Faculty, Adana, Turkey

A. Bat, F. Boran, S. Cerci⁵³, S. Damarseckin⁵⁴, Z.S. Demiroglu, F. Dolek, C. Dozen, I. Dumanoglu, G. Gokbulut, EmineGurpinar Guler⁵⁵, Y. Guler, I. Hos⁵⁶, C. Isik, E.E. Kangal⁵⁷, O. Kara, A. Kayis Topaksu, U. Kiminsu, M. Oglakci, G. Onengut, K. Ozdemir⁵⁸, S. Ozturk⁵⁹, A. Polatoz, B. Tali⁵³, U.G. Tok, S. Turkcapar, I.S. Zorbakir, C. Zorbilmez

Middle East Technical University, Physics Department, Ankara, Turkey

B. Isildak⁶⁰, G. Karapinar⁶¹, M. Yalvac, M. Zeyrek

Bogazici University, Istanbul, Turkey

I.O. Atakisi, E. Gülmez, M. Kaya⁶², O. Kaya⁶³, Ö. Özçelik, S. Ozkorucuklu⁶⁴, S. Tekten, E.A. Yetkin⁶⁵

Istanbul Technical University, Istanbul, Turkey

A. Cakir, K. Cankocak, Y. Komurcu, S. Sen⁶⁶

**Institute for Scintillation Materials of National Academy of Science of Ukraine,
Kharkov, Ukraine**

B. Grynyov

**National Scientific Center, Kharkov Institute of Physics and Technology,
Kharkov, Ukraine**

L. Levchuk

University of Bristol, Bristol, United Kingdom

F. Ball, J.J. Brooke, D. Burns, E. Clement, D. Cussans, O. Davignon, H. Flacher, J. Goldstein, G.P. Heath, H.F. Heath, L. Kreczko, D.M. Newbold⁶⁷, S. Paramesvaran, B. Penning, T. Sakuma, D. Smith, V.J. Smith, J. Taylor, A. Titterton

Rutherford Appleton Laboratory, Didcot, United Kingdom

K.W. Bell, A. Belyaev⁶⁸, C. Brew, R.M. Brown, D. Cieri, D.J.A. Cockerill, J.A. Coughlan, K. Harder, S. Harper, J. Linacre, K. Manolopoulos, E. Olaiya, D. Petyt, T. Reis, T. Schuh, C.H. Shepherd-Themistocleous, A. Thea, I.R. Tomalin, T. Williams, W.J. Womersley

Imperial College, London, United Kingdom

R. Bainbridge, P. Bloch, J. Borg, S. Breeze, O. Buchmuller, A. Bundock, D. Colling, P. Dauncey, G. Davies, M. Della Negra, R. Di Maria, P. Everaerts, G. Hall, G. Iles, T. James, M. Komm, C. Laner, L. Lyons, A.-M. Magnan, S. Malik, A. Martelli, V. Milosevic, J. Nash⁶⁹, A. Nikitenko⁸, V. Palladino, M. Pesaresi, D.M. Raymond, A. Richards, A. Rose, E. Scott, C. Seez, A. Shtipliyski, G. Singh, M. Stoye, T. Strebler, S. Summers, A. Tapper, K. Uchida, T. Virdee¹⁷, N. Wardle, D. Winterbottom, J. Wright, S.C. Zenz

Brunel University, Uxbridge, United Kingdom

J.E. Cole, P.R. Hobson, A. Khan, P. Kyberd, C.K. Mackay, A. Morton, I.D. Reid, L. Teodorescu, S. Zahid

Baylor University, Waco, U.S.A.

K. Call, J. Dittmann, K. Hatakeyama, H. Liu, C. Madrid, B. McMaster, N. Pastika, C. Smith

Catholic University of America, Washington, DC, U.S.A.

R. Bartek, A. Dominguez

The University of Alabama, Tuscaloosa, U.S.A.

A. Buccilli, O. Charaf, S.I. Cooper, C. Henderson, P. Rumerio, C. West

Boston University, Boston, U.S.A.

D. Arcaro, T. Bose, Z. Demiragli, D. Gastler, S. Girgis, D. Pinna, C. Richardson, J. Rohlf, D. Sperka, I. Suarez, L. Sulak, D. Zou

Brown University, Providence, U.S.A.

G. Benelli, B. Burkley, X. Coubez, D. Cutts, M. Hadley, J. Hakala, U. Heintz, J.M. Hogan⁷⁰, K.H.M. Kwok, E. Laird, G. Landsberg, J. Lee, Z. Mao, M. Narain, S. Sagir⁷¹, R. Syarif, E. Usai, D. Yu

University of California, Davis, Davis, U.S.A.

R. Band, C. Brainerd, R. Breedon, D. Burns, M. Calderon De La Barca Sanchez, M. Chertok, J. Conway, R. Conway, P.T. Cox, R. Erbacher, C. Flores, G. Funk, W. Ko, O. Kukral, R. Lander, M. Mulhearn, D. Pellett, J. Pilot, M. Shi, D. Stolp, D. Taylor, K. Tos, M. Tripathi, Z. Wang, F. Zhang

University of California, Los Angeles, U.S.A.

M. Bachtis, C. Bravo, R. Cousins, A. Dasgupta, A. Florent, J. Hauser, M. Ignatenko, N. Mccoll, S. Regnard, D. Saltzberg, C. Schnaible, V. Valuev

University of California, Riverside, Riverside, U.S.A.

E. Bouvier, K. Burt, R. Clare, J.W. Gary, S.M.A. Ghiasi Shirazi, G. Hanson, G. Karapostoli, E. Kennedy, O.R. Long, M. Olmedo Negrete, M.I. Paneva, W. Si, L. Wang, H. Wei, S. Wimpenny, B.R. Yates

University of California, San Diego, La Jolla, U.S.A.

J.G. Branson, P. Chang, S. Cittolin, M. Derdzinski, R. Gerosa, D. Gilbert, B. Hashemi, A. Holzner, D. Klein, G. Kole, V. Krutelyov, J. Letts, M. Masciovecchio, S. May, D. Olivito, S. Padhi, M. Pieri, V. Sharma, M. Tadel, J. Wood, F. Würthwein, A. Yagil, G. Zevi Della Porta

University of California, Santa Barbara — Department of Physics, Santa Barbara, U.S.A.

N. Amin, R. Bhandari, C. Campagnari, M. Citron, V. Dutta, M. Franco Sevilla, L. Gouskos, R. Heller, J. Incandela, H. Mei, A. Ovcharova, H. Qu, J. Richman, D. Stuart, S. Wang, J. Yoo

California Institute of Technology, Pasadena, U.S.A.

D. Anderson, A. Bornheim, J.M. Lawhorn, N. Lu, H.B. Newman, T.Q. Nguyen, J. Pata, M. Spiropulu, J.R. Vlimant, R. Wilkinson, S. Xie, Z. Zhang, R.Y. Zhu

Carnegie Mellon University, Pittsburgh, U.S.A.

M.B. Andrews, T. Ferguson, T. Mudholkar, M. Paulini, M. Sun, I. Vorobiev, M. Weinberg

University of Colorado Boulder, Boulder, U.S.A.

J.P. Cumalat, W.T. Ford, F. Jensen, A. Johnson, E. MacDonald, T. Mulholland, R. Patel, A. Perloff, K. Stenson, K.A. Ulmer, S.R. Wagner

Cornell University, Ithaca, U.S.A.

J. Alexander, J. Chaves, Y. Cheng, J. Chu, A. Datta, K. Mcdermott, N. Mirman, J. Monroy, J.R. Patterson, D. Quach, A. Rinkevicius, A. Ryd, L. Skinnari, L. Soffi, S.M. Tan, Z. Tao, J. Thom, J. Tucker, P. Wittich, M. Zientek

Fermi National Accelerator Laboratory, Batavia, U.S.A.

S. Abdullin, M. Albrow, M. Alyari, G. Apollinari, A. Apresyan, A. Apyan, S. Banerjee, L.A.T. Bauerdick, A. Beretvas, J. Berryhill, P.C. Bhat, K. Burkett, J.N. Butler, A. Canepa, G.B. Cerati, H.W.K. Cheung, F. Chlebana, M. Cremonesi, J. Duarte, V.D. Elvira, J. Freeman, Z. Gecse, E. Gottschalk, L. Gray, D. Green, S. Grünendahl, O. Gutsche, J. Hanlon,

R.M. Harris, S. Hasegawa, J. Hirschauer, Z. Hu, B. Jayatilaka, S. Jindariani, M. Johnson, U. Joshi, B. Klima, M.J. Kortelainen, B. Kreis, S. Lammel, D. Lincoln, R. Lipton, M. Liu, T. Liu, J. Lykken, K. Maeshima, J.M. Marraffino, D. Mason, P. McBride, P. Merkel, S. Mrenna, S. Nahn, V. O'Dell, K. Pedro, C. Pena, O. Prokofyev, G. Rakness, F. Ravera, A. Reinsvold, L. Ristori, B. Schneider, E. Sexton-Kennedy, A. Soha, W.J. Spalding, L. Spiegel, S. Stoynev, J. Strait, N. Strobbe, L. Taylor, S. Tkaczyk, N.V. Tran, L. Uplegger, E.W. Vaandering, C. Vernieri, M. Verzocchi, R. Vidal, M. Wang, H.A. Weber

University of Florida, Gainesville, U.S.A.

D. Acosta, P. Avery, P. Bortignon, D. Bourilkov, A. Brinkerhoff, L. Cadamuro, A. Carnes, D. Curry, R.D. Field, S.V. Gleyzer, B.M. Joshi, J. Konigsberg, A. Korytov, K.H. Lo, P. Ma, K. Matchev, N. Menendez, G. Mitselmakher, D. Rosenzweig, K. Shi, J. Wang, S. Wang, X. Zuo

Florida International University, Miami, U.S.A.

Y.R. Joshi, S. Linn

Florida State University, Tallahassee, U.S.A.

T. Adams, A. Askew, S. Hagopian, V. Hagopian, K.F. Johnson, R. Khurana, T. Kolberg, G. Martinez, T. Perry, H. Prosper, A. Saha, C. Schiber, R. Yohay

Florida Institute of Technology, Melbourne, U.S.A.

M.M. Baarmand, V. Bhopatkar, S. Colafranceschi, M. Hohlmann, D. Noonan, M. Rahmani, T. Roy, M. Saunders, F. Yumiceva

University of Illinois at Chicago (UIC), Chicago, U.S.A.

M.R. Adams, L. Apanasevich, D. Berry, R.R. Betts, R. Cavanaugh, X. Chen, S. Dittmer, O. Evdokimov, C.E. Gerber, D.A. Hangal, D.J. Hofman, K. Jung, C. Mills, M.B. Tonjes, N. Varelas, H. Wang, X. Wang, Z. Wu, J. Zhang

The University of Iowa, Iowa City, U.S.A.

M. Alhusseini, B. Bilki⁵⁵, W. Clarida, K. Dilsiz⁷², S. Durgut, R.P. Gandrajula, M. Haytmyradov, V. Khristenko, O.K. Köseyan, J.-P. Merlo, A. Mestvirishvili, A. Moeller, J. Nachtman, H. Ogul⁷³, Y. Onel, F. Ozok⁷⁴, A. Penzo, C. Snyder, E. Tiras, J. Wetzel

Johns Hopkins University, Baltimore, U.S.A.

B. Blumenfeld, A. Cocoros, N. Eminizer, D. Fehling, L. Feng, A.V. Gritsan, W.T. Hung, P. Maksimovic, J. Roskes, U. Sarica, M. Swartz, M. Xiao

The University of Kansas, Lawrence, U.S.A.

A. Al-bataineh, P. Baringer, A. Bean, S. Boren, J. Bowen, A. Bylinkin, J. Castle, S. Khalil, A. Kropivnitskaya, D. Majumder, W. Mcbrayer, M. Murray, C. Rogan, S. Sanders, E. Schmitz, J.D. Tapia Takaki, Q. Wang

Kansas State University, Manhattan, U.S.A.

S. Duric, A. Ivanov, K. Kaadze, D. Kim, Y. Maravin, D.R. Mendis, T. Mitchell, A. Modak, A. Mohammadi

Lawrence Livermore National Laboratory, Livermore, U.S.A.

F. Rebassoo, D. Wright

University of Maryland, College Park, U.S.A.

A. Baden, O. Baron, A. Belloni, S.C. Eno, Y. Feng, C. Ferraioli, N.J. Hadley, S. Jabeen, G.Y. Jeng, R.G. Kellogg, J. Kunkle, A.C. Mignerey, S. Nabili, F. Ricci-Tam, M. Seidel, Y.H. Shin, A. Skuja, S.C. Tonwar, K. Wong

Massachusetts Institute of Technology, Cambridge, U.S.A.

D. Abercrombie, B. Allen, V. Azzolini, A. Baty, R. Bi, S. Brandt, W. Busza, I.A. Cali, M. D'Alfonso, G. Gomez Ceballos, M. Goncharov, P. Harris, D. Hsu, M. Hu, M. Klute, D. Kovalskyi, Y.-J. Lee, P.D. Luckey, B. Maier, A.C. Marini, C. McGinn, C. Mironov, S. Narayanan, X. Niu, C. Paus, D. Rankin, C. Roland, G. Roland, Z. Shi, G.S.F. Stephans, K. Sumorok, K. Tatar, D. Velicanu, J. Wang, T.W. Wang, B. Wyslouch

University of Minnesota, Minneapolis, U.S.A.

A.C. Benvenuti[†], R.M. Chatterjee, A. Evans, P. Hansen, J. Hiltbrand, Sh. Jain, S. Kalafut, M. Krohn, Y. Kubota, Z. Lesko, J. Mans, R. Rusack, M.A. Wadud

University of Mississippi, Oxford, U.S.A.

J.G. Acosta, S. Oliveros

University of Nebraska-Lincoln, Lincoln, U.S.A.

E. Avdeeva, K. Bloom, D.R. Claes, C. Fangmeier, L. Finco, F. Golf, R. Gonzalez Suarez, R. Kamalieddin, I. Kravchenko, J.E. Siado, G.R. Snow, B. Stieger

State University of New York at Buffalo, Buffalo, U.S.A.

A. Godshalk, C. Harrington, I. Iashvili, A. Kharchilava, C. Mclean, D. Nguyen, A. Parker, S. Rappoccio, B. Roozbahani

Northeastern University, Boston, U.S.A.

G. Alverson, E. Barberis, C. Freer, Y. Haddad, A. Hortiangtham, G. Madigan, D.M. Morse, T. Orimoto, A. Tishelman-charny, T. Wamorkar, B. Wang, A. Wisecarver, D. Wood

Northwestern University, Evanston, U.S.A.

S. Bhattacharya, J. Bueghly, T. Gunter, K.A. Hahn, N. Odell, M.H. Schmitt, K. Sung, M. Trovato, M. Velasco

University of Notre Dame, Notre Dame, U.S.A.

R. Bucci, N. Dev, R. Goldouzian, M. Hildreth, K. Hurtado Anampa, C. Jessop, D.J. Karmgard, K. Lannon, W. Li, N. Loukas, N. Marinelli, F. Meng, C. Mueller, Y. Musienko⁴⁰, M. Planer, R. Ruchti, P. Siddireddy, G. Smith, S. Taroni, M. Wayne, A. Wightman, M. Wolf, A. Woodard

The Ohio State University, Columbus, U.S.A.

J. Alimena, L. Antonelli, B. Bylsma, L.S. Durkin, S. Flowers, B. Francis, C. Hill, W. Ji, A. Lefeld, T.Y. Ling, W. Luo, B.L. Winer

Princeton University, Princeton, U.S.A.

S. Cooperstein, G. Dezoort, P. Elmer, J. Hardenbrook, N. Haubrich, S. Higginbotham, A. Kalogeropoulos, S. Kwan, D. Lange, M.T. Lucchini, J. Luo, D. Marlow, K. Mei, I. Ojalvo, J. Olsen, C. Palmer, P. Piroué, J. Salfeld-Nebgen, D. Stickland, C. Tully

University of Puerto Rico, Mayaguez, U.S.A.

S. Malik, S. Norberg

Purdue University, West Lafayette, U.S.A.

A. Barker, V.E. Barnes, S. Das, L. Gutay, M. Jones, A.W. Jung, A. Khatiwada, B. Mahakud, D.H. Miller, N. Neumeister, C.C. Peng, S. Piperov, H. Qiu, J.F. Schulte, J. Sun, F. Wang, R. Xiao, W. Xie

Purdue University Northwest, Hammond, U.S.A.

T. Cheng, J. Dolen, N. Parashar

Rice University, Houston, U.S.A.

Z. Chen, K.M. Ecklund, S. Freed, F.J.M. Geurts, M. Kilpatrick, Arun Kumar, W. Li, B.P. Padley, R. Redjimi, J. Roberts, J. Rorie, W. Shi, Z. Tu, A. Zhang

University of Rochester, Rochester, U.S.A.

A. Bodek, P. de Barbaro, R. Demina, Y.t. Duh, J.L. Dulemba, C. Fallon, T. Ferbel, M. Galanti, A. Garcia-Bellido, J. Han, O. Hindrichs, A. Khukhunaishvili, E. Ranken, P. Tan, R. Taus

Rutgers, The State University of New Jersey, Piscataway, U.S.A.

B. Chiarito, J.P. Chou, Y. Gershtein, E. Halkiadakis, A. Hart, M. Heindl, E. Hughes, S. Kaplan, S. Kyriacou, I. Laflotte, A. Lath, R. Montalvo, K. Nash, M. Osherson, H. Saka, S. Salur, S. Schnetzer, D. Sheffield, S. Somalwar, R. Stone, S. Thomas, P. Thomassen

University of Tennessee, Knoxville, U.S.A.

H. Acharya, A.G. Delannoy, J. Heideman, G. Riley, S. Spanier

Texas A&M University, College Station, U.S.A.

O. Bouhali⁷⁵, A. Celik, M. Dalchenko, M. De Mattia, A. Delgado, S. Dildick, R. Eusebi, J. Gilmore, T. Huang, T. Kamon⁷⁶, S. Luo, D. Marley, R. Mueller, D. Overton, L. Perniè, D. Rathjens, A. Safonov

Texas Tech University, Lubbock, U.S.A.

N. Akchurin, J. Damgov, F. De Guio, P.R. Duderov, S. Kunori, K. Lamichhane, S.W. Lee, T. Mengke, S. Muthumuni, T. Peltola, S. Undleeb, I. Volobouev, Z. Wang, A. Whitbeck

Vanderbilt University, Nashville, U.S.A.

S. Greene, A. Gurrola, R. Janjam, W. Johns, C. Maguire, A. Melo, H. Ni, K. Padeken, F. Romeo, P. Sheldon, S. Tuo, J. Velkovska, M. Verweij, Q. Xu

University of Virginia, Charlottesville, U.S.A.

M.W. Arenton, P. Barria, B. Cox, R. Hirosky, M. Joyce, A. Ledovskoy, H. Li, C. Neu, Y. Wang, E. Wolfe, F. Xia

Wayne State University, Detroit, U.S.A.

R. Harr, P.E. Karchin, N. Poudyal, J. Sturdy, P. Thapa, S. Zaleski

University of Wisconsin — Madison, Madison, WI, U.S.A.

J. Buchanan, C. Caillol, D. Carlsmith, S. Dasu, I. De Bruyn, L. Dodd, B. Gomber⁷⁷,
 M. Grothe, M. Herndon, A. Hervé, U. Hussain, P. Klabbers, A. Lanaro, K. Long,
 R. Loveless, T. Ruggles, A. Savin, V. Sharma, N. Smith, W.H. Smith, N. Woods

†: Deceased

- 1: Also at Vienna University of Technology, Vienna, Austria
- 2: Also at Skobeltsyn Institute of Nuclear Physics, Lomonosov Moscow State University, Moscow, Russia
- 3: Also at IRFU, CEA, Université Paris-Saclay, Gif-sur-Yvette, France
- 4: Also at Universidade Estadual de Campinas, Campinas, Brazil
- 5: Also at Federal University of Rio Grande do Sul, Porto Alegre, Brazil
- 6: Also at Université Libre de Bruxelles, Bruxelles, Belgium
- 7: Also at University of Chinese Academy of Sciences, Beijing, China
- 8: Also at Institute for Theoretical and Experimental Physics, Moscow, Russia
- 9: Also at Joint Institute for Nuclear Research, Dubna, Russia
- 10: Also at Cairo University, Cairo, Egypt
- 11: Also at Suez University, Suez, Egypt
- 12: Now at British University in Egypt, Cairo, Egypt
- 13: Also at Zewail City of Science and Technology, Zewail, Egypt
- 14: Also at Purdue University, West Lafayette, U.S.A.
- 15: Also at Université de Haute Alsace, Mulhouse, France
- 16: Also at Tbilisi State University, Tbilisi, Georgia
- 17: Also at CERN, European Organization for Nuclear Research, Geneva, Switzerland
- 18: Also at RWTH Aachen University, III. Physikalisches Institut A, Aachen, Germany
- 19: Also at University of Hamburg, Hamburg, Germany
- 20: Also at Brandenburg University of Technology, Cottbus, Germany
- 21: Also at Institute of Physics, University of Debrecen, Debrecen, Hungary
- 22: Also at Institute of Nuclear Research ATOMKI, Debrecen, Hungary
- 23: Also at MTA-ELTE Lendület CMS Particle and Nuclear Physics Group, Eötvös Loránd University, Budapest, Hungary
- 24: Also at Indian Institute of Technology Bhubaneswar, Bhubaneswar, India
- 25: Also at Institute of Physics, Bhubaneswar, India
- 26: Also at Shoolini University, Solan, India
- 27: Also at University of Visva-Bharati, Santiniketan, India
- 28: Also at Isfahan University of Technology, Isfahan, Iran
- 29: Also at Plasma Physics Research Center, Science and Research Branch, Islamic Azad University, Tehran, Iran
- 30: Also at Italian National Agency for New Technologies, Energy and Sustainable Economic Development, Bologna, Italy
- 31: Also at Centro Siciliano di Fisica Nucleare e di Struttura della Materia, Catania, Italy
- 32: Also at Università degli Studi di Siena, Siena, Italy
- 33: Also at Scuola Normale e Sezione dell'INFN, Pisa, Italy
- 34: Also at Kyung Hee University, Department of Physics, Seoul, Korea
- 35: Also at Riga Technical University, Riga, Latvia

- 36: Also at International Islamic University of Malaysia, Kuala Lumpur, Malaysia
- 37: Also at Malaysian Nuclear Agency, MOSTI, Kajang, Malaysia
- 38: Also at Consejo Nacional de Ciencia y Tecnología, Mexico City, Mexico
- 39: Also at Warsaw University of Technology, Institute of Electronic Systems, Warsaw, Poland
- 40: Also at Institute for Nuclear Research, Moscow, Russia
- 41: Now at National Research Nuclear University ‘Moscow Engineering Physics Institute’ (MEPhI), Moscow, Russia
- 42: Also at St. Petersburg State Polytechnical University, St. Petersburg, Russia
- 43: Also at University of Florida, Gainesville, U.S.A.
- 44: Also at P.N. Lebedev Physical Institute, Moscow, Russia
- 45: Also at California Institute of Technology, Pasadena, U.S.A.
- 46: Also at Budker Institute of Nuclear Physics, Novosibirsk, Russia
- 47: Also at Faculty of Physics, University of Belgrade, Belgrade, Serbia
- 48: Also at University of Belgrade — Faculty of Physics, Belgrade, Serbia
- 49: Also at INFN Sezione di Pavia^a, Università di Pavia^b, Pavia, Italy
- 50: Also at National and Kapodistrian University of Athens, Athens, Greece
- 51: Also at Universität Zürich, Zurich, Switzerland
- 52: Also at Stefan Meyer Institute for Subatomic Physics (SMI), Vienna, Austria
- 53: Also at Adiyaman University, Adiyaman, Turkey
- 54: Also at Sirtak University, SIRTAK, Turkey
- 55: Also at Beykent University, Istanbul, Turkey
- 56: Also at Istanbul Aydin University, Istanbul, Turkey
- 57: Also at Mersin University, Mersin, Turkey
- 58: Also at Piri Reis University, Istanbul, Turkey
- 59: Also at Gaziosmanpasa University, Tokat, Turkey
- 60: Also at Ozyegin University, Istanbul, Turkey
- 61: Also at Izmir Institute of Technology, Izmir, Turkey
- 62: Also at Marmara University, Istanbul, Turkey
- 63: Also at Kafkas University, Kars, Turkey
- 64: Also at Istanbul University, Faculty of Science, Istanbul, Turkey
- 65: Also at Istanbul Bilgi University, Istanbul, Turkey
- 66: Also at Hacettepe University, Ankara, Turkey
- 67: Also at Rutherford Appleton Laboratory, Didcot, United Kingdom
- 68: Also at School of Physics and Astronomy, University of Southampton, Southampton, United Kingdom
- 69: Also at Monash University, Faculty of Science, Clayton, Australia
- 70: Also at Bethel University, St. Paul, U.S.A.
- 71: Also at Karamanoğlu Mehmetbey University, Karaman, Turkey
- 72: Also at Bingol University, Bingol, Turkey
- 73: Also at Sinop University, Sinop, Turkey
- 74: Also at Mimar Sinan University, Istanbul, Istanbul, Turkey
- 75: Also at Texas A&M University at Qatar, Doha, Qatar
- 76: Also at Kyungpook National University, Daegu, Korea
- 77: Also at University of Hyderabad, Hyderabad, India